学位論文（要約）

# Architectonics of π-Conjugated Low-dimensional Nanomaterials at Liquid Interfaces

（液相界面を駆使したπ共役低次元ナノ物質の構築）

平成２８年１２月　博士（理学）申請

東京大学大学院理学系研究科化学専攻

松岡　亮太

# Abstract

本内容の一部については、5 年以内に雑誌等で刊行予定のため、非公開。

Use of a liquid/liquid or gas/liquid interface is an effective approach to construct low-dimensional polymeric or assembled nanomaterials with well-defined morphologies in a bottom-up fashion. However, the diversity in chemical bonding or interaction employed in this method has not been extensively explored, resulted in restriction of the accessible structural motifs. This thesis describes architectonics of several kinds of π-conjugated low-dimensional nanomaterials at liquid interfaces.

In **Chapter 1**, general research background and the focus and concept of this thesis are described.

In **Chapter 2**, π-conjugated one-dimensional coordination polymers comprising the bis(dipyrrinato)metal(II) complex motif are studied. The liquid/liquid interfacial synthesis affords single crystals of the desired linear polymer chains, where the chains are aligned in a parallel manner with each other. The Zn-centered coordination polymer features good proessability by being dispersed in an organic solvent, realizing applications to thermoelectric and photoelectric conversion systems.

**Chapter 3**

**Chapter 4**

**Chapter 5** summarizes the research achievement in this thesis as a series of concluding remarks.

# Contents


## Abstract

## Chapter 1 General Introduction and Scientific Background 1

1-1 Low-dimensional nanomaterials 2

1-2 Preparation of low-dimensional nanomaterials 3

1-2-1 Top-down method 3

1-2-2 Bottom-up method 5

1-3 Liquid interfaces 9

1-3-1 Gas/liquid interface 9

1-3-2 Liquid/liquid interface 11

1-4 Aim of this research 13

1-5 References 16

## Chapter 2 Bis(dipyrrinato)metal(II) One-dimensional Coordination Polymers 23

2-1 Introduction 24

2-1-1 One-dimensional coordination polymers 24

2-1-2 Dipyrrin and its 1D CPs 25

2-2 Experimental section 27

2-2-1 Materials 27

2-2-2 Syntheses 27

2-2-3 Instruments and experimental methods 31

2-3 Results and discussion 35

2-3-1 Single-phase synthesis of bulk MCP 35

2-3-2 Spectroscopic characterization of MCP 36

2-3-3 Liquid/liquid interfacial synthesis of MCP 40

2-3-4 Single wire exfoliation 46

2-3-5 Thermoelectric conversion upon conjugation with SWCNT 48

2-3-6 Photoelectric conversion 54
2-4 Conclusions 59
2-5 References 60

**Chapter 3 Graphdiyne Nanosheets 63**
3-1 Introduction 64
3-1-1 Nanosheets based on C–C bond 64
3-1-2 Graphdiyne 65
3-2 Experimental Section 67
3-2-1 Materials 67
3-2-2 Syntheses 67
3-2-3 Instruments and experimental methods 70
3-3 Results and discussion 72
3-3-1 Liquid/liquid interfacial synthesis of graphdiyne 72
3-3-2 Microscopic observation of multi-layer graphdiyne 74
3-3-3 2D Periodicity of multi-layer graphdiyne 75
3-3-4 Spectroscopic characterization of multi-layer graphdiyne 78
3-3-5 Gas/liquid interfacial synthesis of graphdiyne 81
3-3-6 Microscopic observations of few-layer graphdiyne 82
3-3-7 2D Periodicity of few-layer graphdiyne 87
3-3-8 Spectroscopic characterization of few-layer graphdiyne 90
3-4 Conclusions 92
3-5 References 93

**Chapter 4 Triphenylene-cored diyne Nanosheet 97**
4-1 Introduction 98
4-2 Experimental Section 99
4-2-1 Materials 99
4-2-2 Syntheses 99
4-2-3 Instruments and experimental methods 101
4-3 Results and discussion 102

4-3-1 Liquid/liquid interfacial synthesis of HETP-2DP 102
4-3-2 Microscopic observation of HETP-2DP 103
4-3-3 Spectroscopic characterization of HETP-2DP 105
4-4 Conclusions 108
4-5 References 109

**Chapter 5 Concluding Regards 111**

**Appendix 115**
Crystalographic data of **ZnCP** 116
Crystalographic data of **CuCP** 121
Crystalographic data of **NiCP** 126

**Acknowledgement 132**

**List of publications 135**

# Chapter 1

# General Introduction and Scientific Background

## 1-1 Low-dimensional nanomaterials

Low-dimensional (LD) nanomaterials describe substances of which size in specific dimensions is less than 100 nm–1 μm. As the name implies, their structures extend in low dimensions and can be classified by their dimensionality. A representative example of LD nanomaterials is a series of allotropes of carbon: Fullerenes,[1] carbon nanotubes,[2] and graphene[3] as zero-, one-, and two-dimensional (0D, 1D, and 2D) nanomaterials respectively (Fig. 1-1). Depending on the dimensionality, these carbon allotropes feature distinct chemical and physical properties as well as their structures. Fullerenes behave like conventional molecules in terms of electronic structures and solubility in organic solvents; carbon nanotubes and graphene have electronic band structures and insolubility due to their quasi-infinite structures. In addition, the dimensionality of the 1D nanotubes and 2D sheet significantly changes their electronic structures and induces unique anisotropic properties. Recently such LD nanomaterials have attracted much interest as a new class of functional materials in electronics,[4,5] optics,[6,7] spintronics,[8,9] and nanomechanics.[10,11]

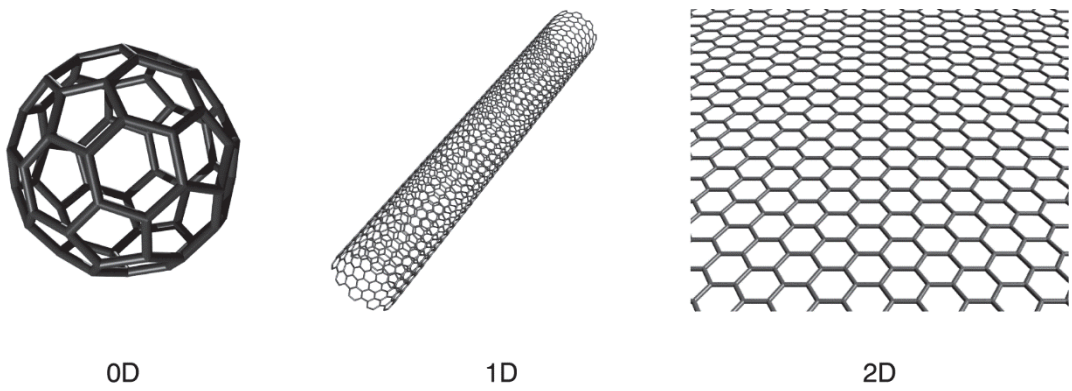


**Figure 1-1 | Dimensionality of nanomaterials**. Structure of [60]fullerene (left), single-walled carbon nanotube (middle), and graphene (right) as 0D, 1D, amd 2D carbon nanomaterials.

## 1-2 Preparation of low-dimensional nanomaterials

### 1-2-1 Top-down method

LD nanomaterial motifs occur in some bulk crystals, and can be sometimes exfoliated into individual wires or sheets in a top-down fashion. The top-down approaches to prepare LD materials have been reviewed.[12,13] As for 2D materials, the pioneering study has been made by Novoselov and coworkers, in which they mechanically exfoliated bulk graphite into individual graphene sheets.[3] This strategy is applicable to other layered materials where each nanosheet stacks via van der Waals interaction including transition metal dichalcogenide (TMD)[14] and hexagonal boron nitride (hBN).[15] LD materials can be also exfoliated in liquid media.[16] A straightforward way of liquid-phase exfoliation is application of mechanical force by ultrasonication. In this case, the yield of exfoliated products strongly depends on dispersants. For example, carbon nanotubes and graphene are effectively dispersed and stabilized in *N*-methylpyrrolidone and *N*,*N*-dimethylformamide[17] while black phosphorus in *N*-cyclohexyl-2-pyrrolidone.[18] More improved exfoliation of graphite into graphene has been achieved by the use of microwaves and molecularly engineered ionic liquids (Fig. 1-2).[19] Layered TMD can be exfoliated into nanosheets at higher concentration with the assistance of amine-terminated polymers.[20] Similarly, delamination of layered metal-organic frameworks has been realized in the presence of amine.[21] Positively charged inorganic nanosheets have been isolated from layered double hydroxides by the intercalation of anionic surfactants.[22] Acid-base treatment solubilizes single fibers of 1D coordination polymers: Protonation/deprotonation of the constitutive ligands gives positive/negative charge to the polymer chain, inducing the electrostatic repulsion between the chains.[23] An anthracene-based covalent organic framework has been delaminated into individual sheets by the chemical addition of *N*-hexylmaleimide through [4+2] Diels-Alder cycloaddition reaction (Fig. 1-2).[24] As another example of the top-down approach, Huang and coworkers have reported the evaporative thinning of layered bismuth selenide and antimony telluride down to monolayer thickness.[25]

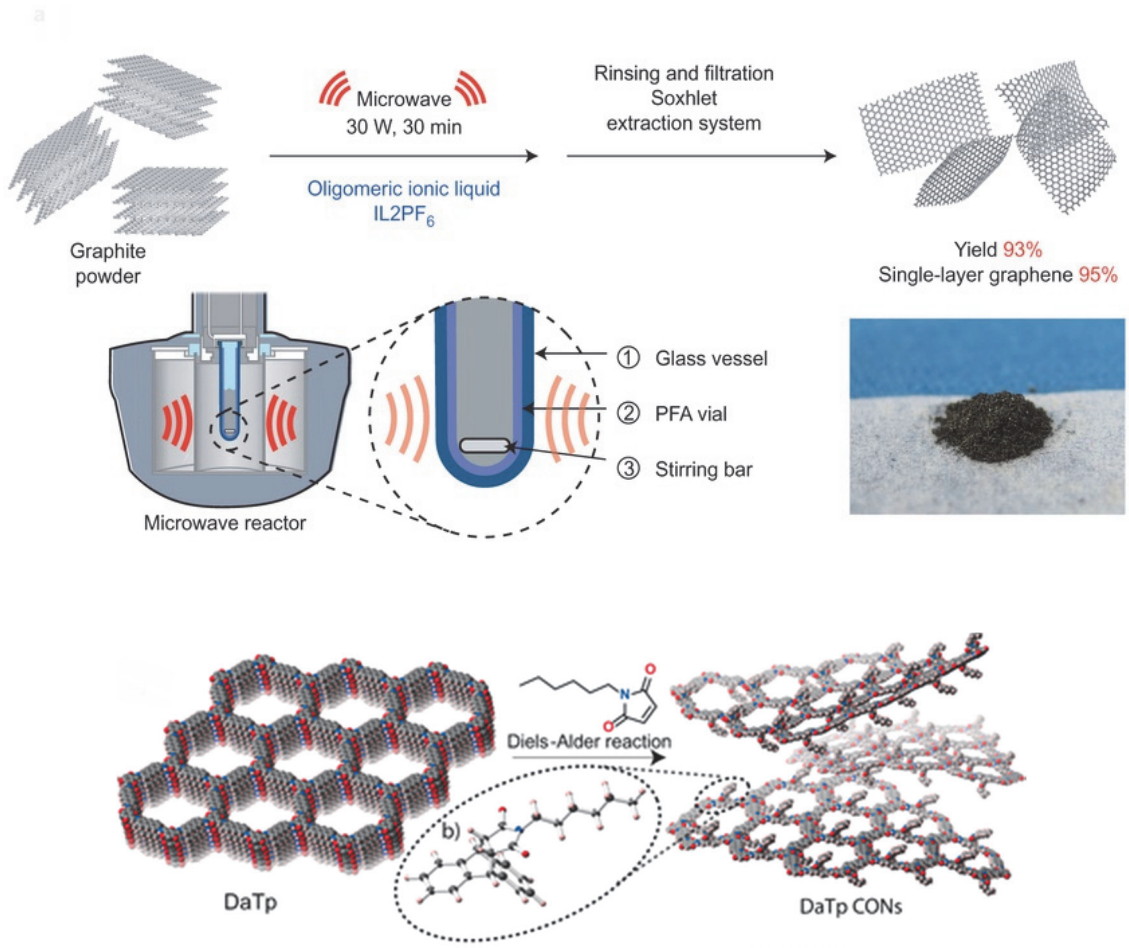


**Figure 1-2 | Top-down exfoliation of LD nanomaterials**. Microwave-assisted liquid-phase exfoliation of graphite in ionic liquids (top) and chemical exfoliation of a layered COF through [4+2] Diels-Alder cycloaddition reaction (bottom). Adapted by permission from Macmillan Publishers Ltd: Nature Chemistry ref. 19, copyright 2015 (top); From Khayum, *Chemically Delaminated Free-Standing Ultrathin Covalent Organic Nanosheets* (ref. 24), Copyright © 2016 by John Wiley & Sons, Inc. Adapted by permission of John Wiley & Sons, Inc. (bottom)

## 1-2-2 Bottom-up method

Although top-down approaches take advantages in scalability and inexpensiveness, diversity in structures and chemical composition of the products is highly limited. To realize more diverse and precisely designed LD materials, chemists have synthesized them in direct bottom-up fashions using atomic, ionic, and molecular components. The bottom-up approaches can be categorized according to the method of construction: in a solution, at a solid surface, and at a liquid surface.

### Solution-based syntheses

The solution-based approach often gives LD materials as layered or aligned crystals. Typical examples are coordination polymers: the moderate bond strength of metal-ligand interaction allows structural correction in the polymer, giving rise to thermodynamically stable crystals in solutions. A large number of 1D and 2D coordination polymers composed of various ligands and metal ions have been reported so far. For exsample, Papaefstathiou and coworkers employed a paracyclophane-based ligand to construct a 2D MOF with multiple cavities.[26] Nozaki and coworkers inserted coronene molecules to stabilize the 2D framework with a large mesh of 39 × 29 Å diameters.[27] Rodenas and coworkers developed diffusion-mediated growth of a 2D MOF as freestanding nanosheets that can be easily dispersed into a polymer matrix.[28] Many studies pursuing the functionality of coordination polymers have also been reported: solid state luminescence,[29,30] superprotonic conductivity,[31] electrical conductivity,[32,33] electrochromism,[34] and paramagnetism.[35]

Solvothermal syntheses of imine- or boronate-based covalent organic frameworks are also based on reversible bond formation and have been studied intensively.[36–38] Although many functionalities of the COFs have been sought (e.g. pseudocapacitive energy storage,[39] electrical conductivity,[40,41] and $CO_2$ reduction[42]), they are often polycrystalline powders. Several efforts to improve the crystallinity of these materials

have been made. Kandambeth and coworkers have introduced hydroxyl functionalities adjacent to the Schiff base centers in COFs to induce irreversible proton tautomerism to the keto-enamine form, which enhances the chemical stability and crystallinity of COFs.[43,44] Very recently Ascherl and coworkers realized COFs with long-range periodicity and well-defined crystal facets by utilizing the propeller-shaped molecular building units, which defines the position of each building block and preclude lattice strain and defects in successive layer (Fig. 1-3).[45]

As for inorganics, it is easier to obtain crystalline LD materials with well-defined structures. Oriented attachment of crystalline nanoparticles (e.g. lead sulfide) often results in the formation of 1D or 2D superstructures with good crystallinity.[46] Another pervasive strategy is the use of surfactants.[47] The surfactants adsorb on certain crystal facets of the crystal seeds and therefore slow down the crystal growth in these direction. The surfactant molecules can be removed after the formation of the nanostructure. Besides them, Yoo and coworkers reported on the crystal growth of single-layer TMDs in oleylamine with controlled influx of hydrogen sulfide, a chalcogen source.[48]

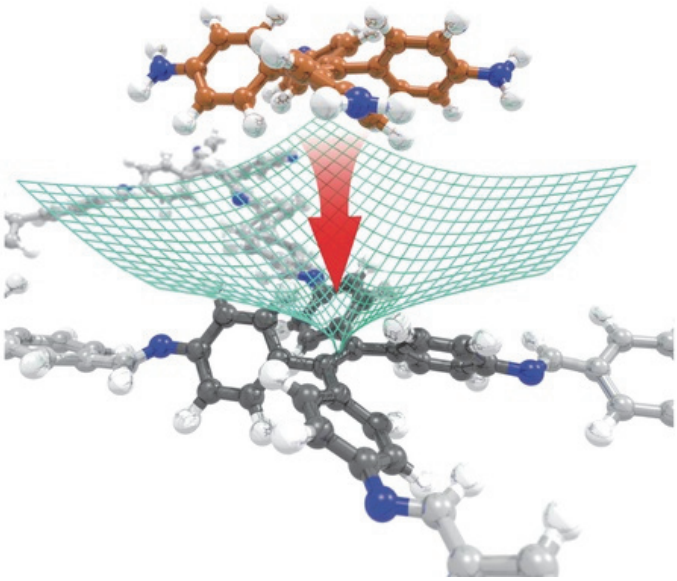

**Figure 1-3 | Solution-based bottom-up synthesis of LD nanomaterials**. Molecular docking sites designed for the generation of highly crystalline COFs. Adapted by permission from Macmillan Publishers Ltd: Nature Chemistry ref. 45, copyright 2016.

### On-surface syntheses

It is useful to get the help of solid surfaces to organize nanomaterials in one- or two-dimension because the building blocks adsorbed on a solid surface diffuse and assemble without the displacement away from there. The prototype of this strategy is the formation of self-assembled monolayers (SAMs), which are single layers of surface-adsorbed molecules with high degree of orientation and packing. As an early study of SAMs, in 1946, Zisman and coworkers reported a molecular adsorption of surfactant molecules on a clean metal surface immersed in a solution.[49] Later, the SAM study have become popular from the end of 1970s and many SAM systems stabilized by chemical bonding, van der Waals interaction, hydrogen bonding, and dipolar coupling have been discovered.[50–52] Recently, this strategy has been applied to construct more stable LD nanomaterials based on stronger chemical bond formation. Tanoue and coworkers constructed 1D and 2D imine-based covalent nanoarchetectures on

iodine-modified Au(111) surfaces in water.[53] Similar Shiff-base 2D networks have been synthesized at octanoic acid/highly oriented pyrolytic graphite (HOPG)[54] and octanoic acid/graphene-copper interfaces[55] by Xu and coworkers. Dienstmaier and coworkers reported on the growth of a COF monolayer based on boronic acid condensation at the interface between HOPG and various organic solvents.[56] Huang and coworkers prepared ultrathin hexagonal close-packed gold nanostructures at a mixed organic solvent/graphene oxide interface.[57] In addition, such kinds of polymer networks can be obtained under an ultra-high vacuum condition. Constitutive building blocks are deposited on solid surfaces by physical vapor deposition. The obtained LD networks are based on imine condensation,[58] metal-ligand coordination,[59,60] polyimide formation,[61,62] and boronic acid condensation (Fig. 1-4).[63]

Chemical vapor deposition (CVD) on solid surfaces is another important method to synthesize LD nanomaterials.[64] Several sophisticated techniques have been established in this strategy (e.g. on-spot synthesis[65] and lateral heterojunction[66–70]). However, the materials scope of CVD are still limited to metals,[71] inorganics,[72] carbon allotropes,[73] conventional organic polymers,[74] and several MOFs.[75]

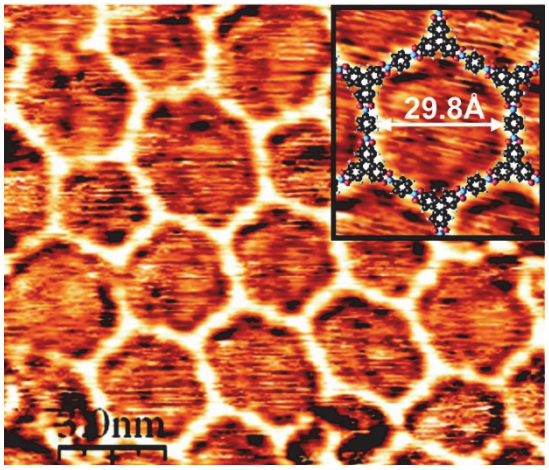


**Figure 1-4 | Surface-assisted bottom-up synthesis of LD nanomaterials**. STM image of the 2D COF based on boronic acid condensation. Adapted with permission from ref. 63. Copyright 2008 American Chemical Society.

## 1-3 Liquid interfaces

As described above, enormous efforts have been made to create LD nanomaterials in solutions and at solid surfaces. The solution-based synthetic strategy, however, cannot avoid a random encounter between building blocks which generates undesired kinetic products. This problem strongly restricts the accessible structural motifs. The on-surface syntheses can access various structural motifs unavailable via solution-based reactions. However, they often suffer from small domain size of the products due to the strong interaction between building blocks and underlying substrates. In this context, use of a liquid/liquid or gas/liquid interface is an important strategy for expanding the series of synthetic low-dimensional nanomaterials. Its interface has long been adopted for realizing various polymerized or self-assembled membranes with long-range 2D organization.[76,77] In addition, the interface can serve as a 2D reaction space for the reactants.[78] For these reasons many researchers have employed liquid/liquid and gas/liquid interfaces to synthesize low-dimensional nanomaterials.

### 1-3-1 Gas/liquid interface

A hundred years ago, Langmuir discovered that stearic acid spreads on a water surface (*i.e.* gas/water interface) with its carboxyl group in contact with the water to form a molecularly thin 2D assembly.[79] Since the hydrocarbon chain of each stearic acid molecule is nearly perpendicular to the water surface, the obtained film features uniform thickness and internal periodicity. His finding has inspired chemists to utilize a gas/liquid interface as a tool of molecular organization. In 1935, Gee and coworkers reported the polymerization of $\beta$-elaeostearin at the gas/water interface.[76] A remarkable progress in this research field has been made very recently thanks to the development of nanotechnology. For example, self-assembly or merging of nanometer-sized inorganic crystals creates well-organized superstructures at the gas/liquid interface.[80,81] Direct syntheses of inorganic 2D nanomaterials has also been

reported. Therein, self-assembled surfactant monolayers on a water surface serve as templates guiding the growth of the nanosheets (Fig. 1-5).[82,83] Another example has demonstrated pH-modulated Langmuir-Blodgett assemblies of supramolecular containers which varies the surface hydrophilicities along with the orientation of the supramolecules in the films.[84] A covalent organic nanosheet constructed by imine condensation has been obtained at an air/water interface.[85] In addition, an increasing number of metal-organic nanosheets (coordination nanosheets, CONASHs) have been synthesized at a gas/liquid interface in recent years. CONASHs are built via the successive coordination reactions between metal ions in water and ligands floating on the water surface. The combinations of metal ions and ligands include $Cu^{2+}$ or $Cd^{2+}$/tetrapyridylporphyrin,[86] $Cu^{2+}$/tetrakis(4-carboxyphenyl)porphyrin,[87] $Ni^{2+}$/benzene-hexathiol,[88] $Co^{2+}$/benzenehexathiol or triphenylenehexathiol,[89] $Fe^{2+}$/6-fold terpyridine ligand,[90] and $Zn^{2+}$/3-fold dipyrrin ligand.[91] Some of CONASHs exhibit characteristic functionalities owing to the metal complexes incorporated in the 2D polymers.[88,89,91]

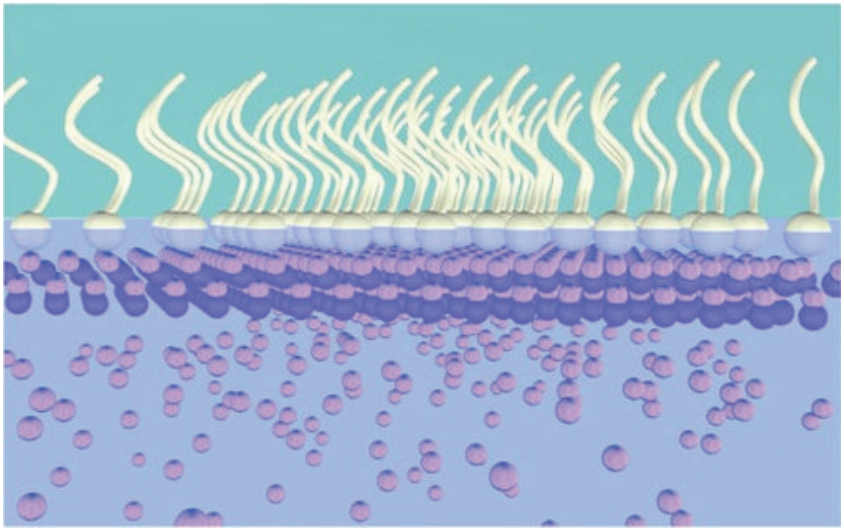

**Figure 1-5 | Bottom-up construction of LD nanomaterials at a gas/liquid interface**. Surfactant-assisted synthesis of inorganic 2D nanomaterials at a gas/liquid interface. Adapted from ref. 83.

### 1-3-2 Liquid/liquid interface

A liquid/liquid interface has a long history of use in polymer chemistry. In 1959, Wittbecker and Morgan synthesized nylon-6,10 by polycondensation of sebacoyl chloride and hexamethylenediamine at a benzene/water interface.[92] Since the diacid chloride and diamine are dissolved in different immiscible solvents, the condensation reaction occurs only at the flat liquid/liquid interface, thereby forming a thin film as the product. This approach is called as interfacial polymerization and has been widely used to manufacture polyamides, polyesters, polyurethanes, polysulfonamides and polycarbonates. In recent years, chemists have further developed the utilization of the liquid/liquid interface to the fabrication of low-dimensional nanomaterials. Matsui and coworkers created poly(3,4-ethylenedioxythiophene) (PEDOT) nanocrystals via the oxidative polymerization of 3,4-ethylenedioxythiophene at a dichloromethane/water interface.[93,94] Jana and coworkers reported on the liquid/liquid interfacial synthesis of self-assembled films composed of PbSe single crystallites.[95] Pfeffermann and coworkers demonstrated the creation of a free-Standing monolayer 2D supramolecular organic framework at a toluene/water interface.[96] Solomon and coworkers synthesized microporous polyarylate nanofilms through hexane/water interfacial polymerization.[97] Nishihara and coworkers have used the liquid/liquid interface for synthesizing multi-layered CONASHs based on metalladithiolene,[88] metal bis(terpyridine) (Fig. 1-6),[98] and metal bis(dipyrrinate) complex motifs.[91] Huang and coworkers conducted the similar reaction to prepare Cu-benzenehexathiol 2D polymer.[99]

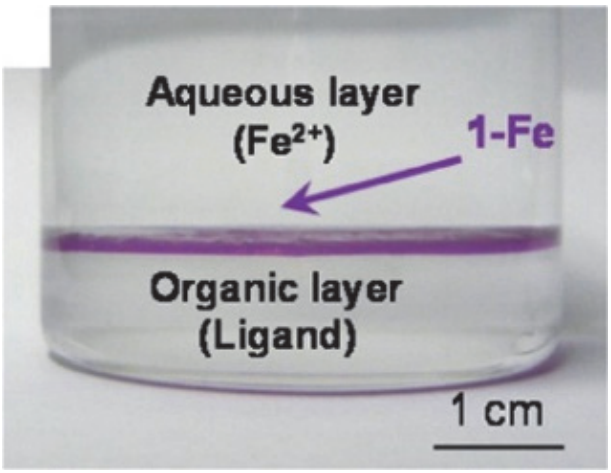


**Figure 1-6 | Bottom-up construction of LD nanomaterials at a liquid/liquid interface**. Photograph of the liquid/liquid interfacial synthesis of bis(terpyridine)iron(II) complex nanosheet. Adapted with permission from ref. 98. Copyright 2015 American Chemical Society.

## 1-4 Aim of this research

As described above, the liquid interfaces have a potential to provide a platform for constructing versatile low-dimensional supramolecular or polymeric nanomaterials. Chemists have begun to take possession of this platform in certain research fields. However, the diversity in chemical bonding or interaction employed in this method has not been extensively explored, resulted in restriction of the accessible structural motifs. In other words, we still leave room for further development of liquid interfacial synthetic chemistry.

The aim of my research is to expand the scope of the liquid interfacial syntheses to versatile low-dimensional nanomaterials. In the master course I have developed synthesis and ordered alignment of a 1D CP comprising bis(dithioleto)nickel(II) complex motif at a liquid/liquid or gas/liquid interface (Figure 1-7).[100] Therein, generated 1D chains formed a film-like secondary nanostructure in which the chains aligned in a parallel manner with each other. The π-π interaction between the chains of planer bis(dithiolato)nickel(II) 1D CP promoted the parallel assembly of the linear fibers and formation of the hierarchical nanostructure.

In my Ph.D research, I focus on two distinct structural concepts as other typical examples: the van der Waals induced organization of linear coordination polymers and construction of covalent 2D polymers based on π-conjugated carbon–carbon bond formation (Figure 1-8).

For the first concept, non-planer bis(dipyrrinato)metal(II) 1D CPs are newly designed and synthesized at a liquid /liquid interface (Chapter 2). These quasi-cylindrical chains feature ordered alignment in a different manner from that in the previous bis(dithiolene) polymer. I also investigated the processability and applicability of the Zn-centered polymer to electric conversion systems.

Then I take on further challenge to develop a liquid/liquid or gas/liquid interfacial synthesis of a 2D polymer woven by π-conjugated carbon–carbon bond (Chapters 3, 4).

The interfaces are employed as the 2D reaction fields of catalytic alkyne-alkyne homocoupling to generate extended 2D polymer networks. Their morphology, chemical composition, and in-plane periodicity are investigated comprehensively. The adaptability to the construction of a nanosheet with different monomer unit is also investigated.

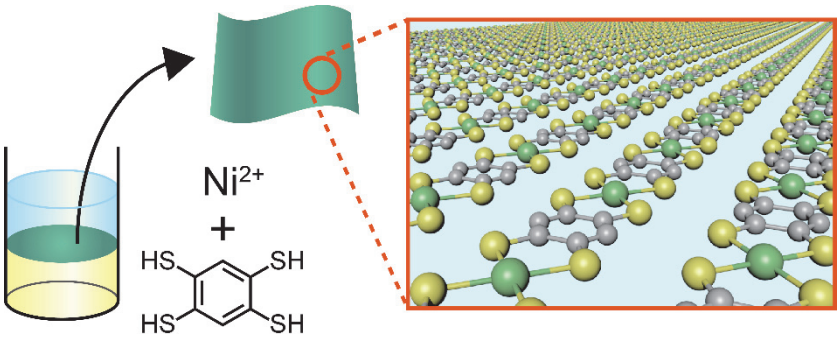


**Figure 1-7 | Conceptual scheme showing my previous study.** Adapted from Ref. 100 with permission from The Royal Society of Chemistry.

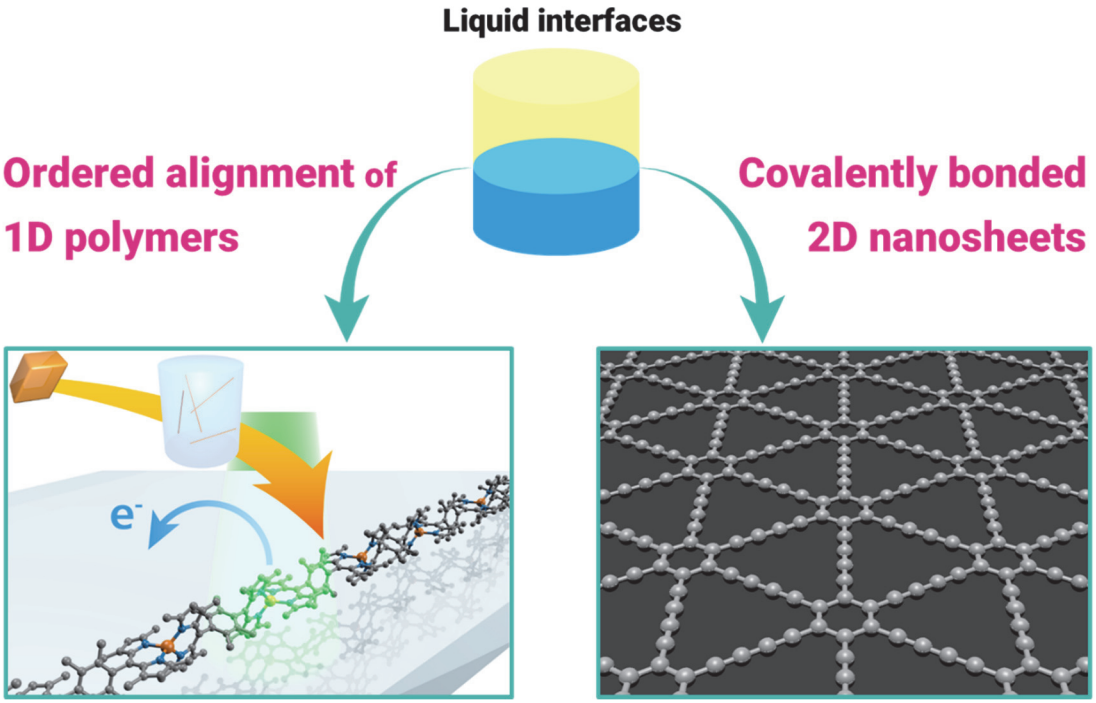


**Figure 1-8 | Conceptual scheme showing the studies in my Ph.D course.**

## 1-5 References


(1) Kroto, H. W.; Heath, J. R.; O'Brien, S. C.; Curl, R. F.; Smalley, R. E. *Nature* **1985**, *318*, 162–163.

(2) Iijima, S. *Nature* **1991**, *354*, 56–58.

(3) Novoselov, K. S. *Science* **2004**, *306*, 666–669.

(4) Geim, A. K.; Novoselov, K. S. *Nat. Mater.* **2007**, *6*, 183–191.

(5) Lin, Y.-M.; Dimitrakopoulos, C.; Jenkins, K. A.; Farmer, D. B.; Chiu, H.-Y.; Grill, A.; Avouris, P. *Science* **2010**, *327*, 662–662.

(6) Bonaccorso, F.; Sun, Z.; Hasan, T.; Ferrari, A. C. *Nat. Photonics* **2010**, *4*, 611–622.

(7) Kim, Y. D.; Kim, H.; Cho, Y.; Ryoo, J. H.; Park, C.-H.; Kim, P.; Kim, Y. S.; Lee, S.; Li, Y.; Park, S.-N.; Shim Yoo, Y.; Yoon, D.; Dorgan, V. E.; Pop, E.; Heinz, T. F.; Hone, J.; Chun, S.-H.; Cheong, H.; Lee, S. W.; Bae, M.-H.; Park, Y. D. *Nat. Nanotechnol.* **2015**, *10*, 676–681.

(8) Son, Y.-W.; Cohen, M. L.; Louie, S. G. *Nature* **2006**, *444*, 347–349.

(9) Maassen, J.; Ji, W.; Guo, H. *Nano Lett.* **2011**, *11*, 151–155.

(10) Nicholl, R. J. T.; Conley, H. J.; Lavrik, N. V; Vlassiouk, I.; Puzyrev, Y. S.; Sreenivas, V. P.; Pantelides, S. T.; Bolotin, K. I. *Nat. Commun.* **2015**, *6*, 8789.

(11) Qian, D.; Wagner, G. J.; Liu, W. K.; Yu, M.-F.; Ruoff, R. S. *Appl. Mech. Rev.* **2002**, *55*, 495.

(12) Yi, M.; Shen, Z. *J. Mater. Chem. A* **2015**, *3*, 11700–11715.

(13) Nicolosi, V.; Chhowalla, M.; Kanatzidis, M. G.; Strano, M. S.; Coleman, J. N. *Science* **2013**, *340*, 1226419–1226419.

(14) Li, H.; Yin, Z.; He, Q.; Li, H.; Huang, X.; Lu, G.; Fam, D. W. H.; Tok, A. I. Y.; Zhang, Q.; Zhang, H. *Small* **2012**, *8*, 63–67.

(15) Pacilé, D.; Meyer, J. C.; Girit, Ç. Ö.; Zettl, A. *Appl. Phys. Lett.* **2008**, *92*, 133107.

(16) Coleman, J. N.; Lotya, M.; O'Neill, A.; Bergin, S. D.; King, P. J.; Khan, U.; Young, K.; Gaucher, A.; De, S.; Smith, R. J.; Shvets, I. V.; Arora, S. K.; Stanton, G.; Kim, H.-Y.; Lee, K.; Kim, G. T.; Duesberg, G. S.; Hallam, T.; Boland, J. J.; Wang, J. J.; Donegan, J. F.; Grunlan, J. C.; Moriarty, G.; Shmeliov, A.; Nicholls, R. J.; Perkins, J. M.; Grieveson, E. M.; Theuwissen, K.; McComb, D. W.; Nellist, P. D.; Nicolosi, V. *Science* **2011**, *331*, 568–571.

(17) Hernandez, Y.; Nicolosi, V.; Lotya, M.; Blighe, F.; Sun, Z.; De, S.; McGovern, I. T.; Holland, B.; Byrne, M.; Gunko, Y.; Boland, J.; Niraj, P.; Duesberg, G.; Krishnamurti, S.; Goodhue, R.; Hutchison, J.; Scardaci, V.; Ferrari, A. C.; Coleman, J. N. *Nat. Nanotechnol.* **2008**, *3*, 563–568.

(18) Hanlon, D.; Backes, C.; Doherty, E.; Cucinotta, C. S.; Berner, N. C.; Boland, C.; Lee, K.; Harvey, A.; Lynch, P.; Gholamvand, Z.; Zhang, S.; Wang, K.; Moynihan, G.; Pokle, A.; Ramasse, Q. M.; McEvoy, N.; Blau, W. J.; Wang, J.; Abellan, G.; Hauke, F.; Hirsch, A.; Sanvito, S.; O'Regan, D. D.; Duesberg, G. S.; Nicolosi, V.; Coleman, J. N. *Nat. Commun.* **2015**, *6*, 8563.

(19) Matsumoto, M.; Saito, Y.; Park, C.; Fukushima, T.; Aida, T. *Nat. Chem.* **2015**, *7*, 730–736.

(20) Velusamy, D. B.; Kim, R. H.; Cha, S.; Huh, J.; Khazaeinezhad, R.; Kassani, S. H.; Song, G.; Cho, S. M.; Cho, S. H.; Hwang, I.; Lee, J.; Oh, K.; Choi, H.; Park, C. *Nat. Commun.* **2015**, 8063.

(21) Li, P.-Z.; Maeda, Y.; Xu, Q. *Chem. Commun.* **2011**, *47*, 8436.

(22) Ma, R.; Liu, Z.; Li, L.; Iyi, N.; Sasaki, T. *J. Mater. Chem.* **2006**, *16*, 3809.

(23) Mas-Ballesté, R.; Gómez-Herrero, J.; Zamora, F. *Chem. Soc. Rev.* **2010**, *39*, 4220.

(24) Khayum, M. A.; Kandambeth, S.; Mitra, S.; Nair, S. B.; Das, A.; Nagane, S. S.; Mukherjee, R.; Banerjee, R. *Angew. Chemie Int. Ed.* **2016**, *55*, 15604–15608.

(25) Huang, Y.-K.; Cain, J. D.; Peng, L.; Hao, S.; Chasapis, T.; Kanatzidis, M. G.; Wolverton, C.; Grayson, M.; Dravid, V. P. *ACS Nano* **2014**, *8*, 10851–10857.

(26) Papaefstathiou, G. S.; Frišc ̌ić, T.; MacGillivray, L. R. *J. Am. Chem. Soc.* **2005**, *127*, 14160–14161.

(27) Nozaki, T.; Kosaka, W.; Miyasaka, H. *CrystEngComm* **2012**, *14*, 5398.

(28) Rodenas, T.; Luz, I.; Prieto, G.; Seoane, B.; Miro, H.; Corma, A.; Kapteijn, F.; Llabrés i Xamena, F. X.; Gascon, J. *Nat. Mater.* **2014**, *14*, 48–55.

(29) Liu, G.-F.; Zhang, W.-H.; Chen, Y.; Liu, D.; Lang, J.-P. *Inorg. Chem. Commun.* **2007**, *10*, 1049–1053.

(30) Gallina, M. E.; Bergamini, G.; Di Motta, S.; Sakamoto, J.; Negri, F.; Ceroni, P. *Photochem. Photobiol. Sci.* **2014**, *13*, 997.

(31) Xu, G.; Otsubo, K.; Yamada, T.; Sakaida, S.; Kitagawa, H. *J. Am. Chem. Soc.* **2013**, *135*, 7438–7441.

(32) Sheberla, D.; Sun, L.; Blood-Forsythe, M. A.; Er, S.; Wade, C. R.; Brozek, C. K.; Aspuru-Guzik, A.; Dincă, M. *J. Am. Chem. Soc.* **2014**, *136*, 8859–8862.

(33) Cui, J.; Xu, Z. *Chem. Commun.* **2014**, *50*, 3986.

(34) AlKaabi, K.; Wade, C. R.; Dincă, M. *Chem* **2016**, *1*, 264–272.

(35) Furukawa, S.; Ohba, M.; Kitagawa, S. *Chem. Commun.* **2005**, *2661*, 865.

(36) Zeng, Y.; Zou, R.; Luo, Z.; Zhang, H.; Yao, X.; Ma, X.; Zou, R.; Zhao, Y. *J. Am. Chem. Soc.* **2015**, *137*, 1020–1023.

(37) Nagai, A.; Chen, X.; Feng, X.; Ding, X.; Guo, Z.; Jiang, D. *Angew. Chemie Int. Ed.* **2013**, *52*, 3770–3774.

(38) Bisbey, R. P.; DeBlase, C. R.; Smith, B. J.; Dichtel, W. R. *J. Am. Chem. Soc.* **2016**, *138*, 11433–11436.

(39) DeBlase, C. R.; Silberstein, K. E.; Truong, T.-T.; Abruña, H. D.; Dichtel, W. R. *J. Am. Chem. Soc.* **2013**, *135*, 16821–16824.

(40) Calik, M.; Auras, F.; Salonen, L. M.; Bader, K.; Grill, I.; Handloser, M.; Medina, D. D.; Dogru, M.; Löbermann, F.; Trauner, D.; Hartschuh, A.; Bein, T. *J. Am. Chem. Soc.* **2014**, *136*, 17802–17807.

(41) Jin, S.; Sakurai, T.; Kowalczyk, T.; Dalapati, S.; Xu, F.; Wei, H.; Chen, X.; Gao, J.; Seki, S.; Irle, S.; Jiang, D. *Chem. - A Eur. J.* **2014**, *20*, 14608–14613.

(42) Lin, S.; Diercks, C. S.; Zhang, Y.-B.; Kornienko, N.; Nichols, E. M.; Zhao, Y.; Paris, A. R.; Kim, D.; Yang, P.; Yaghi, O. M.; Chang, C. J. *Science* **2015**, *349*, 1208–1213.

(43) Kandambeth, S.; Shinde, D. B.; Panda, M. K.; Lukose, B.; Heine, T.; Banerjee, R. *Angew. Chemie Int. Ed.* **2013**, *52*, 13052–13056.

(44) Kandambeth, S.; Mallick, A.; Lukose, B.; Mane, M. V.; Heine, T.; Banerjee, R. *J. Am. Chem. Soc.* **2012**, *134*, 19524–19527.

(45) Ascherl, L.; Sick, T.; Margraf, J. T.; Lapidus, S. H.; Calik, M.; Hettstedt, C.; Karaghiosoff, K.; Döblinger, M.; Clark, T.; Chapman, K. W.; Auras, F.; Bein, T. *Nat. Chem.* **2016**, *8*, 310–316.

(46) Schliehe, C.; Juarez, B. H.; Pelletier, M.; Jander, S.; Greshnykh, D.; Nagel, M.; Meyer, A.; Foerster, S.; Kornowski, A.; Klinke, C.; Weller, H. *Science* **2010**, *329*, 550–553.

(47) Wang, F.; Wang, X. *Nanoscale* **2014**, *6*, 6398.

(48) Yoo, D.; Kim, M.; Jeong, S.; Han, J.; Cheon, J. *J. Am. Chem. Soc.* **2014**, *136*, 14670–14673.

(49) Bigelow, W. C.; Pickett, D. L.; Zisman, W. a. *J. Colloid Sci.* **1946**, *1*, 513–538.

(50) Sagiv, J.; Polymeropoulos, E. E. *Berichte der Bunsengesellschaft für Phys. Chemie* **1978**, *82*, 883–883.

(51) Nuzzo, R. G.; Allara, D. L. *J. Am. Chem. Soc.* **1983**, *105*, 4481–4483.

(52) Vericat, C.; Vela, M. E.; Corthey, G.; Pensa, E.; Cortés, E.; Fonticelli, M. H.; Ibañez, F.; Benitez, G. E.; Carro, P.; Salvarezza, R. C. *RSC Adv.* **2014**, *4*, 27730.

(53) Tanoue, R.; Higuchi, R.; Enoki, N.; Miyasato, Y.; Uemura, S.; Kimizuka, N.; Stieg, A. Z.; Gimzewski, J. K.; Kunitake, M. *ACS Nano* **2011**, *5*, 3923–3929.

(54) Xu, L.; Zhou, X.; Yu, Y.; Tian, W. Q.; Ma, J.; Lei, S. *ACS Nano* **2013**, *7*, 8066–8073.

(55) Xu, L.; Zhou, X.; Tian, W. Q.; Gao, T.; Zhang, Y. F.; Lei, S.; Liu, Z. F. *Angew. Chemie Int. Ed.* **2014**, *53*, 9564–9568.

(56) Dienstmaier, J. F.; Gigler, A. M.; Goetz, A. J.; Knochel, P.; Bein, T.; Lyapin, A.; Reichlmaier, S.; Heckl, W. M.; Lackinger, M. *ACS Nano* **2011**, *5*, 9737–9745.

(57) Huang, X.; Li, S.; Huang, Y.; Wu, S.; Zhou, X.; Li, S.; Gan, C. L.; Boey, F.; Mirkin, C. a; Zhang, H. *Nat. Commun.* **2011**, *2*, 292.

(58) Weigelt, S.; Busse, C.; Bombis, C.; Knudsen, M. M.; Gothelf, K. V.; Lægsgaard, E.; Besenbacher, F.; Linderoth, T. R. *Angew. Chemie Int. Ed.* **2008**, *47*, 4406–4410.

(59) Dmitriev, A.; Spillmann, H.; Lin, N.; Barth, J. V.; Kern, K. *Angew. Chemie Int. Ed.* **2003**, *42*, 2670–2673.

(60) Stepanow, S.; Lingenfelder, M.; Dmitriev, A.; Spillmann, H.; Delvigne, E.; Lin, N.; Deng, X.; Cai, C.; Barth, J. V; Kern, K. *Nat. Mater.* **2004**, *3*, 229–233.

(61) Treier, M.; Fasel, R.; Champness, N. R.; Argent, S.; Richardson, N. V. *Phys. Chem. Chem. Phys.* **2009**, *11*, 1209.

(62) Treier, M.; Richardson, N. V.; Fasel, R. *J. Am. Chem. Soc.* **2008**, *130*, 14054–14055.

(63) Zwaneveld, N. a a; Pawlak, R.; Abel, M.; Catalin, D.; Gigmes, D.; Bertin, D.; Porte, L. *J. Am. Chem. Soc.* **2008**, *130*, 6678–6679.

(64) Yu, J.; Li, J.; Zhang, W.; Chang, H. *Chem. Sci.* **2015**, *6*, 6705–6716.

(65) Wu, T.; Zhang, X.; Yuan, Q.; Xue, J.; Lu, G.; Liu, Z.; Wang, H.; Wang, H.; Ding, F.; Yu, Q.; Xie, X.; Jiang, M. *Nat. Mater.* **2015**, *15*, 43–47.

(66) Liu, Z.; Ma, L.; Shi, G.; Zhou, W.; Gong, Y.; Lei, S.; Yang, X.; Zhang, J.; Yu, J.; Hackenberg, K. P.; Babakhani, A.; Idrobo, J.-C.; Vajtai, R.; Lou, J.; Ajayan, P. M. *Nat. Nanotechnol.* **2013**, *8*, 119–124.

(67) Liu, L.; Park, J.; Siegel, D. a.; McCarty, K. F.; Clark, K. W.; Deng, W.; Basile, L.; Idrobo, J. C.; Li, A.-P.; Gu, G. *Science* **2014**, *343*, 163–167.

(68) Huang, C.; Wu, S.; Sanchez, A. M.; Peters, J. J. P.; Beanland, R.; Ross, J. S.; Rivera, P.; Yao, W.; Cobden, D. H.; Xu, X. *Nat. Mater.* **2014**, *13*, 1096–1101.

(69) Duan, X.; Wang, C.; Shaw, J. C.; Cheng, R.; Chen, Y.; Li, H.; Wu, X.; Tang, Y.; Zhang, Q.; Pan, A.; Jiang, J.; Yu, R.; Huang, Y.; Duan, X. *Nat. Nanotechnol.* **2014**, *9*, 1024–1030.

(70) Gong, Y.; Lin, J.; Wang, X.; Shi, G.; Lei, S.; Lin, Z.; Zou, X.; Ye, G.; Vajtai, R.; Yakobson, B. I.; Terrones, H.; Terrones, M.; Tay, B. K.; Lou, J.; Pantelides, S. T.; Liu, Z.; Zhou, W.; Ajayan, P. M. *Nat. Mater.* **2014**, *13*, 1135–1142.

(71) Mond, L.; Langer, C.; Quincke, F. *J. Chem. Soc., Trans.* **1890**, *57*, 749–753.

(72) Tai, G.; Hu, T.; Zhou, Y.; Wang, X.; Kong, J.; Zeng, T.; You, Y.; Wang, Q. *Angew. Chemie Int. Ed.* **2015**, *54*, 15473–15477.

(73) Mohsin, A.; Liu, L.; Liu, P.; Deng, W.; Ivanov, I. N.; Li, G.; Dyck, O. E.; Duscher, G.; Dunlap, J. R.; Xiao, K.; Gu, G. *ACS Nano* **2013**, *7*, 8924–8931.

(74) Coclite, A. M.; Howden, R. M.; Borrelli, D. C.; Petruczok, C. D.; Yang, R.; Yagüe, J. L.; Ugur, A.; Chen, N.; Lee, S.; Jo, W. J.; Liu, A.; Wang, X.; Gleason, K. K. *Adv. Mater.* **2013**, *25*, 5392–5423.

(75) Stassen, I.; Styles, M.; Grenci, G.; Gorp, H. Van; Vanderlinden, W.; Feyter, S. De; Falcaro, P.; Vos, D. De; Vereecken, P.; Ameloot, R. *Nat. Mater.* **2015**, *15*, 304–310.

(76) Gee, G.; Rideal, E. K. *Proc. R. Soc. A Math. Phys. Eng. Sci.* **1935**, *153*, 116–128.

(77) Blodgett, K. B.; Langmuir, I. *Phys. Rev.* **1937**, *51*, 964–982.

(78) Piradashvili, K.; Alexandrino, E. M.; Wurm, F. R.; Landfester, K. *Chem. Rev.* **2016**, *116*, 2141–2169.

(79) Langmuir, I. *J. Am. Chem. Soc.* **1917**, *39*, 1848–1906.

(80) Evers, W. H.; Goris, B.; Bals, S.; Casavola, M.; de Graaf, J.; Roij, R. Van; Dijkstra, M.; Vanmaekelbergh, D. *Nano Lett.* **2013**, *13*, 2317–2323.

(81) Boneschanscher, M. P.; Evers, W. H.; Geuchies, J. J.; Altantzis, T.; Goris, B.; Rabouw, F. T.; van Rossum, S. a. P.; van der Zant, H. S. J.; Siebbeles, L. D. a.; Van Tendeloo, G.; Swart, I.; Hilhorst, J.; Petukhov, A. V.; Bals, S.; Vanmaekelbergh, D. *Science* **2014**, *344*, 1377–1380.

(82) Wang, F.; Seo, J.; Ma, Z.; Wang, X. *ACS Nano* **2012**, *6*, 2602–2609.

(83) Wang, F.; Seo, J.-H.; Luo, G.; Starr, M. B.; Li, Z.; Geng, D.; Yin, X.; Wang, S.; Fraser, D. G.; Morgan, D.; Ma, Z.; Wang, X. *Nat. Commun.* **2016**, *7*, 10444.

(84) Netzer, N. L.; Dai, F.-R.; Wang, Z.; Jiang, C. *Angew. Chemie Int. Ed.* **2014**, *53*, 10965–10969.

(85) Dai, W.; Shao, F.; Szczerbiński, J.; McCaffrey, R.; Zenobi, R.; Jin, Y.; Schlüter, A. D.; Zhang, W. *Angew. Chemie Int. Ed.* **2016**, *55*, 213–217.

(86) Ruggles, J. L.; Foran, G. J.; Tanida, H.; Nagatani, H.; Jimura, Y.; Watanabe, I.; Gentle, I. R. *Langmuir* **2006**, *22*, 681–686.

(87) Makiura, R.; Motoyama, S.; Umemura, Y.; Yamanaka, H.; Sakata, O.; Kitagawa, H. *Nat. Mater.* **2010**, *9*, 565–571.

(88) Kambe, T.; Sakamoto, R.; Hoshiko, K.; Takada, K.; Miyachi, M.; Ryu, J.-H.; Sasaki, S.; Kim, J.; Nakazato, K.; Takata, M.; Nishihara, H. *J. Am. Chem. Soc.* **2013**, *135*, 2462–2465.

(89) Clough, A. J.; Yoo, J. W.; Mecklenburg, M. H.; Marinescu, S. C. *J. Am. Chem. Soc.* **2015**, *137*, 118–121.

(90) Bauer, T.; Zheng, Z.; Renn, A.; Enning, R.; Stemmer, A.; Sakamoto, J.; Schlüter, A. D. *Angew. Chemie Int. Ed.* **2011**, *50*, 7879–7884.

(91) Sakamoto, R.; Hoshiko, K.; Liu, Q.; Yagi, T.; Nagayama, T.; Kusaka, S.; Tsuchiya, M.; Kitagawa, Y.; Wong, W.-Y.; Nishihara, H. *Nat. Commun.* **2015**, *6*, 6713.

(92) Wittbecker, E. L.; Morgan, P. W. *J. Polym. Sci.* **1959**, *40*, 289–297.

(93) Su, K.; Nuraje, N.; Zhang, L.; Chu, I.-W.; Peetz, R. M.; Matsui, H.; Yang, N.-L. *Adv. Mater.* **2007**, *19*, 669–672.

(94) Nuraje, N.; Su, K.; Yang, N. I.; Matsui, H. *ACS Nano* **2008**, *2*, 502–506.

(95) Jana, M. K.; Murali, B.; Krupanidhi, S. B.; Biswas, K.; Rao, C. N. R. *J. Mater. Chem. C* **2014**, *2*, 6283–6289.

(96) Pfeffermann, M.; Dong, R.; Graf, R.; Zajaczkowski, W.; Gorelik, T.; Pisula, W.; Narita, A.; Müllen, K.; Feng, X. *J. Am. Chem. Soc.* **2015**, *137*, 14525–14532.

(97) Jimenez-Solomon, M. F.; Song, Q.; Jelfs, K. E.; Munoz-Ibanez, M.; Livingston, A. G. *Nat. Mater.* **2016**, *15*, 760–767.

(98) Takada, K.; Sakamoto, R.; Yi, S.-T.; Katagiri, S.; Kambe, T.; Nishihara, H. *J. Am. Chem. Soc.* **2015**, *137*, 4681–4689.

(99) Huang, X.; Sheng, P.; Tu, Z.; Zhang, F.; Wang, J.; Geng, H.; Zou, Y.; Di, C.; Yi, Y.; Sun, Y.; Xu, W.; Zhu, D. *Nat. Commun.* **2015**, *6*, 7408.

(100) Matsuoka, R.; Sakamoto, R.; Kambe, T.; Takada, K.; Kusamoto, T.; Nishihara, H. *Chem. Commun.* **2014**, *50*, 8137.

# Chapter 2

# Bis(dipyrrinato)metal(II) One-dimensional Coordination Polymers

# 2-1 Introduction

## 2-1-1 One-dimensional coordination polymers

Coordination polymers (CPs) are infinite structures based on the combination of metal ions and ligands. Their bottom-up fabrication from constituents allows diversity in both composition and physical properties. In addition, their syntheses are often by self-assembly. In the last decade, a considerable number of CPs have been reported expecting potential applicability in electronics,[1–3] optics,[4,5] and magnetic devices.[6,7]

Two- and three-dimensional CPs such as coordination nanosheets (CONASHs),[8–10] metal-organic frameworks (MOFs),[11–13] and porous coordination polymers (PCPs)[14–16] have attracted intense interest. On the other hand, the physical flexibility of one-dimensional coordination polymers (1D CPs) makes them useful for conjugation with micro and nano-sized functional materials such as carbon nanotubes,[17–19] although difficulties in handling have prevented 1D CPs from widespread application. Many 1D coordination chains are stable only in the solid phase, and they dissociate into constitutive ligands and metals readily in solution. Furthermore, 1D CPs tend to aggregate randomly and amorphously, and there are few examples of 1D CPs where both crystalline phase and isolated single chain phase coexist.[4,20,21]

## 2-1-2 Dipyrrin and its 1D CPs

Dipyrrin, or dipyrromethane, is a compound composed of two pyrrole rings bridged with a methine carbon atom. Its structure is also called as half-porphyrin, and works as a mono-valent bidentate ligand. Due to the π-conjugation extending across the whole molecule, dipyrrin exhibits strong visible-light absorption (and sometimes fluorescence) assignable to π-π* transition both in a free-base and metal complex. Therefore, dipyrrins, their complexes, and their diverse derivatives have been the subject of intense research over 70 years.[22,23]

The dipyrrin-metal complex is an attractive molecular motif for coordination polymers. Dipyrrin ligands accept various metal ions, and in most cases the complexation reaction proceeds spontaneously even in the absence of a base. This feature is desirable for synthesizing supramolecules[24,25] and coordination polymers.[26–28] However, no 1D CP based on the dipyrrin-metal complex has demonstrated crystallinity, single-chain isolation, and potential applicability at the same time.

In the present work, I synthesize 1D CP **MCP** featuring the bis(dipyrrinato)metal(II) complex motif, which is composed of bridging dipyrrin ligand 5,5′-(2,3,5,6-tetramethyl-1,4-phenylene)bis((3,5-dimethyl-2H-pyrrol-2-ylidene)methylene))bis(2,4-dimethyl-1H-pyrrole) **L1** and divalent metal ion $\mathbf{M}^{2+}$ (**M** = Zn, Ni, and Cu, Fig. 2-1a). A liquid/liquid interfacial reaction is effective for ordering **MCP**, giving rise to single crystals suitable for X-ray diffraction analysis (XRD). Single fibers of **ZnCP** are isolated from the single crystal upon ultrasonication, and then visualized by atomic force microscopy (AFM). The dispersibility of the exfoliated fibers of **ZnCP** affords good processability, giving rise to a conjugate with single-wall carbon nanotubes (SWCNTs), and a thin film of **ZnCP** on a transparent $SnO_2$ electrode. These processed materials may be applied in thermo- and photoelectric conversion systems, thereby demonstrating the utility of **ZnCP** (Fig. 2-1b).

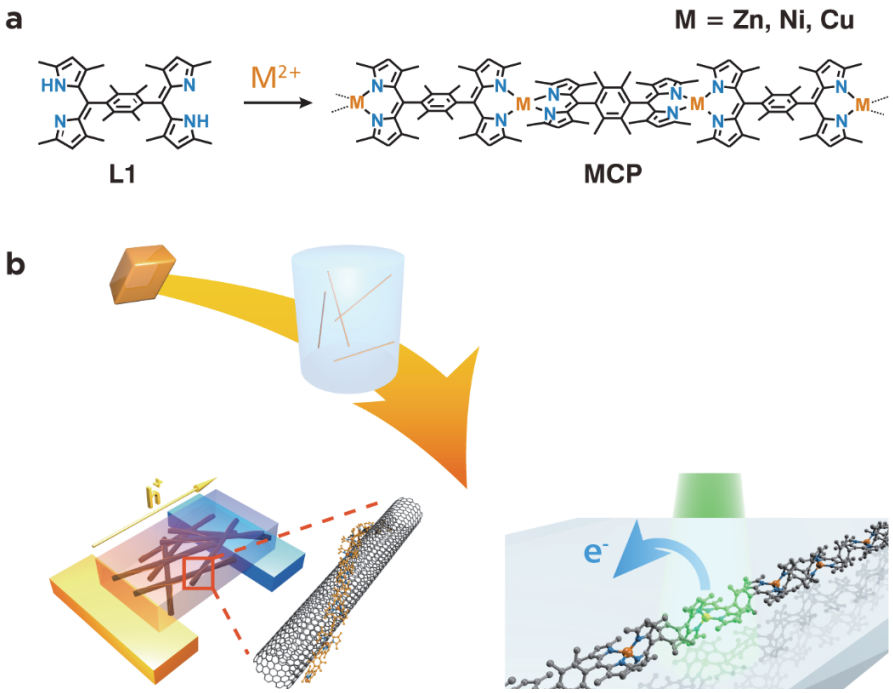


**Figure 2-1 | Concept of this research on Metal(II) Bis(dipyrrinate) 1D CPs**. **a**, Chemical structures of bridging dipyrrin ligands **L1** and corresponding 1D CPs **MCP** (**M** = Zn, Ni, Cu). **b**, Schematic illustration of the synthesis, crystallization, exfoliation into isolated single fibers of **MCP**, and its application to electric conversion systems.

## 2-2 Experimental Section

### 2-2-1 Materials

All chemicals were purchased from Tokyo Chemical Industry Co., Ltd., Kanto Chemical Co., or Wako Pure Chemical Industries, Ltd., unless otherwise stated. They were used without further purification, except for $Zn(OAc)_2{\cdot}2H_2O$, which was recrystallized from water. Water was purified using a Milli-Q purification system (Merck KGaA). HOPG was purchased from Alliance Biosystems, Inc. (Grade SPI-1, 10 ×10 × 2 mm) and was cleaved with adhesive tape just before use. Tranparent $SnO_2$ electrode (on ITO-coated glass, 5 Ω $sq^{-1}$) was purchaced from Geomatec co., ltd. It was sonicated in acetone (10 min), and nonionic detergent (white 7-P, UI Kasei Co., Ltd.) in water (30 min×2). Then the substrate was washed with water till the bubble of the detergent disappeared, and sonicated in water (10 min). The cleaned substrate was stored in water, and dried by nitrogen blow just prior to use. **Ac-Zn$_{mono}$** was synthesized according to the method described previously.[29] SWCNTs (HP-grade, >80% carbon purity, diameter 1.0–1.4 nm, length 5–50 μm, semiconductor content >80%) were purchased from KH Chemicals Co., Ltd. 2-((3,5-Dimethyl-2H- pyrrol-2-ylidene)(2,6-dimethylphenyl)methyl)-3,5-dimethyl-1H-pyrrole (**L$_{mono}$**) was prepared according to the method described previously.[30]

### 2-2-2 Syntheses

**Mononuclear bis(dipyrrinato)zinc(II) complex (Zn$_{mono}$).**

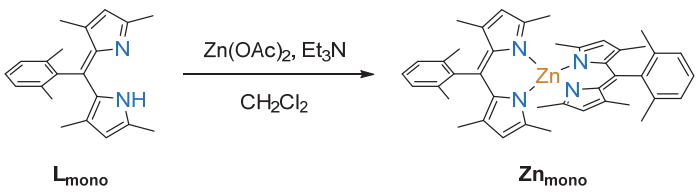


Zinc(II) acetate (36.7 mg, 0.200 mol) and triethylamine (0.11 mL, 0.79 mmol) were added to a dichloromethane solution (20 mL) of 2-((3,5-dimethyl-2H-

pyrrol-2-ylidene)(2,6-dimethylphenyl)methyl)-3,5-dimethyl-1H-pyrrole, $\mathbf{L_{mono}}$[30] (122 mg, 0.401 mmol), and the reaction mixture was stirred overnight at room temperature. Methanol (20 mL) was added to recrystallize the product as an orange solid (60.5 mg, 45.0%). $^{1}$H NMR (500 MHz, $CDCl_3$): δ = 7.21 (t, *J* = 7.6 Hz, 2H), 7.11 (d, *J* = 7.6 Hz, 4H), 5.91 (s, 4H), 2.16 (s, 12H), 2.04 (s, 12H), 1.28 (s, 12H); $^{13}$C NMR (125 MHz, $CDCl_3$): δ = 156.07, 143.26, 143.06, 139.18, 135.95, 134.27, 127.98, 127.88, 119.74, 19.33, 16.13, 14.70; HR-FAB-MS: 670.3011 $[M]^+$, calcd. for: $C_{42}H_{46}N_4Zn^+$: 670.3014.

**5,5'-(2,3,5,6-tetramethyl-1,4-phenylene)bis((3,5-dimethyl-2*H*-pyrrol-2-ylidene)methylene))bis(2,4-dimethyl-1*H*-pyrrole) (L1) .**

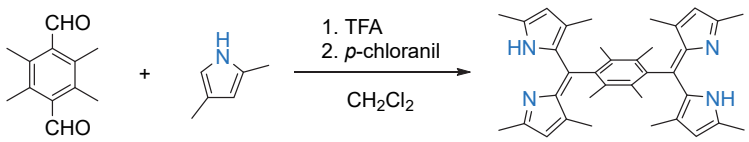


**L1**

2,3,5,6-Tetramethylterephthalaldehyde (457 mg, 2.4 mmol), 2,4-dimethylpyrrole (1.0 mL, 9.7 mmol), and trifluoroacetate (10 μL) were added to dry dichloromethane (100 mL), and the resultant solution was stirred overnight in the dark at room temperature. Then, *p*-chloranil (1.182 g, 4.8 mmol) was added, and the reaction mixture was stirred for 2 h. After removal of the solvent under reduced pressure, the crude product was purified by alumina column chromatography (Eluent: hexane:dichloromethane = 1:1, then dichloromethane). The yellow–orange band was collected and evaporated under reduced pressure to give a brown powder, which was recrystallized further from dichloromethane and hexane to give **L1** as a brown–orange powder (642 mg, 50%). $^{1}$H NMR (400 MHz, $CDCl_3$): δ = 13.89 (br, 2 H), 5.85 (s, 4 H), 2.36 (s, 12 H), 2.15 (s, 12 H), 1.56 (s, 12 H); $^{13}$C NMR (100 MHz, $CDCl_3$): δ =151.1, 139.5, 139.0, 137.2, 136.0, 133.1, 118.7, 17.1, 16.1, 15.6; HR-FAB-MS: 531.3484 $[M+H]^+$, calcd. for: $C_{36}H_{43}N_4^+$: 531.3482.

**Bis(dipyrrinato)zinc(II) one-dimensional coordination polymer (ZnCP) by means a single-phase reaction.**

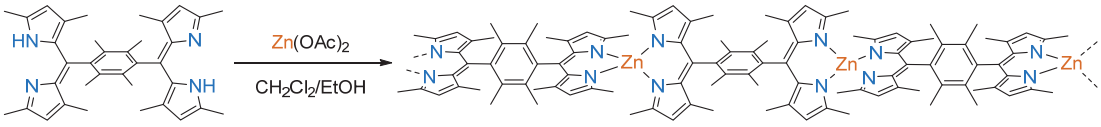


L1 ZnCP

An ethanol solution of zinc(II) acetate (2.6 mg, 12 μmol) was added dropwise to a dichloromethane solution (25 mL) of **L1** (5.6 mg, 11 μmol) over a period of 30 min. After stirring for 1 d at room temperature, the resulting orange precipitate was filtered, washed with dichloromethane and ethanol, and dried under a reduced pressure to give **ZnCP** as a dark-orange powdery solid (5.0 mg, 80%). The formation of **ZnCP** was confirmed by XPS, disclosing a nitrogen-to-zinc abundance ratio of 79.8 : 20.2 (calcd. 4 : 1, Fig. 2-5a).

**Bis(dipyrrinato)nickel(II) one-dimensional coordination polymer (NiCP) by means a single-phase reaction.**

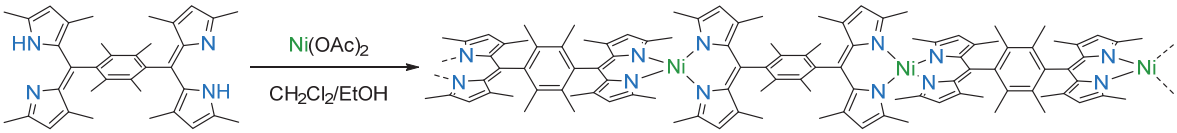


L1 NiCP

The same procedure as **ZnCP** was employed, except for nickel(II) acetate as the metal source, to give a dark-red solid (3.0 mg, 51%). The formation of **NiCP** was confirmed by XPS, disclosing a nitrogen-to-nickel abundance ratio of 80.2 : 19.8 (calcd. 4 : 1, Fig. 2-5c).

**Bis(dipyrrinato)copper(II) one-dimensional coordination polymer (CuCP) by means a single-phase reaction.**

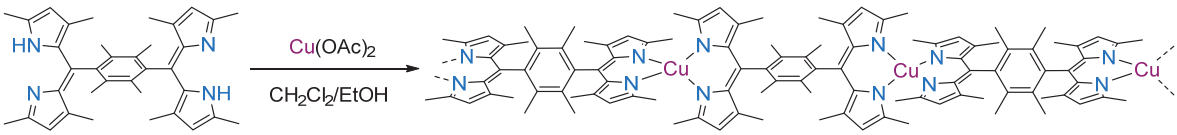


L1 CuCP

The same procedure as **ZnCP** was employed, except for copper(II) acetate as the metal source, to give a green solid (4.8 mg, 81%). The formation of **CuCP** was confirmed by XPS, disclosing a nitrogen-to-nickel abundance ratio of 80.3 : 19.7 (calcd. 4 : 1, Fig. 2-5d).

**Bis(dipyrrinato)zinc(II) one-dimensional coordination polymer (ZnCP) by means of a liquid/liquid interfacial reaction.**

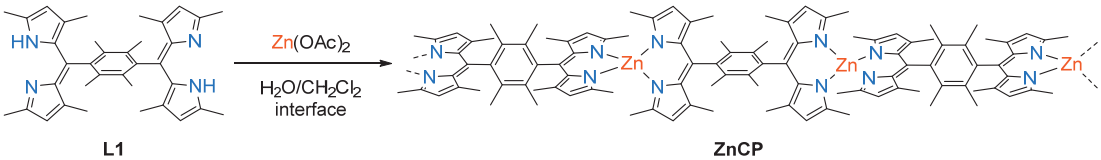


**L1** (1.5 mg) was added to dichloromethane (10 mL) in a glass cylinder with a diameter of 40 mm, to obtain a solution with a concentration of 0.28 mM. The dichloromethane solution was then covered with pure water (10 mL), such that a two-phase system was formed. An aqueous solution (10 mL) of zinc(II) acetate (50 mM) was added gently to the water phase. The reaction system was kept undisturbed for 30 d in the dark, and **ZnCP** was observed as orange crystals floating on the interface, or sinking at the bottom of the reaction container. The crystals were collected by filtration.

**Bis(dipyrrinato)nickel(II) one-dimensional coordination polymer (NiCP) by means of a liquid/liquid interfacial reaction.**

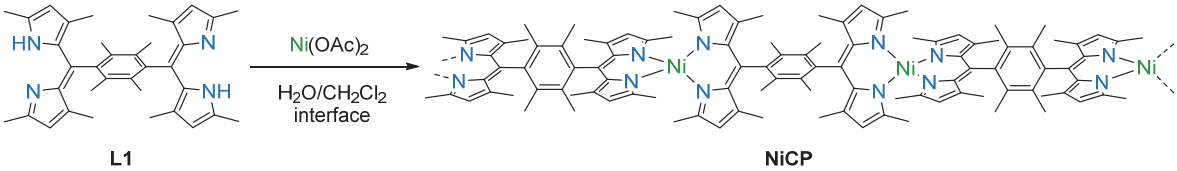


The same procedure as **ZnCP** was employed, except for nickel(II) acetate as the metal source, and 90 d as the reaction time. **NiCP** was obtained as orange crystals floating on the interface, or sinking at the bottom of the reaction container.

**Bis(dipyrrinato)copper(II) one-dimensional coordination polymer (CuCP) by means of a liquid/liquid interfacial reaction.**

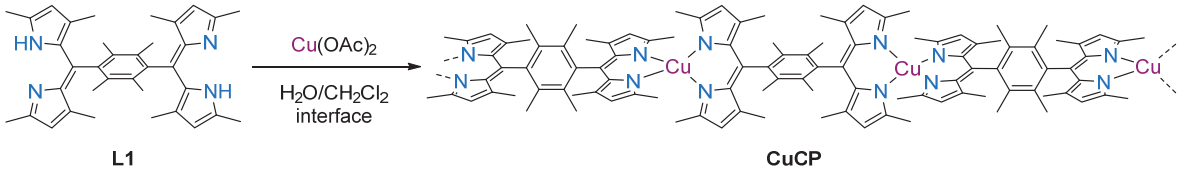


The same procedure as **ZnCP** was employed, except for copper(II) acetate as the metal source, and 20 d as the reaction time. **CuCP** was obtained as dark-green crystals floating on the interface, or sinking at the bottom of the reaction container.

**Synthesis of a conjugate of ZnCP and SWCNTs (ZnCP-SWCNT).**

Crystals of **ZnCP** (0.1 mg) and SWCNTs (1 mg) were suspended in DMF (10 mL) by ultrasonication (38 kHz, 80 W) for 90 min. The orange suspension was then shaken using a laboratory shaker (300 oscillation/min) for 24 h, which resulted in the disappearance of the orange color derived from **ZnCP**: This change indicates that **ZnCP** was adsorbed onto SWCNTs. The residue was filtered using a polytetrafluoroethylene membrane filter (pore size: 450 nm), washed thoroughly with DMF and dichloromethane to remove small molecules, and dried under a reduced pressure at 80°C, to produce a round, thin disk of **ZnCP-SWCNT** 1 cm in diameter and 64 μm thick. A film of pristine SWCNTs was fabricated using the same method, with DMSO as a solvent and without **ZnCP**, and a disk 1 cm in diameter and 86 μm thick was obtained.

## 2-2-3 Instruments and experimental methods

**Instrumentation.**

$^{1}$H and $^{13}$C NMR data were collected in $CDCl_3$, and were recorded on a Bruker DRX 500, a JEOL ECX-500, and a Bruker US500 spectrometer. Tetramethylsilane ($\delta_H$ = 0.00) was used as

an internal standard for the $^{1}H$ NMR spectra, and $CDCl_3$ ($\delta_C$ = 77.00) was used as an internal standard for the $^{13}C$ NMR spectra. High-resolution fast-atom bombardment mass spectroscopy (HR-FAB-MS) was performed on a JEOL JMS-700 MStation mass spectrometer. XPS data were acquired using an ULVAC-PHI PHI 5000 VersaProbe spectrometer. Al Kα (15 kV, 25 W) was used as the X-ray source, and the beam was focused on a 100 $\mu m^2$ area. The spectra were analyzed using MultiPak Software and standardized using the C 1s peak at 284.6 eV. AFM measurements were carried out using an Agilent Technologies 5500 scanning probe microscope under ambient conditions in high-amplitude mode (tapping mode) with a silicon cantilever Nano World PPP-NCL probe. UV–vis spectra were recorded on a JASCO V-570 spectrometer. Fluorescence spectrum was collected with a HITACHI F-4500 spectrometer. Absolute photo luminescent quantum yields were measured by a Hamamatsu Photonics C9920-02G. TEM images were recorded at an accelerating voltage of 300 kV using a JEOL JEM-3100FEF. Raman spectra were recorded on a JASCO NRS-5100. Electrochemical measurements were carried out using ALS 650DT electrochemical analyzer (BAS. Co., Ltd.). A homemade $Ag^+$/Ag reference electrode (0.01 M $AgClO_4$ in 0.1 M $Bu_4NClO_4$/acetonitrile) and a Pt wire counter electrode were implemented in order to establish a three-electrode system. $Bu_4NClO_4$, acting as a supporting electrolyte, was recrystallised from EtOH and put under vacuum for 24 h. Ferrocene was used as an internal standard.

### X-ray crystallography.

Single-crystal X-ray diffraction (XRD) data for **MCP** were collected at 100 K. The diffractions were recorded on a large cylindrical imaging plate with synchrotron radiation of $\lambda$ = 0.7000 Å at SPring-8 beam line BL02B1 (Hyogo, Japan).[31] The structures were solved by direct methods using SIR-92,[32] and were refined by the full-matrix least-squares techniques against $F^2$ implementing SHELXL-2013.[33] CCDC 1012353 (for **ZnCP**), 1044669 (for **NiCP**), and 1044670 (for **CuCP)** contain the supplementary crystallographic data for this paper. These

data may be obtained free of charge from The Cambridge Crystallographic Data Centre via www.ccdc.cam.ac.uk/data_request/cif.

### DFT calculation.

In order to estimate the heights of **ZnCP**, A DFT calculation for $\mathbf{Zn_{mono}}$ was carried out. The Gausian 09 program[34] was used for the geometrical optimization. The structures were optimised without any symmetry constraint. The B3LYP hybrid exchange-correlation functional[35] was employed. The LanL2DZ basis set[36] was used for the Zn atoms, and the 6-31G(d) basis set[37] for the other atoms. Visualization of the result was performed using GaussView 5.0.8 software[38].

### Thermoelectric conversion properties.

The DC electrical conductivity was measured using a Mitsubishi Chemical Loresta GP MCP-T610 with the four-point probe method. The thermoelectric voltage was recorded using a Seebeck coefficient measurement system K20SB100-3R (MMR technology) equipped with a Joule-Thomson effect temperature controller. The buckypaper films were transferred onto the sample stage of the measurement system, and silver paste was used to create the electrical connection.

### Photoelectric conversion.

A dispersion of **ZnCP** in acetonitrile was dropcasted on a transparent $SnO_2$ electrode, so that the coordination polymer was deposited in the range of a 5mmϕ circle. The polymers deposited on the $SnO_2$ electrodes were always subjected to UV/vis spectroscopy prior to photoelectric conversion. The modified $SnO_2$ electrode was used as a working electrode (photoanode). An $Ag^+/Ag$ reference electrode (0.01 M $AgClO_4$ in 0.1 M $Bu_4NClO_4$/acetonitrile) and a Pt wire counter electrode were implemented in order to establish

a three-electrode system. The three electrodes were built into a photoelectrochemical cell shown in Fig. 2-16. The cell was filled with an acetonitrile solution of tetrabutylammonium perchlorate (0.1 M, as a supporting electrolyte) containing triethanolamine (TEOA, 0.05 M, as a sacrificial donor reagent). The photoelectrochemical cell was sealed, and was deoxygenized by Ar bubbling for 5 min prior to a measurement. Monochromatic light for the action spectra shown in Fig. 2-17b (430–600 nm in every 10 nm) was extracted from Xe lamp (MAX-302, Asahi Spectra Co., Ltd.), the photon flux of which was monochromated by a monochrometer (CT-10, JASCO Corporation). For the photocurrent responses shown in Fig. 2-17a and 2-19c, monochromic light was provided by the Xe lamp equipped with a band-pass filter (500 nm). The active area of the electrode was 0.264 $cm^2$, which was determined by a fluorocarbon rubber o-ring. The electrode potentials were controlled using an electrochemical analyzer (ALS 750A, BAS Inc.). The potential of the photoanode was fixed at near the open circuit potential (−0.35 V vs $Ag^+/Ag$) such that a negligible dark current was observed. The photocurrent was also collected through the electrochemical analyzer. A photon counter (8230E and 82311B, ADC Corporation) was employed to quantify the photon flux of the incident light.

## 2-3 Results and Discussion

### 2-3-1 Single-phase synthesis of bulk MCP

Initially, a conventional single-phase reaction was performed to synthesize **MCP** (**M** = Zn, Cu, and Ni, Fig. 2-2a). Equimolar amounts of bridging dipyrrin ligand **L1** and metal(II) acetate were reacted in a mixture of dichloromethane and ethanol. The reaction mixture was stirred at room temperature for 1 day, leading to the spontaneous complexation of divalent metal ions with the bidentate dipyrrin ligand. This process resulted in precipitation of **MCP** as an insoluble powder. The obtained powders were collected by filtration and washed with ethanol and dichloromethane. As depicted in Fig. 2-2b–d, the powders of **ZnCP**, **CuCP**, and **NiCP** are dark-orange, green, and red in color, respectively.

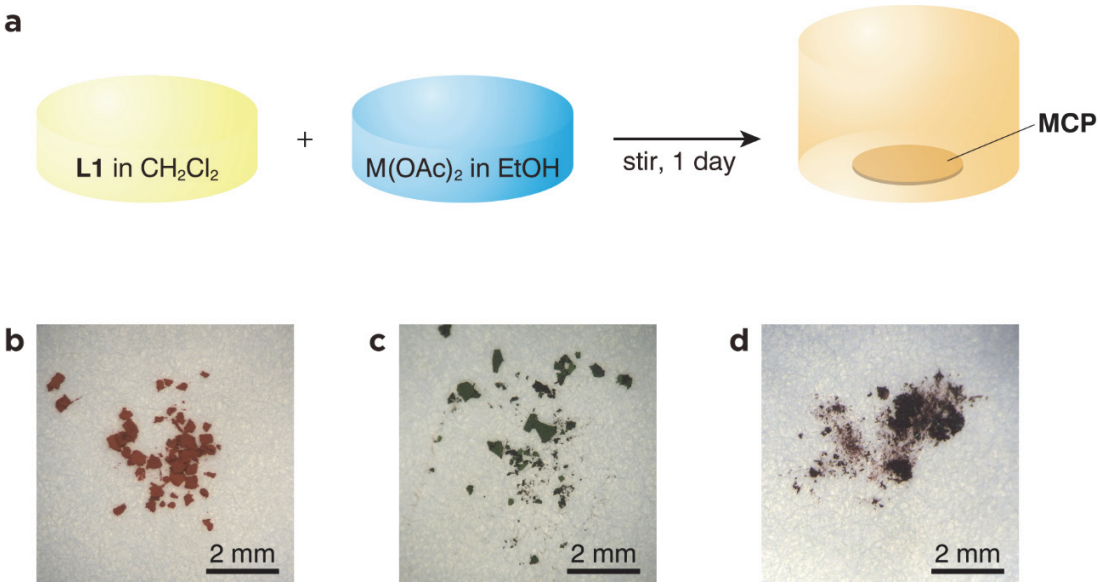


**Figure 2-2 | Single-phase syntheses of MCP**. **a**, Schematic illustration of the syntheses. **b–d**, Photographs of powdery **ZnCP** (**b**), **CuCP** (**c**), and **NiCP** (**d**).

## 2-3-2 Spectroscopic characterization of MCP

The elemental composition and chemical bonding of **MCP** were analyzed by X-ray photoelectron spectroscopy (XPS) and UV/vis absorption spectroscopy. For XPS, the powders of **MCP** were placed on a double-sided adhesive carbon tape. The XPS survey spectrum of **MCP** displays the presence of four elements: carbon, nitrogen, oxygen and the metal corresponding to each metal(II) source (Fig. 2-3). The presence of both nitrogen and the metal elements indicates the inclusion of both **L1** and metal(II) ions in the powders of **MCP**.

The chemical environment of elements in **ZnCP** was inspected by high-resolution XPS using **L1** and mononuclear bis(dipyrrinato)zinc(II) complex $\mathbf{Zn_{mono}}$ as references (Fig. 2-4). The Zn 2p 3/2 peak is only visible in $\mathbf{Zn_{mono}}$ and **ZnCP**, which is consistent with the presence of zinc ions. Another distinctive fingerprint of the coordination between the dipyrrin ligand and zinc(II) ions occurs in the N 1s region. Free base **L1** features two peaks (397.5 and 399.1 eV) arising from the iminic and pyrrolic nitrogens that are chemically different from one another.[39] In contrast, $\mathbf{Zn_{mono}}$ shows a single N 1s peak, which stems from the homogenization of the two nitrogen atoms upon coordination to the zinc center. A solitary N 1s peak is also observed for **ZnCP**. In addition, the nitrogen-to-zinc abundance ratio calculated from the peak area corrected by the photoionization cross-section is consistent with the ideal value of N:Zn = 4:1 (79.8:20.2 and 79.5:20.5 for **ZnCP** and $\mathbf{Zn_{mono}}$, respectively). Likewise, the nitrogen-to-copper and nitrogen-to-nickel abundance ratio of **CuCP** and **NiCP** are 80.3 : 19.7 and 80.2 : 19.8, respectively, both consistent with the chemical composition of the corresponding coordination polymers (N:Cu and N:Ni = 4:1, Fig. 2-5). These results indicate the formation of the desired coordination polymer **MCP** consisting of the bis(dipyrrinato)metal(II) complex.

The presence of the bis(dipyrrinato)metal(II) complex motif was also confirmed by UV/vis absorption spectroscopy (Fig. 2-6). For this measurement, **ZnCP** was dispersed in *N*,*N*-dimethylformamide (DMF) by ultrasonication, while **L1** and $\mathbf{Zn_{mono}}$ were dissolved in the same solvent. An intense absorption with a maximum at 445 nm in **L1** stems from the $^{1}\pi$–$\pi^{*}$

transition of the free-base dipyrrin moiety.[40] However, the $^{1}\pi$–$\pi^{*}$ band is red-shifted by 44 nm in $\mathbf{Zn_{mono}}$ (489 nm), which is typical of zinc(II) complexation with a dipyrrin ligand.[40] The $^{1}\pi$–$\pi^{*}$ band of **ZnCP** has the same absorption maximum (489 nm) as that of $\mathbf{Zn_{mono}}$, which also shows that **ZnCP** formed the bis(dipyrrinato)zinc(II) coordination polymer.

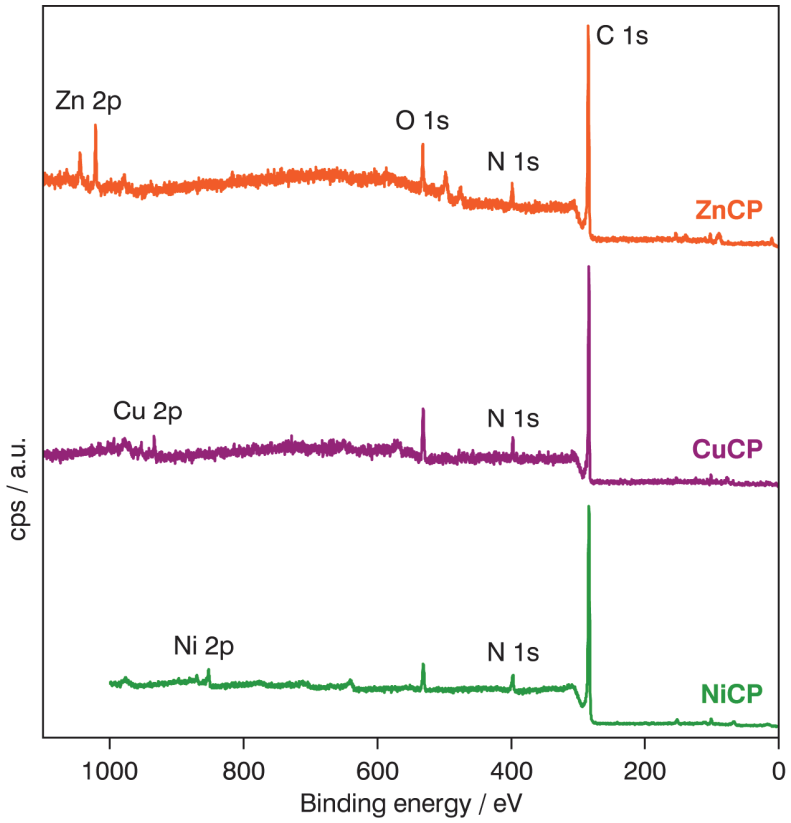


**Figure 2-3 | Survey XPS of MCP**. XPS of **ZnCP** (orange), **CuCP** (purple), and **NiCP** (green).

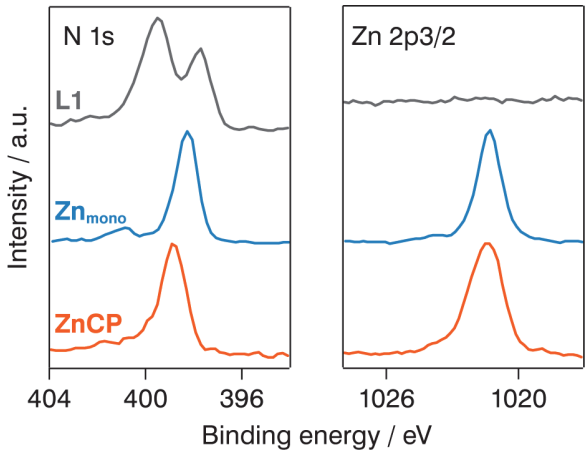


**Figure 2-4 | High-resolution XPS.** XPS of **L1** (gray), **Zn$_{mono}$** (blue), and **ZnCP** (orange) focusing on the N 1s and Zn 2p 3/2 regions.

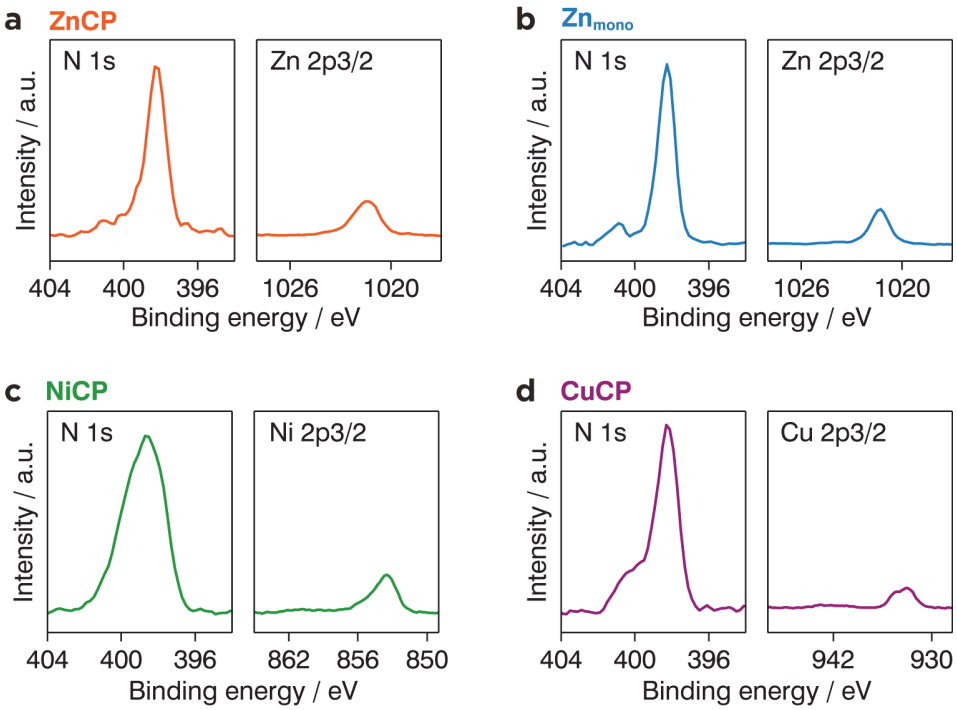


**Figure 2-5 | High-resolution XPS of ZnCP, Zn$_{mono}$, NiCP, and CuCP.** XPS of (**a**) **ZnCP** focusing on the N 1s and Zn 2p 3/2 regions, (**b**) **Zn$_{mono}$** focusing on the N 1s and Zn 2p 3/2 regions, (**c**) **NiCP** focusing on the N 1s and Ni 2p 3/2 regions, and (**d**) **CuCP** focusing on the N 1s and Cu 2p 3/2 regions. The baselines were corrected and the intensity was corrected by the photoionization cross-section.

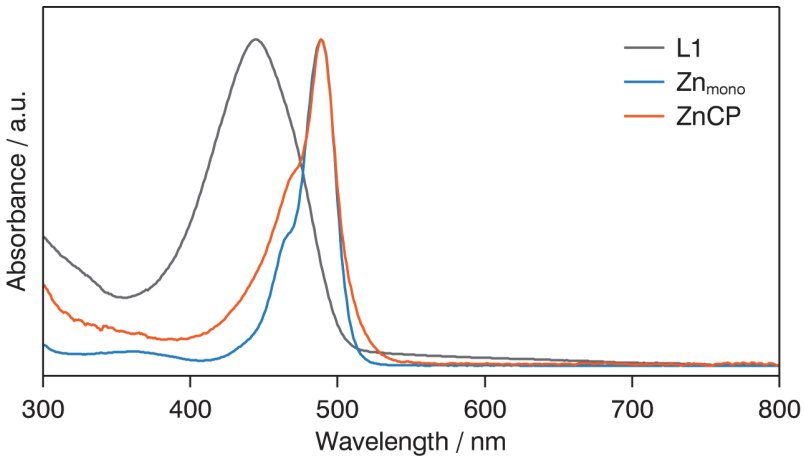


**Figure 2-6 |** UV/vis spectra of **L1** (gray), **Zn$_{mono}$** (blue), and **ZnCP** (orange) in DMF.

### 2-3-3 Liquid/liquid interfacial synthesis of MCP

I next attempted to produce **MCP** at the interface between two immiscible liquids. The upper aqueous layer contained metal(II) acetate (**M**$(OAc)_2$, **M** = Zn, Ni, and Cu, Fig. 2-7a); the lower dichloromethane layer contained the bridging dipyrrin ligand **L1**. The organic layer was initially overlaid with pure water, which allowed the liquid/liquid interface to remain still while the aqueous solution was added. This process allowed us to circumvent a random encounter between **L1** and divalent metal ions $\mathbf{M}^{2+}$. Under a static condition, the successive coordination reaction led to the growth of 1D polymeric chain, giving rise to small crystals of **MCP** that floated on the liquid/liquid interface or sank to the bottom of the reaction container (Fig. 2-7b). Photographs of a typical single crystals for **MCP** are shown in Fig. 2-7c–e. The crystals of **ZnCP**, **CuCP**, and **NiCP** are orange, green, and reddish orange in color, respectively, consistent with those of powdery **MCP**. This series of crystals was analyzed by synchrotron radiation X-ray diffraction (Fig. 2-8 and Table 2-1–3). The crystal structures are almost identical to each other for the three metal centers. They show the desired 1D polymeric chains, propagating along the [1 0 −1] crystallographic axis. The metal centers adopt slightly distorted tetrahedral coordination spheres with dihedral angles of 81.29°, 81.11°, and 87.36° for Zn, Ni, and Cu, respectively. The average metal-nitrogen bond lengths are, respectively, 1.9181, 1.9151, and 1.9032 Å for Zn, Ni, and Cu. This series of dihedral angles and metal-nitrogen bond lengths are typical of bis(dipyrrinato)metal(II) complexes bearing α-methylated dipyrrin ligands.[40,41] Divalent nickel and copper generally prefer square-planar coordination spheres, though, the methyl group at the α-position induces tetrahedral coordination spheres even to the Ni and Cu centers because of steric hindrance. The dipyrrinato ligand is orthogonal to the bridging 2,3,4,5-tetramethylphenyl group with dihedral angles of 101.18°, 100.02°, and 98.93° for Zn, Ni, and Cu, respectively, reflecting steric hindrance between the two moieties.

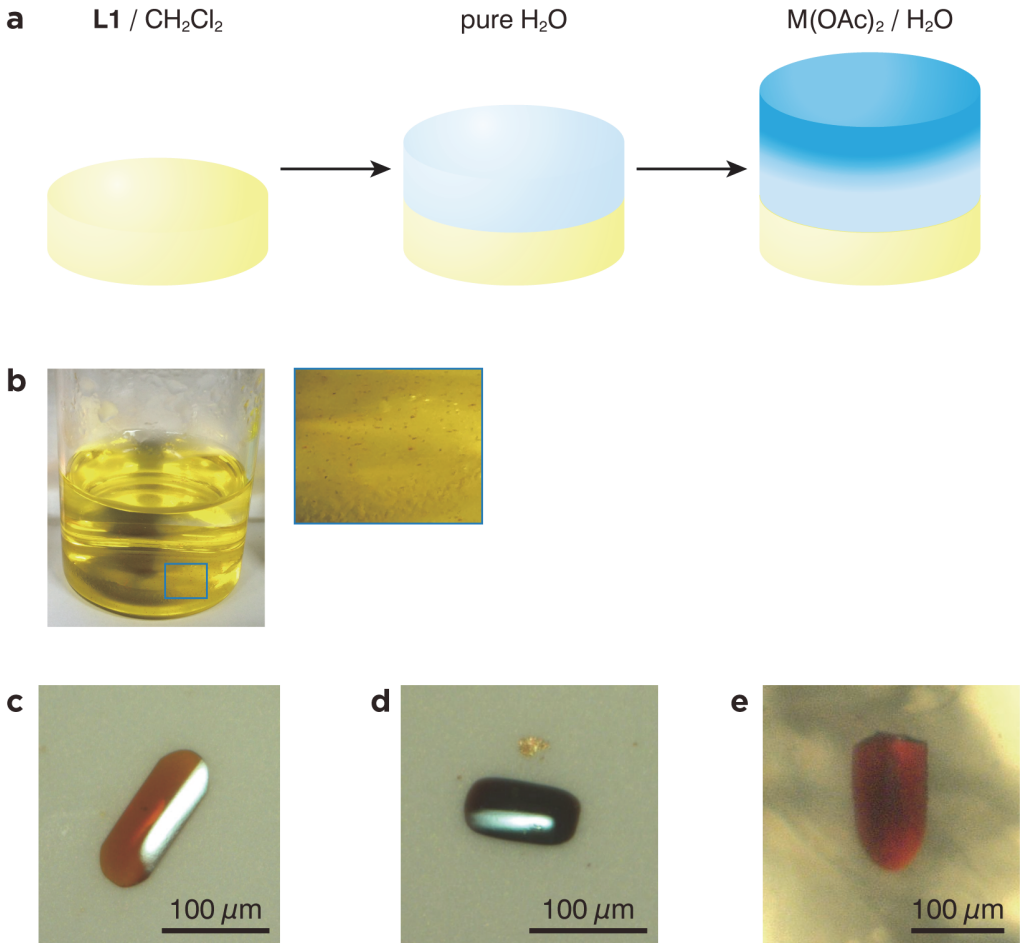


**Figure 2-7 | Liquid/liquid interfacial syntheses and crystal structures of MCP. a**, Schematic illustration of the liquid/liquid interfacial synthesis for **MCP**. **b,** Photograph of the reaction system after the emergence of single crystals of **ZnCP** (left) and close-up image at the liquid/liquid interface (blue square, right). **c–e**, Photographs of typical single crystals of **ZnCP** (**c**), **CuCP** (**d**), and **NiCP** (**e**).

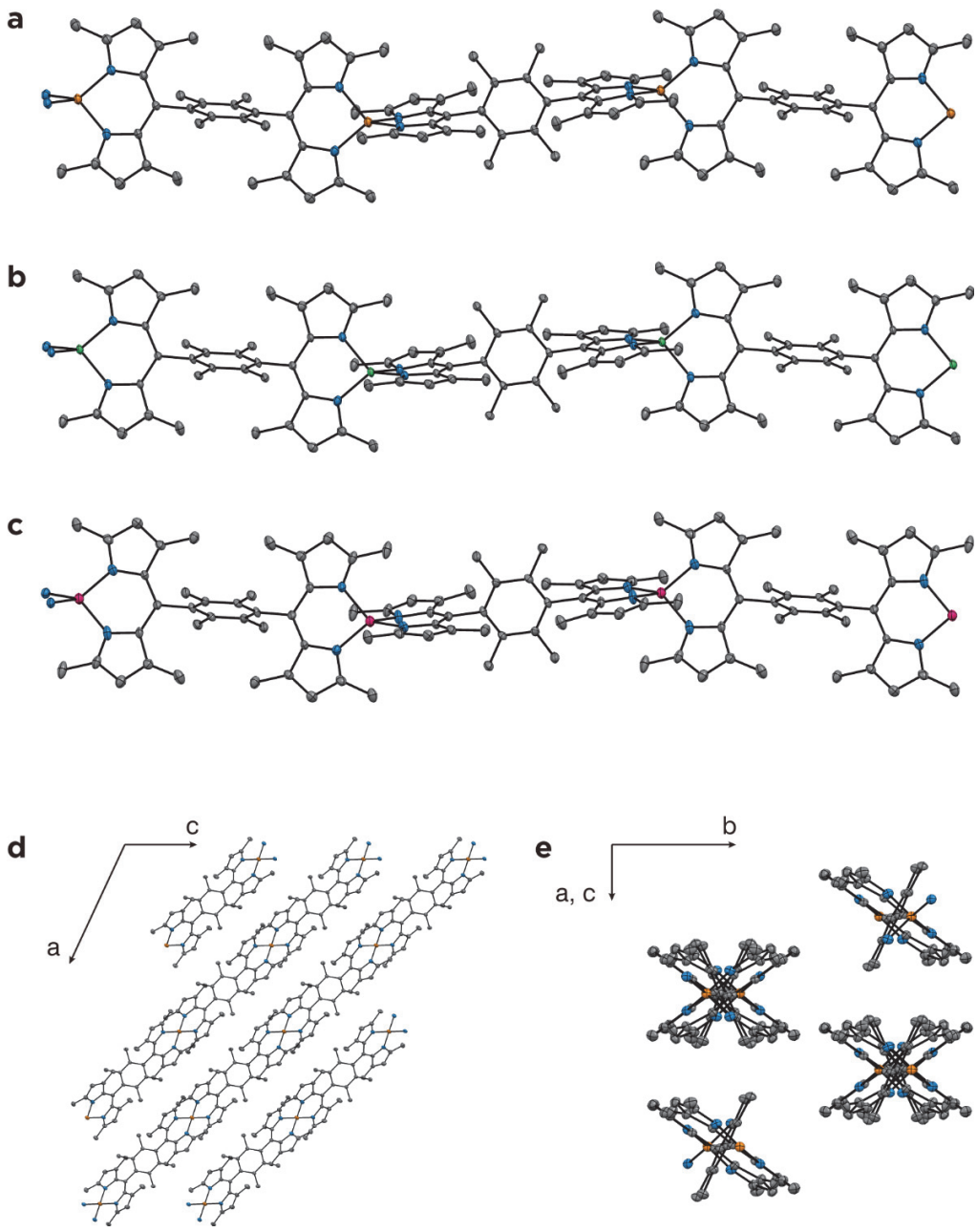


**Figure 2-8 | Crystal structures. a–c**, ORTEP drawing of **ZnCP** (**a**), **NiCP** (**b**), and **CuCP** (**c**) with a thermal ellipsoid set at the 50% probability level (C, gray; N, blue; Zn, orange; Ni, green; Cu, purple). Hydrogen atoms are omitted for clarity. **d,e,** Perspective views of 3D packing of **ZnCP** along the b (**d**) and [1 0 –1] (**e**) crystallographic axes, respectively.

**Table 2-1** Crystallographic data of **ZnCP**.

| | |
|---|---|
| Empirical formula | $C_{36}H_{40}N_4Zn_{0.5}$ |
| Formula weight | 561.40 |
| Temperature | 100(2) K |
| Wavelength | 0.7000 Å Crystal |
| system | Monoclinic |
| Space group | C2/c (no. 15) |
| Unit cell dimensions | $a$ = 18.8182(4) Å, $\alpha$ =90° |
| | $b$ = 15.9892(3) Å, $\beta$ = 114.760(8)° |
| | $c$ = 10.4062(2) Å, $\gamma$ =90° |
| Volume ($V$) | 2843.26(19) Å$^3$ |
| Z | 4 |
| Density (calculated) | 1.311 g/cm$^3$ |
| Absorption coefficient | 0.430 mm$^{-1}$ |
| F(000) | 1196 |
| Crystal size | 0.15 × 0.07 × 0.01 mm$^3$ |
| Theta range for data collection | 2.317 to 35.683° |
| Index ranges | -37<=h<=30, -24<=k<=28, -18<=l<=20 |
| Reflections collected | 67,218 |
| Independent reflections | 6,635 ($R_{int}$ = 0.0451) |
| Completeness to theta = 24.835° | 100.0% |
| Refinement method | Full-matrix least-squares against $F^2$ |
| Data / restraints / parameters | 6635 / 0 / 190 |
| Goodness-of-fit on $F^2$ | 0.995 |
| Final $R$ indices [$I$ >2σ($I$)] | $R_1$ = 0.0529, $wR_2$ = 0.1394 |
| $R$ indices (all reflections) | $R_1$ = 0.0653, $wR_2$ = 0.1500 |
| Largest diff. peak and hole | 0.617 and -0.641 eÅ$^{-3}$ |

**Table 2-2** Crystallographic data of **CuCP**.

| | |
|---|---|
| Empirical formula | $C_{36}H_{40}N_4Cu_{0.5}$ |
| Formula weight | 560.49 |
| Temperature | 100(2) K |
| Wavelength | 0.7000 Å Crystal |
| system | Monoclinic |
| Space group | C2/c (no. 15) |
| Unit cell dimensions | $a$ = 18.8080(8) Å, $\alpha$ =90° |
| | $b$ = 16.1023(7) Å, $\beta$ = 115.201(8)° |
| | $c$ = 10.3382(4) Å, $\gamma$ =90° |
| Volume ($V$) | 2832.9(3) Å$^3$ |
| Z | 4 |
| Density (calculated) | 1.314 g/cm$^3$ |
| Absorption coefficient | 0.386 mm$^{-1}$ |
| F(000) | 1194 |
| Crystal size | 0.09 × 0.07 × 0.01 mm$^3$ |
| Theta range for data collection | 1.715 to 27.496° |
| Index ranges | -31<=h<=31, -26<=k<=25, -17<=l<=17 |
| Reflections collected | 39,666 |
| Independent reflections | 3,319 ($R_{int}$ = 0.0787) |
| Completeness to theta = 24.835° | 98.9% |
| Refinement method | Full-matrix least-squares against $F^2$ |
| Data / restraints / parameters | 3319 / 0 / 189 |
| Goodness-of-fit on $F^2$ | 0.891 |
| Final $R$ indices [$I$ >2σ($I$)] | $R_1$ = 0.0570, $wR_2$ = 0.0975 |
| $R$ indices (all reflections) | $R_1$ = 0.0818, $wR_2$ = 0.1169 |
| Largest diff. peak and hole | 0.399 and -0.525 eÅ$^{-3}$ |

**Table 2-3** Crystallographic data of **NiCP**.

| | |
|---|---|
| Empirical formula | $C_{36}H_{40}N_4Ni_{0.5}$ |
| Formula weight | 558.07 |
| Temperature | 100(2) K |
| Wavelength | 0.7000 Å Crystal |
| system | Monoclinic |
| Space group | C2/c (no. 15) |
| Unit cell dimensions | $a$ = 18.8249(10) Å, $\alpha$ =90° |
| | $b$ = 15.9650(10) Å, $\beta$ = 114.696(8)° |
| | $c$ = 10.4056(6) Å, $\gamma$ =90° |
| Volume ($V$) | 2841.3(3) Å$^3$ |
| Z | 4 |
| Density (calculated) | 1.305 g/cm$^3$ |
| Absorption coefficient | 0.343 mm$^{-1}$ |
| F(000) | 1192 |
| Crystal size | 0.07 × 0.06 × 0.01 mm$^3$ |
| Theta range for data collection | 1.72 to 27.5° |
| Index ranges | -34<=h<=26, -31<=k<=31, -15<=l<=20 |
| Reflections collected | 64,773 |
| Independent reflections | 3,297 ($R_{int}$ = 0.0598) |
| Completeness to theta = 24.835° | 98.4% |
| Refinement method | Full-matrix least-squares against $F^2$ |
| Data / restraints / parameters | 3297 / 0 / 189 |
| Goodness-of-fit on $F^2$ | 1.129 |
| Final $R$ indices [$I$ >2σ($I$)] | $R_1$ = 0.0578, $wR_2$ = 0.1218 |
| $R$ indices (all reflections) | $R_1$ = 0.0629, $wR_2$ = 0.1291 |
| Largest diff. peak and hole | 0.535 and -0.589 eÅ$^{-3}$ |

## 2-3-4 Single wire exfoliation

Upon ultrasonication, the single crystal of **ZnCP** could be dispersed in dichloromethane, and showed Tyndall scattering (Fig. 2-9a). The dispersion was cast onto highly ordered pyrolytic graphite (HOPG), which was then subjected to atomic force microscopy (AFM). A representative height image shows several straight white lines traversing the steps of the HOPG substrate (Fig. 2-9b). The cross-sectional analysis shows that the height of the lines is ca. 0.7 nm (Fig. 2-9c), which is consistent with the size of $\mathbf{Zn_{mono}}$ estimated by means of DFT calculation (Fig. 2-9d). This indicates that **ZnCP** is stable enough both chemically and physically to be isolated as single chains. The length of the isolated chains reaches 3 μm, corresponding to ca. 2,500 mers of the bis(dipyrrinato)zinc(II) repeating unit (the Zn–Zn distance is estimated to be 1.26 nm from the crystal structure). I note that the width of **ZnCP** is overestimated by AFM. This is common in 1D polymer systems and AFM resolution.[42]

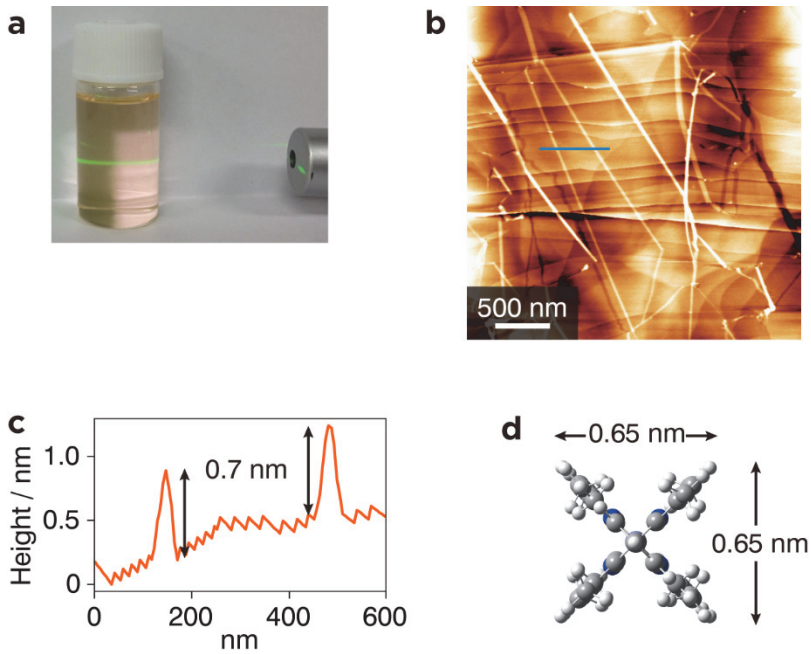


**Figure 2-9 | Exfoliation of single fibers.** **a**, Tyndall scattering form a dichloromethane colloidal suspension of **ZnCP** upon illumination with a green luminous flux. **b**, AFM topographic image of exfoliated fibers of **ZnCP** on HOPG. **c**, AFM cross-sectional profile along the blue line in (**b**). **d**, Molecular size of $\mathbf{Zn_{mono}}$ estimated by means of DFT calculation.

## 2-3-5 Thermoelectric conversion upon conjugation with SWCNT

The good dispersibility of **ZnCP** is useful in practical applications. For example, we can make composite materials by mixing a dispersed 1D CP with other nanomaterials; we also can make a thin film by coating the dispersion on a substrate. In order to demonstrate the processability of **ZnCP**, the author employed these methods to build electric conversion systems.

Themoelectric materials based on SWCNT-polymer composites are the promising candidates for future flexible power generators though those comprising 1D CPs have not been reported.[43] Here I fabricated a composite of **ZnCP** and SWCNTs (**ZnCP-SWCNT**). A mixture of **ZnCP** and SWCNTs with a weight ratio of 1:10 was dispersed in DMF by ultrasonication for 90 min, and the dispersion was then shaken for 1 day. This process resulted in the disappearance of the orange color of **ZnCP** from DMF, which indicated that **ZnCP** was adsorbed onto SWCNTs. Upon filtration, the conjugate spontaneously assembled into a free-standing membrane with a thickness of 64 μm (Fig. 2-10). The conjugate was then subjected to microscopic and spectroscopic analyses. Fig. 2-11 shows TEM images of bundles of SWCNTs with some debundled tubes. On the other hand, electron energy-loss spectroscopy (EELS) reveals the presence of zinc, which is scattered uniformly across the carbon scaffold derived from the SWCNT skeleton (Fig. 2-12). Raman spectroscopy shows an intense G band (1590 $cm^{-1}$) and a weak D band (1350 $cm^{-1}$), which stem from intact and damaged SWCNTs, respectively (Fig. 2-13).[44] These results indicate that **ZnCP** wraps around the SWCNT uniformly without destroying the SWCNT structure. A preliminary experiment disclosed the thermoelectric conversion ability of **ZnCP-SWCNT** (Fig. 2-14). The film of pristine SWCNTs used herein possessed a positive Seebeck coefficient, $\alpha$, of +56.1 μV $K^{-1}$. Thus, its electrical conductivity, $\sigma$ (29.5 S $cm^{-1}$), is dominated by hole conduction (p-type semiconductor). On the other hand, a film of **ZnCP-SWCNT** features greater $\alpha$ and $\sigma$ values of +66.2 μV $K^{-1}$ and 75.6 S $cm^{-1}$, respectively. As a result, **ZnCP-SWCNT** has a power factor ($\alpha^2\sigma$, 33 μW $m^{-1}$ $K^{-2}$) between three and four times greater than that of

pristine SWCNTs (9.3 μW $m^{-1}$ $K^{-2}$). It has been reported that additive substances sandwiched among the SWCNT fibrils enhance the semiconductivity of the SWCNTs.[45] The electrochemical measurements (Figure 2-15) and UV–vis spectroscopy (Figure 2-6) show that the valence band and conduction band levels of **1** are −5.4 eV and −2.9 eV (vs the vacuum level), respectively. Those of the SWCNTs with a diameter of 1.3 nm are −5.0 eV and −4.3 eV, respectively.[46] The similarity of the energy levels of the valence bands in **1** and in the SWCNTs should enhance the positive Seebeck effect. I note that the power factor presented here is even greater than those derived from conjugates between SWCNTs and organic molecules (26 μW $m^{-1}$ $K^{-2}$ at most).[47]

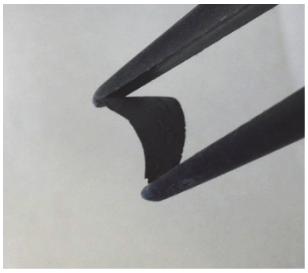

**Figure 2-10 |** Free-standing, flexible, round film of **ZnCP-SWCNT** with a thickness of 64 μm.

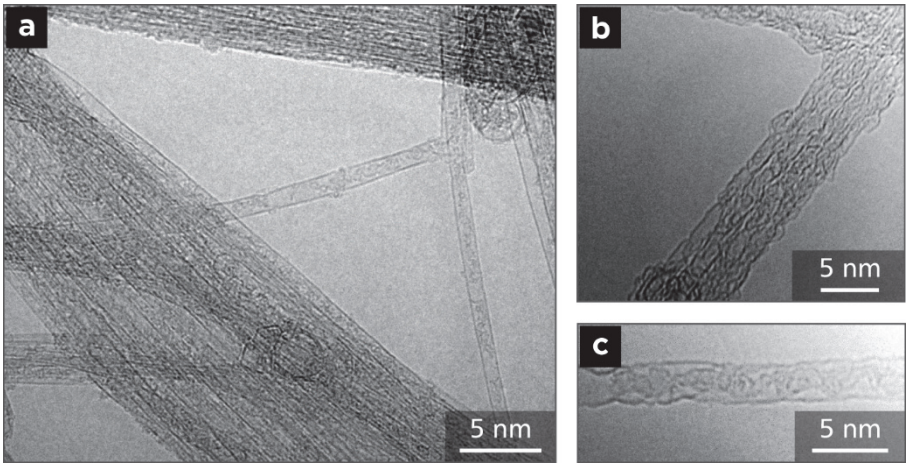


**Figure 2-11 |** TEM images of **ZnCP-SWCNT** on a Cu grid.

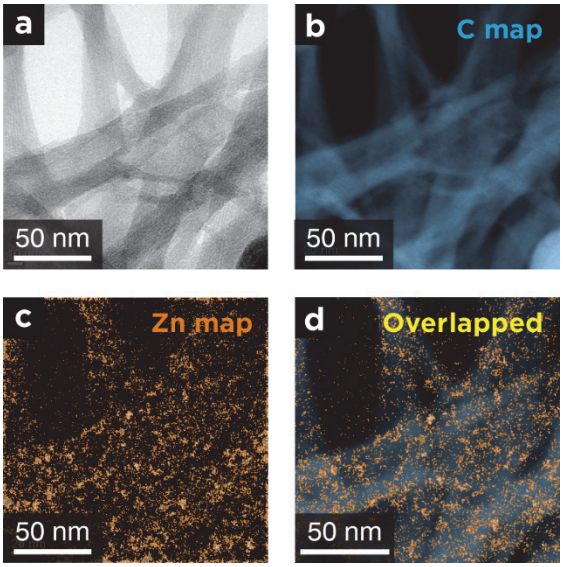


**Figure 2-12 | EELS mapping. a,** Bright-field-TEM image of **ZnCP-SWCNT** subjected to EELS mapping. **b,c**, EELS mapping for: (**b**) Carbon K edge intensity and (**c**) Zinc M2 and M3 edge intensities. **d**, Overlapped image of (**b**) and (**c**).

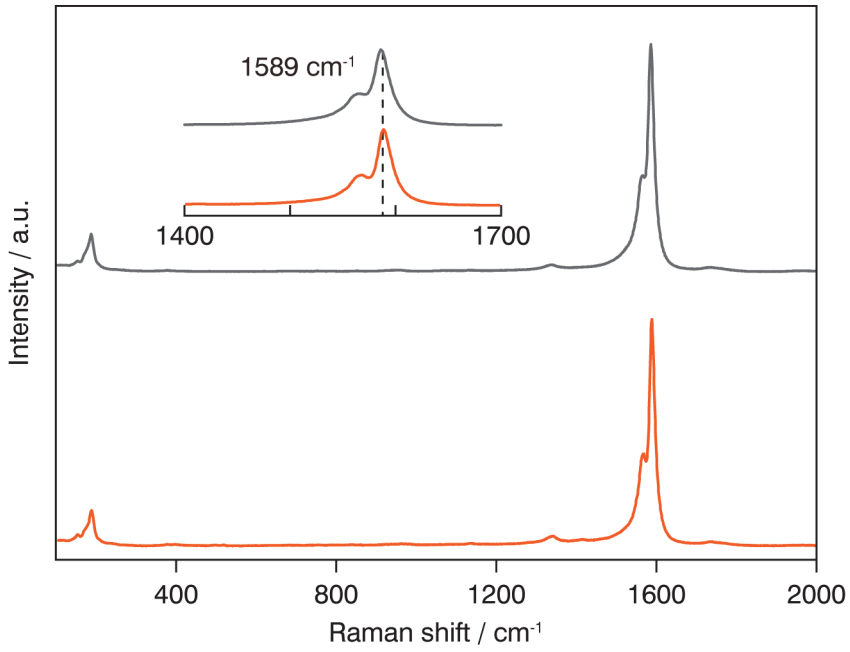


**Figure 2-13 |** Raman spectra of pristine SWCNTs (gray) and **ZnCP-SWCNT** (orange).

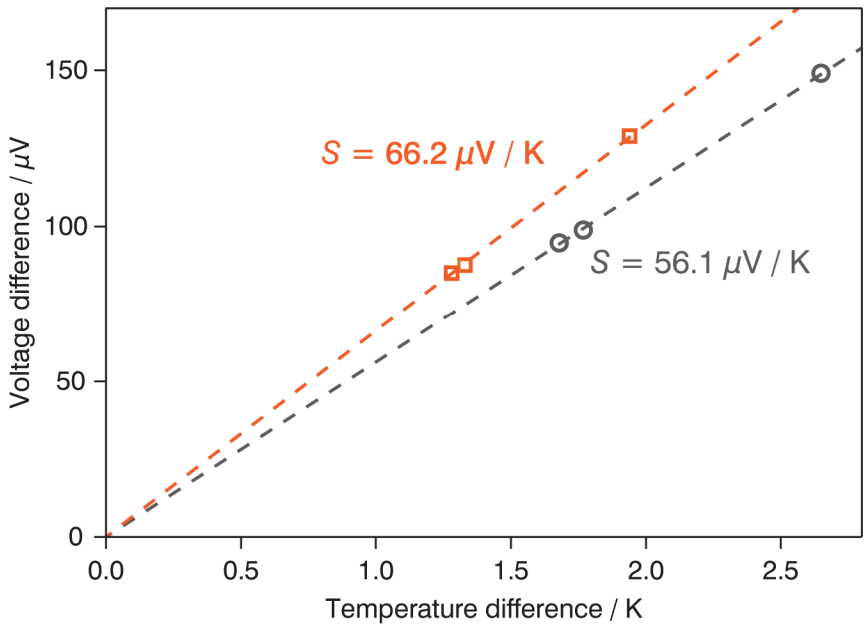


**Figure 2-14 | Thermoelectric conversion ability.** Voltage-difference/temperature difference plots for pristine **SWCNTs** (black) and **ZnCP-SWCNT** (orange).

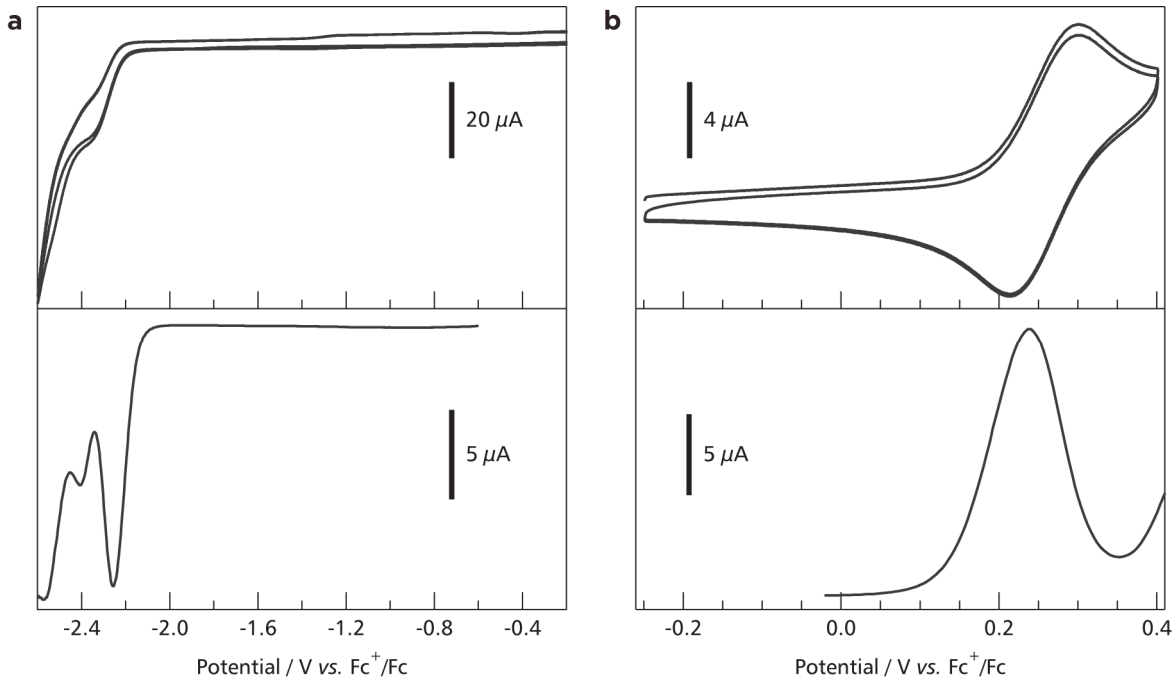


**Figure 2-15 | Electrochemical measurement for $Zn_{mono}$. a,** Cyclic voltammograms (top) and differential pulse voltammograms (bottom) of $\mathbf{Zn_{mono}}$ scanned between −2.6 V and −0.2 V vs. ferrocenium/ferrocene ($Fc^+$/Fc). **b**, Voltammograms scanned between −0.3 V and 0.4 V. The electrolyte solution comprised 0.1 M Bu4NClO4--dichloromethane and the analyte with a concentration of 0.5 mM.

$\mathbf{Zn_{mono}}$ shows the first one-electron oxidation and reduction at $E_{1/2}$ = 0.26 V and -2.23 V *vs.* ferrocenium/ferrocene ($Fc^+$/Fc), respectively. They are assignable to the redox of the dipyrrinato ligand.[48] These electrochemical potentials are converted into the highest occupied and lowest unoccupied molecular orbital levels (HOMO and LUMO) standardized with the vacuum level:[49]

$$E_{HOMO} \text{ / eV} = -5.16 - E_{1/2}(\text{ox}) \text{ / V } vs. \text{ Fc}^+ \text{ / Fc} \quad \text{(S1)}$$

$$E_{LUMO} \text{ / eV} = -5.16 - E_{1/2}(\text{red}) \text{ / V } vs. \text{ Fc}^+ \text{ / Fc} \quad \text{(S2)}$$

Therefore, $E_{HOMO}$ and $E_{LUMO}$ of $\mathbf{Zn_{mono}}$ are quantified as -5.42 and -2.93 eV, respectively.

**ZnCP** and **$Zn_{mono}$** feature $^1\pi$-$\pi^*$ absorption bands with the same peak at 489 nm. This fact indicates that the bis(dipyrrinato)zinc(II) complex moieties in **ZnCP** show no (or negligible) electronic delocalization with one other. In this scheme, the valence band and conduction band levels of **ZnCP** may be approximated by the HOMO and LUMO levels of mononuclear complex **$Zn_{mono}$**, respectively. Therefore, **1ZnCP** is estimated to possess the valence band level of –5.42 eV, and the conduction band level of –2.93 eV.

## 2-3-6 Photoelectric conversion

Thanks to intense light absorption disclosed in Fig. 2-6, **ZnCP** is expected to show photofunctionality. As one of such demonstrations, **ZnCP** was built into a photoelectric conversion system. Dispersion of **ZnCP** was deposited onto transparent $SnO_2$ electrodes, such that thin films of **ZnCP** was formed (Fig. 2-15): This also ensures the good processability of **ZnCP**. A three-electrode electrochemical cell was then set up (Fig. 2-16), where the modified $SnO_2$ electrode was employed as a photoanode. An anodic photocurrent was observed only when the **ZnCP**-modified $SnO_2$ electrode was illumunated with 500 nm light (Fig. 2-17a). In addition, the action spectrum for the photocurrent coincided with the absoption spectrum of **ZnCP** on a $SnO_2$ electrode (Fig. 2-17b). This series of facts indicates that **ZnCP** functions as an active layer for the photoelectric conversion system. This system retained 91% of photocurrent after 500 on/off cycles, suggesting the good durability of **ZnCP** (Fig. 2-17c). I then investigated the photoelectric conversion efficiency (Fig. 2-18). As shown in Fig. 2-18a, the photocurrent reaches the maximal value with the optical density of the film at 500 nm of ~0.005. On the other hand, the quantum yield for the photoelectric conversion decreased as the growth of the film, showing the maximal value of 1.0% in an acetonitrile medium (Fig. 2-18b). To demonstrate the predominance of **ZnCP**, the authors also prepared mononuclear bis(dipyrrinato)zinc(II) complex **Ac-Zn$_{mono}$** with carboxy groups, which forms a self-assembled monolayer (SAM) on a $SnO_2$ electrode upon chemisorption (Fig. 2-19a). The SAM of **Ac-Zn$_{mono}$** performed a much lower conversion efficiency (0.069%, Fig. 2-19b,c), thus justifying the predominance of **ZnCP** over conventional molecular films. It has been reported that bis(dipyrrinato)zinc(II) complexes exhibit exciton transfer from one dipyrrin moiety to the adjacent dipyrrins.[30,40] The 1D dipyrrin array of **ZnCP** presumably serves as an exciton transmitter which conveys excited electron to the $SnO_2$ electrode; this feature might make **ZnCP** a better sensitizer.

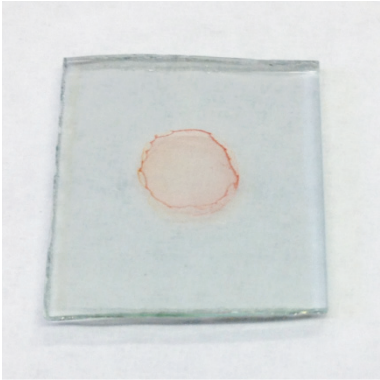

**Figure 2-15 |** Photograph of thin films of **ZnCP** on a $SnO_2$ electrode.

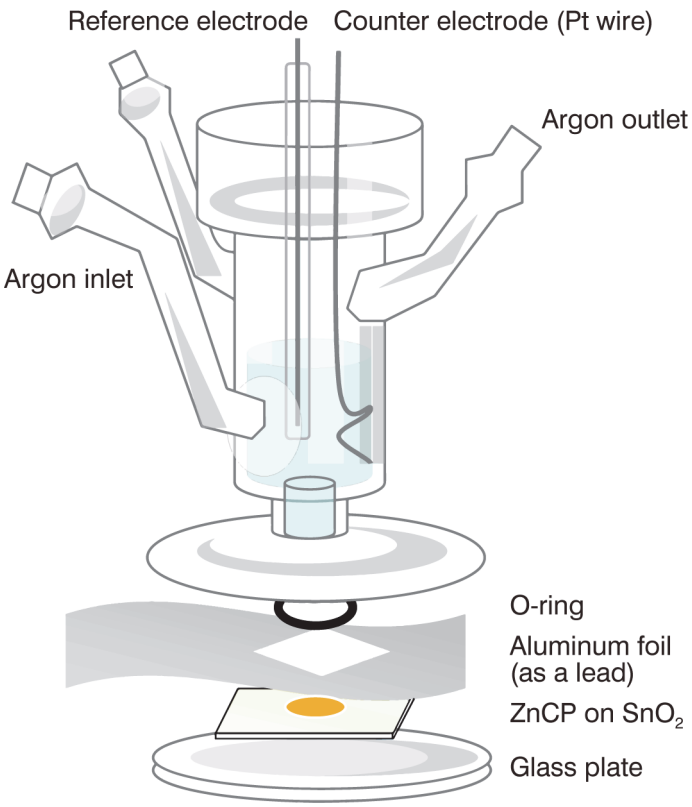


**Figure 2-16 | Photoelectric conversion setup.** Three-electrode electrochemical cell used for the photocurrent generation. The components are clipped in order to ensure sealability. The incident light is illuminated in the direction vertical to the $SnO_2$ electrode (i.e. from the bottom of the cell).

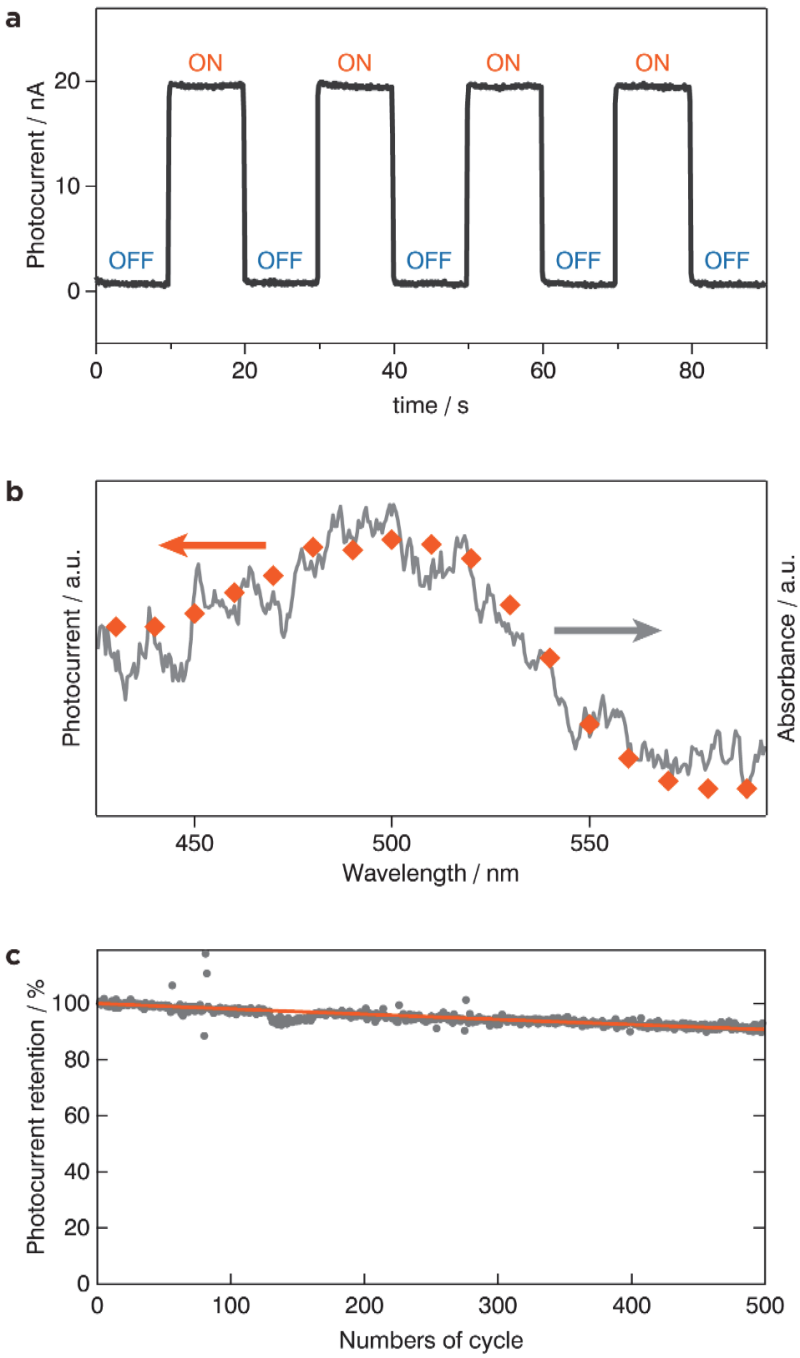


**Figure 2-17 | Photoelectric conversion. a,** Typical anodic photocurrent response upon irradiation of a working electrode ($SnO_2$ substrate modified with **ZnCP** as shown in Fig. 2-15) with intermittent 500 nm light. Light intensity, 0.6 mW. **b,** Action spectrum for the photocurrent generation (orange dots) and absorption spectrum of **ZnCP** on a $SnO_2$ substrate (gray solid line). **c,** Plot of photocurrent decay of **ZnCP** under on $SnO_2$ under intermittent 500 nm light.

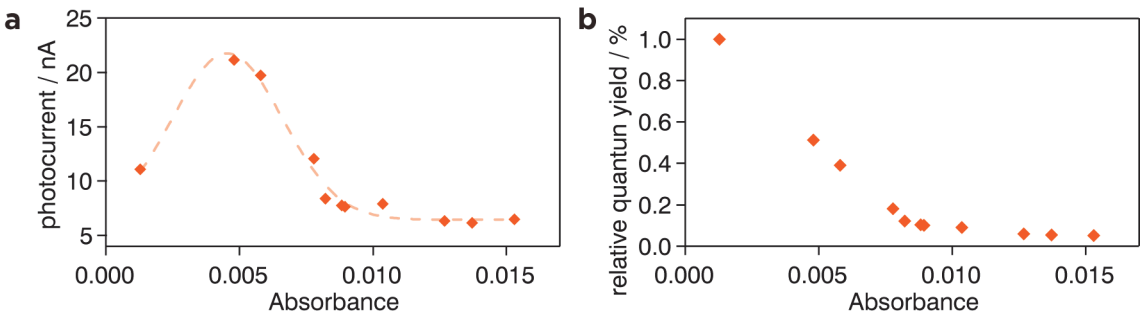


**Figure 2-18 | Photoelectric conversion efficiency of the film of ZnCP. a,b,** Relationship between the absorbance of the film of **ZnCP** and the photocurrent (**a**), and the relative quantum yield of the photoelectric conversion (**b**) upon irradiation with 500 nm light. Light intensity, 0.9 mW.

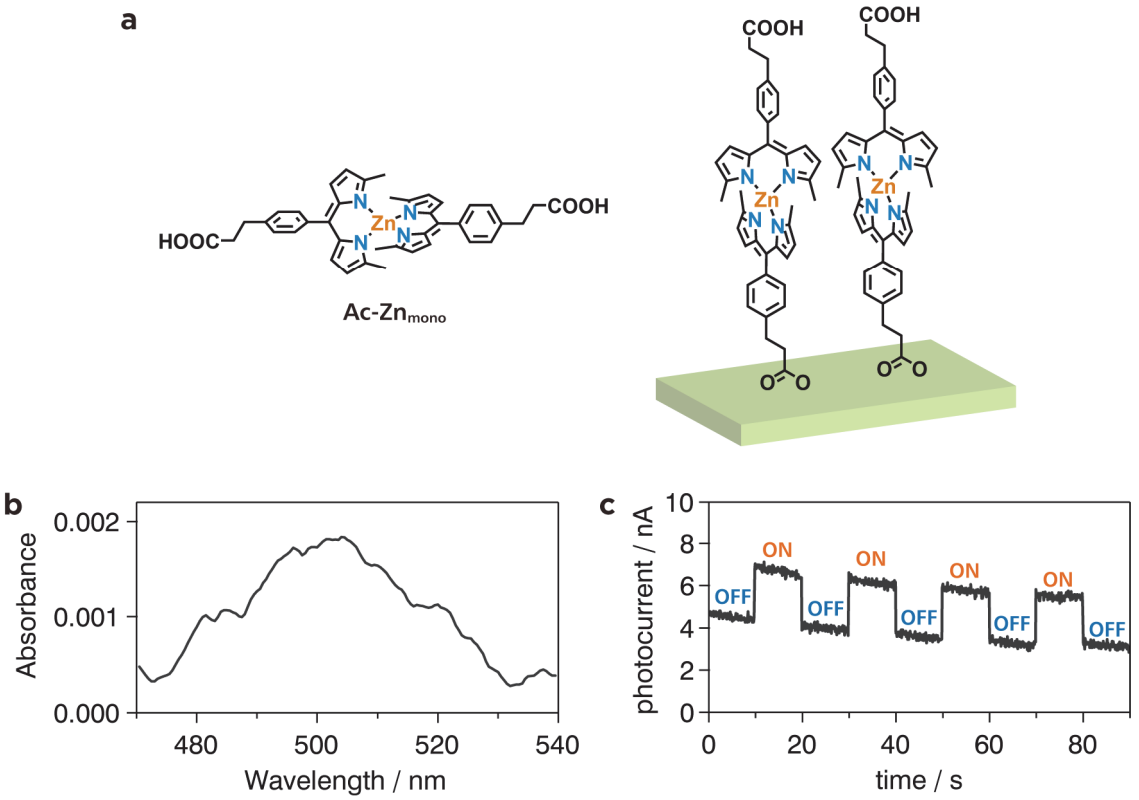


**Figure 2-19 | Determination of the quantum yield for the photoelectric conversion of Ac-Zn$_{mono}$. a,** chemical structure of mononuclear complex **Ac-Zn$_{mono}$**, and a schematic illustration on its self-assembled monolayer (SAM) on a $SnO_2$ electrode. **b,** Absorption spectra of **Ac-Zn$_{mono}$** chemisorbed as a SAM on a $SnO_2$ electrode. This electrode was used for the photocurrent measurement shown in (**c**). **c,** Typical anodic photocurrent response upon irradiation of a working electrode ($SnO_2$ substrate modified with **Ac-Zn$_{mono}$**) with intermittent 500 nm light in an acetonitrile medium. Light intensity, 1.8 mW. This measurement gave a quantum efficiency of 0.069%.

## 2-4 Conclusions

Here I determined the structural and functional features of 1D CPs comprising the bis(dipyrrinato)metal(II) complex motif. Layering bridging dipyrrin ligand **L1** in dichloromethane and metal(II) ions in water produced single crystals of 1D CP **MCP** through a spontaneous coordination reaction at the liquid/liquid interface. X-ray diffraction analysis showed that the fibers of **MCP** were propagated along the [1 0 −1] crystallographic axis. Isolated fibers of **ZnCP** could be exfoliated from the single crystal upon ultrasonication in dichloromethane, and AFM confirmed that the fibers were more than several μm long. The dispersibility of **ZnCP** is sufficient enough to afford a significant advantage in processing them for applications. **ZnCP** formed a conjugate with SWCNTs, where the fibers of **ZnCP** wrapped around SWCNTs uniformly, and which featured thermoelectric conversion. In addition, **ZnCP** could be deposited onto transparent $SnO_2$ electrodes as thin films, which served as photoanodes for a photoelectric conversion system.

## 2-5 References


(1) Mitsumi, M.; Kitamura, K.; Morinaga, A.; Ozawa, Y.; Kobayashi, M.; Toriumi, K.; Iso, Y.; Kitagawa, H.; Mitani, T. *Angew. Chemie Int. Ed.* **2002**, *41*, 2767–2771.

(2) Welte, L.; Calzolari, A.; Di Felice, R.; Zamora, F.; Gómez-Herrero, J. *Nat. Nanotechnol.* **2010**, *5*, 110–115.

(3) Hui, J. K.-H.; Kishida, H.; Ishiba, K.; Takemasu, K.; Morikawa, M.; Kimizuka, N. *Chem. - A Eur. J.* **2016**, *22*, 14213–14218.

(4) Kimizuka, N. *Adv. Mater.* **2000**, *12*, 1461–1463.

(5) Zheng, Z.; Opilik, L.; Schiffmann, F.; Liu, W.; Bergamini, G.; Ceroni, P.; Lee, L.-T.; Schütz, A.; Sakamoto, J.; Zenobi, R.; VandeVondele, J.; Schlüter, A. D. *J. Am. Chem. Soc.* **2014**, *136*, 6103–6110.

(6) Clérac, R.; Miyasaka, H.; Yamashita, M.; Coulon, C. *J. Am. Chem. Soc.* **2002**, *124*, 12837–12844.

(7) Matsukizono, H.; Kuroiwa, K.; Kimizuka, N. *J. Am. Chem. Soc.* **2008**, *130*, 5622–5623.

(8) Sakamoto, R.; Takada, K.; Sun, X.; Pal, T.; Tsukamoto, T.; Phua, E. J. H.; Rapakousiou, A.; Hoshiko, K.; Nishihara, H. *Coord. Chem. Rev.* **2016**, *320–321*, 118–128.

(9) Maeda, H.; Sakamoto, R.; Nishihara, H. *Langmuir* **2016**, *32*, 2527–2538.

(10) Tan, J.-C.; Saines, P. J.; Bithell, E. G.; Cheetham, A. K. *ACS Nano* **2012**, *6*, 615–621.

(11) Furukawa, H.; Cordova, K. E.; O'Keeffe, M.; Yaghi, O. M. *Science* **2013**, *341*, 1230444–1230444.

(12) Sadakiyo, M.; Yamada, T.; Honda, K.; Matsui, H.; Kitagawa, H. *J. Am. Chem. Soc.* **2014**, *136*, 7701–7707.

(13) Li, T.; Kozlowski, M. T.; Doud, E. a; Blakely, M. N.; Rosi, N. L. *J. Am. Chem. Soc.* **2013**, *135*, 11688–11691.

(14) Matsuda, R.; Kitaura, R.; Kitagawa, S.; Kubota, Y.; Belosludov, R. V; Kobayashi, T. C.; Sakamoto, H.; Chiba, T.; Takata, M.; Kawazoe, Y.; Mita, Y. *Nature* **2005**, *436*, 238–241.

(15) Deng, H.; Grunder, S.; Cordova, K. E.; Valente, C.; Furukawa, H.; Hmadeh, M.; Gandara, F.; Whalley, A. C.; Liu, Z.; Asahina, S.; Kazumori, H.; O'Keeffe, M.; Terasaki, O.; Stoddart, J. F.; Yaghi, O. M. *Science* **2012**, *336*, 1018–1023.

(16) Inokuma, Y.; Yoshioka, S.; Ariyoshi, J.; Arai, T.; Hitora, Y.; Takada, K.; Matsunaga, S.; Rissanen, K.; Fujita, M. *Nature* **2013**, *495*, 461–466.

(17) Ren, L.; Yang, L.; Yu, P.; Wang, Y.; Mao, L. *ACS Appl. Mater. Interfaces* **2013**, *5*, 11471–11478.

(18) Culp, J. T.; Sui, L.; Goodman, A.; Luebke, D. *J. Colloid Interface Sci.* **2013**, *393*, 278–285.

(19) Liu, J.; Chen, M.; Qian, D.-J.; Liu, M. *RSC Adv.* **2014**, *4*, 5678.

(20) Olea, D.; Alexandre, S. S.; Amo-Ochoa, P.; Guijarro, A.; de Jesús, F.; Soler, J. M.; de Pablo, P. J.; Zamora, F.; Gómez-Herrero, J. *Adv. Mater.* **2005**, *17*, 1761–1765.

(21) García-Couceiro, U.; Olea, D.; Castillo, O.; Luque, A.; Román, P.; de Pablo, P. J.; Gómez-Herrero, J.; Zamora, F. *Inorg. Chem.* **2005**, *44*, 8343–8348.

(22) Wood, T. E.; Thompson, A. *Chem. Rev.* **2007**, *107*, 1831–1861.

(23) Baudron, S. a. *Dalt. Trans.* **2013**, *42*, 7498.

(24) Maeda, H.; Hashimoto, T. *Chem. - A Eur. J.* **2007**, *13*, 7900–7907.

(25) Maeda, H.; Nishimura, T.; Akuta, R.; Takaishi, K.; Uchiyama, M.; Muranaka, A. *Chem. Sci.* **2013**, *4*, 1204.

(26) Maeda, H.; Hasegawa, M.; Hashimoto, T.; Kakimoto, T.; Nishio, S.; Nakanishi, T. *J. Am. Chem. Soc.* **2006**, *128*, 10024–10025.

(27) Béziau, A.; Baudron, S. a; Guenet, A.; Hosseini, M. W. *Chem. - A Eur. J.* **2013**, *19*, 3215–3223.

(28) Kilduff, B.; Pogozhev, D.; Baudron, S. a; Hosseini, M. W. *Inorg. Chem.* **2010**, *49*, 11231–11239.

(29) Sakamoto, R.; Hoshiko, K.; Liu, Q.; Yagi, T.; Nagayama, T.; Kusaka, S.; Tsuchiya, M.; Kitagawa, Y.; Wong, W.-Y.; Nishihara, H. *Nat. Commun.* **2015**, *6*, 6713.

(30) Tsuchiya, M.; Sakamoto, R.; Kusaka, S.; Kitagawa, Y.; Okumura, M.; Nishihara, H. *Chem. Commun.* **2014**, *50*, 5881.

(31) Sugimoto, K.; Ohsumi, H.; Aoyagi, S.; Nishibori, E.; Moriyoshi, C.; Kuroiwa, Y.; Sawa, H.; Takata, M.; Garrett, R.; Gentle, I.; Nugent, K.; Wilkins, S. In *AIP Conf. Pr*; 2010; Vol. 1234, pp. 887–890.

(32) Altomare, A.; Cascarano, G.; Giacovazzo, C.; Guagliardi, A.; Burla, M. C.; Polidori, G.; Camalli, M. *J. Appl. Crystallogr.* **1994**, *27*, 435–436.

(33) Sheldrick, G. M. *Acta Crystallogr. Sect. A Found. Crystallogr.* **2008**, *64*, 112–122.

(34) M. J. Frisch, G. W. Trucks, H. B. Schlegel, G. E. Scuseria, M. A. Robb, J. R. Cheeseman, G. Scalmani, V. Barone, B. Mennucci, G. A. Petersson, H. Nakatsuji, M. Caricato, X. Li, H. P. Hratchian, A. F. Izmaylov, J. Bloino, G. Zheng, J. L. Sonnenberg, M. Hada, M. Ehara, K. Toyota, R. Fukuda, J. Hasegawa, M. Ishida, T. Nakajima, Y. Honda, O.

Kitao, H. Nakai, T. Vreven, J. A. Montgomery, Jr., J. E. Peralta, F. Ogliaro, M. Bearpark, J. J. Heyd, E. Brothers, K. N. Kudin, V. N. Staroverov, R. Kobayashi, J. Normand, K. Raghavachari, A. Rendell, J. C. Burant, S. S. Iyengar, J. Tomasi, M. Cossi, N. Rega, J. M. Millam, M. Klene, J. E. Knox, J. B. Cross, V. Bakken, C. Adamo, J. Jaramillo, R. Gomperts, R. E. Stratmann, O. Yazyev, A. J. Austin, R. Cammi, C. Pomelli, J. W. Ochterski, R. L. Martin, K. Morokuma, V. G. Zakrzewski, G. A. Voth, P. Salvador, J. J. Dannenberg, S. Dapprich, A. D. Daniels, Ö. Farkas, J. B. Foresman, J. V. Ortiz, J. Cioslowski, and D. J. Fox, Gaussian, Inc., Wallingford CT, **2009**.

(35) Becke, A. D. *J. Chem. Phys.* **1993**, *98*, 5648–5652.

(36) Hay, P. J.; Wadt, W. R. *J. Chem. Phys.* **1985**, *82*, 270.

(37) Hariharan, P. C.; Pople, J. A. *Theor. Chim. Acta* **1973**, *28*, 213–222.

(38) Roy Dennington, Todd Keith, and John Millam, *Semichem Inc.*, Shawnee Mission, KS, **2009**.

(39) Karweik, D. H.; Winograd, N. *Inorg. Chem.* **1976**, *15*, 2336–2342.

(40) Kusaka, S.; Sakamoto, R.; Kitagawa, Y.; Okumura, M.; Nishihara, H. *Chem. - An Asian J.* **2012**, *7*, 907–910.

(41) Miao, Q.; Shin, J.-Y.; Patrick, B. O.; Dolphin, D. *Chem. Commun.* **2009**, 2541.

(42) Olea, D.; García-Couceiro, U.; Castillo, O.; Gómez-Herrero, J.; Zamora, F. *Inorganica Chim. Acta* **2007**, *360*, 48–54.

(43) Piao, M.; Alam, M. R.; Kim, G.; Dettlaff-Weglikowska, U.; Roth, S. *Phys. status solidi* **2012**, *249*, 2353–2356.

(44) Dresselhaus, M. S.; Dresselhaus, G.; Saito, R.; Jorio, A. *Phys. Rep.* **2005**, *409*, 47–99.

(45) Ito, M.; Okamoto, N.; Abe, R.; Kojima, H.; Matsubara, R.; Yamashita, I.; Nakamura, M. *Appl. Phys. Express* **2014**, *7*, 65102.

(46) Kim, K. K.; Yoon, S.-M.; Park, H. K.; Shin, H.-J.; Kim, S. M.; Bae, J. J.; Cui, Y.; Kim, J. M.; Choi, J.-Y.; Lee, Y. H. *New J. Chem.* **2010**, *34*, 2183.

(47) Nonoguchi, Y.; Ohashi, K.; Kanazawa, R.; Ashiba, K.; Hata, K.; Nakagawa, T.; Adachi, C.; Tanase, T.; Kawai, T. *Sci. Rep.* **2013**, *3*, 3344.

(48) Tsuchiya, M.; Sakamoto, R.; Kusaka, S.; Kakinuma, J.; Nishihara, H. *Electrochemistry* **2013**, *81*, 337–339.

(49) Connelly, N. G.; Geiger, W. E. *Chem. Rev.* **1996**, *96*, 877–910.

# Chapter 3

# Graphdiyne Nanosheets

本章については、5 年以内に雑誌等で刊行予定のため、非公開。

# Chapter 4

# Triphenylene-cored Diyne Nanosheet

本章については、5 年以内に雑誌等で刊行予定のため、非公開。

# Chapter 5

# Concluding Remarks

本章の一部については、5 年以内に雑誌等で刊行予定のため、非公開。

As I described in Chapter 1, constructing low-dimensional polymeric nanomaterials with well-defined morphologies is a challenging research target. In this research field, use of a liquid/liquid or gas/liquid interface is an effective approach to organize atomic, ionic, and molecular building blocks in two-dimension. In addition, the interface can serve as a 2D reaction field for the reactants. Therefore, the liquid interfaces could provide a wide variety of low-dimensional polymeric nanomaterials. However, the diversity in chemical bonding or interaction employed in this method has not been extensively explored, resulted in restriction of the accessible structural motifs.

The aim of my Ph.D. research is to expand the scope of the liquid interfacial syntheses to versatile low-dimensional nanomaterials. I focus on two distinct structural concepts as typical examples: the van der Waals induced organization of linear coordination polymers (Chapter 2) and the construction of covalent 2D polymers based on π-conjugated carbon–carbon bond (Chapters 3 and 4).

In Chapter 2, a series of bis(dipyrrinato)metal(II) 1D CPs were prepared at a liquid/liquid interface. Biphasic systems composed of bridging dipyrrin ligand **L1** in dichloromethane and metal(II) ions in water allowed a controlled coordination reaction at the liquid/liquid interface, which resulted in generation of single-crystals of 1D CP **MCP**. X-ray diffraction analysis revealed that the chains of **MCP** were aligned in a parallel manner along the [1 0 -1] crystallographic axis, and their self-organization was induced by van der Waals interaction. Single fibers of **ZnCP** with lengths of several μm could be exfoliated from the single crystal upon sonication. The dispersed wires could be employed to form a conjugate with SWCNTs and a thin film deposited on transparent electrodes; they featured thermoelectric and photoelectric conversion ability, respectively.

In summary, I achieved the expansion of the scope of the liquid interfacial syntheses to low-dimensional nanomaterials with two distinct structural concepts: the van der Waals

induced organization of linear coordination polymers and the construction of covalent 2D polymers based on π-conjugated carbon–carbon bond. In both cases, I realized the creation of single-crystalline nanomaterials and revealed their periodic structures. The strategy demonstrated here opened the door to access versatile functional low-dimensional nanomaterials which have not been synthesized yet. We require only a cup of glass and two immiscible liquids for the synthesis: there is no doubt on a great potential of liquid interfaces.

# Appendix

## Crystallographic data of ZnCP

```
#----------------- SECTION 1. GLOBAL INFORMATION --------------------------#

data_global

#==========================================================
==================
#
# SUBMISSION DETAILS
# Name and address of author for correspondence

_publ_contact_author_name          'Professor Hiroshi Nishihara'
_publ_contact_author_address
;Department of Chemistry, Graduate School of Science, The University of Tokyo,
7-3-1, Hongo, Bunkyo-ku, Tokyo 113-0033, Japan

;
_publ_contact_author_email         nishihara@chem.s.u-tokyo.ac.jp
_publ_contact_author_phone         '+81-3-5841-4346 '
_publ_contact_author_fax           '+81-3-5841-8063 '
loop_
_publ_author_name
'Matsuoka, Ryota'
'Toyoda, Ryojun'
'Sakamoto, Ryota'
'Tsuchiya, Mizuho'
'Hoshiko, Ken'
'Tatsuhiro, Nagayama'
'Nonoguchi, Yoshiyuki'
'Nishibori, Eiji'
'Kawai, Tsuyoshi'
'Nishihara, Hiroshi'

_publ_requested_journal            Chem.Sci.

#==========================================================
==================
#

#-----------------    SECTION 2. COMPOUND(S) DETAILS ------------------------#

#==========================================================
==================

# CHEMICAL DATA

_chemical_name_systematic
;
  ?
;
_chemical_formula_moiety           'C36 H40 N4 Zn0.50'
_chemical_formula_sum              'C36 H40 N4 Zn0.50'
_chemical_formula_weight           561.4

#==========================================================
==================

# CRYSTAL DATA

_symmetry_cell_setting             monoclinic
_symmetry_space_group_name_H-M     'C 2/c'
_symmetry_space_group_name_Hall    '-C 2yc'
loop_
    _symmetry_equiv_pos_as_xyz
'x, y, z'
'-x, y, -z+1/2'
'x+1/2, y+1/2, z'
'-x+1/2, y+1/2, -z+1/2'
'-x, -y, -z'
'x, -y, z-1/2'
'-x+1/2, -y+1/2, -z'
'x+1/2, -y+1/2, z-1/2'

_cell_length_a                     18.8182(4)
_cell_length_b                     15.9892(3)
_cell_length_c                     10.4062(2)
_cell_angle_alpha                  90
_cell_angle_beta                   114.760(8)
_cell_angle_gamma                  90
_cell_volume                       2843.26(19)
_cell_formula_units_Z              4
_cell_measurement_reflns_used      61771
_cell_measurement_theta_min        1.72
_cell_measurement_theta_max        44.4
_cell_measurement_temperature      100(2)
_exptl_crystal_description         platlet
_exptl_crystal_colour              orange
_exptl_crystal_size_max            0.15
_exptl_crystal_size_mid            0.07
_exptl_crystal_size_min            0.01
_exptl_crystal_density_diffrn      1.311
_exptl_crystal_density_method      'not measured'
_exptl_crystal_F_000               1196
_exptl_absorpt_coefficient_mu      0.43
_exptl_absorpt_correction_type     none

#==========================================================
==================

# EXPERIMENTAL DATA

_exptl_special_details
;
  ?
;
_diffrn_ambient_temperature        100(2)
_diffrn_radiation_type             synchrotron
_diffrn_radiation_wavelength       0.7
_diffrn_source                     'bending magnet'
_diffrn_radiation_monochromator    silicon
_diffrn_measurement_device_type
cylindrical_IP_camera_at_SPring-8_BL02B1
_diffrn_measurement_method         'phi or omega oscillation scans'
_diffrn_detector_area_resol_mean   10
_diffrn_reflns_number              67218
_diffrn_reflns_av_R_equivalents    0.0451
_diffrn_reflns_theta_min           2.317
_diffrn_reflns_theta_max           35.683
_diffrn_reflns_theta_full          24.835
_diffrn_measured_fraction_theta_max
                                   0.961
```

```
_diffrn_measured_fraction_theta_full
                                                    1
_diffrn_reflns_Laue_measured_fraction_full
                                                    1
_diffrn_reflns_Laue_measured_fraction_max
                                                    0.961
_diffrn_reflns_point_group_measured_fraction_full
                                                    1
_diffrn_reflns_point_group_measured_fraction_max
                                                    0.961
_diffrn_reflns_limit_h_min                  -37
_diffrn_reflns_limit_h_max                  30
_diffrn_reflns_limit_k_min                  -24
_diffrn_reflns_limit_k_max                  28
_diffrn_reflns_limit_l_min                  -18
_diffrn_reflns_limit_l_max                  20
_diffrn_reflns_reduction_process
;
  Scaled and merged with Sortav
  R.H. Blessing, (1987) Cryst. Rev. 1, 3-58
  R.H. Blessing, (1989) J. Appl. Cryst. 22, 396-397
;

#=============================================================
==================

# STRUCTURE SOLUTION

_atom_sites_solution_hydrogens              geom
```

```
#=============================================================
==================

# REFINEMENT DATA

_refine_special_details
;
  The occupancy of 'ZN01' was fixed as 0.25
  (a half of the ideal value) during the refinement.
;
_reflns_number_total                        6635
_reflns_number_gt                           4038
_reflns_threshold_expression                'I > 2¥s(I)'
_refine_ls_structure_factor_coef            Fsqd
_refine_ls_matrix_type                      full
_refine_ls_R_factor_all                     0.0653
_refine_ls_R_factor_gt                      0.0529
_refine_ls_wR_factor_ref                    0.15
_refine_ls_goodness_of_fit_ref              0.995
_refine_ls_restrained_S_all                 0.995
_refine_ls_number_reflns                    6635
_refine_ls_number_parameters                190
_refine_ls_number_restraints                0
_refine_ls_number_constraints               0
_refine_ls_hydrogen_treatment               constr
_refine_ls_weighting_scheme                 calc
_refine_ls_weighting_details
                    'w=1/[¥s^2^(Fo^2^)+(0.0409P)^2^]                where
P=(Fo^2^+2Fc^2^)/3'
_refine_ls_shift/su_max                     0.001
_refine_ls_shift/su_mean                    0
```

```
_refine_diff_density_max                    0.617
_refine_diff_density_min                    -0.641
_refine_diff_density_rms                    0.065
_refine_ls_extinction_method                none
loop_
    _atom_type_symbol
    _atom_type_description
    _atom_type_scat_dispersion_real
    _atom_type_scat_dispersion_imag
    _atom_type_scat_source
C C 0.003 0.0016 'International Tables Vol C Tables 4.2.6.8 and 6.1.1.4'
H H 0 0 'International Tables Vol C Tables 4.2.6.8 and 6.1.1.4'
N N 0.0059 0.0032 'International Tables Vol C Tables 4.2.6.8 and 6.1.1.4'
Zn Zn 0.2937 1.3977 'International Tables Vol C Tables 4.2.6.8 and 6.1.1.4'

_computing_data_collection                  'CrystalClear (Rigaku/MSC Inc., 2006)'
_computing_cell_refinement                  'CrystalClear (Rigaku/MSC Inc., 2006)'
_computing_data_reduction
                    'CrystalClear (Rigaku/MSC Inc., 2006), SORTAV (Blessing, 1995)'
_computing_structure_solution               'SIR 92'
_computing_structure_refinement             'SHELXL-2014 (Sheldrick, 2014)'
_computing_molecular_graphics               'Mercury 3.3, CCDC, 2013'
_computing_publication_material             'enCIFer 1.4, CCDC, 2011'

#=============================================================
==================

# ATOMIC COORDINATES AND DISPLACEMENT PARAMETERS

loop_
    _atom_site_label
    _atom_site_fract_x
    _atom_site_fract_y
    _atom_site_fract_z
    _atom_site_U_iso_or_equiv
    _atom_site_adp_type
    _atom_site_calc_flag
    _atom_site_occupancy
    _atom_site_disorder_assembly
    _atom_site_disorder_group
    _atom_site_type_symbol
Zn01 1 0.20251(3) 0.75 0.01901(12) Uani d 0.5 . . Zn
N001 0.99726(6) 0.27064(7) 0.90211(11) 0.0205(2) Uani d 1 . . N
N002 0.90830(6) 0.14430(7) 0.73039(11) 0.0197(2) Uani d 1 . . N
C001 0.60230(7) 0.32937(9) 0.81893(13) 0.0212(2) Uani d 1 . . C
H01A 0.5679 0.3321 0.8682 0.032 Uiso calc 1 . . H
H01B 0.6121 0.386 0.7943 0.032 Uiso calc 1 . . H
H01C 0.5771 0.2961 0.7324 0.032 Uiso calc 1 . . H
C002 0.81386(7) 0.04406(9) 0.65822(13) 0.0224(3) Uani d 1 . . C
H002 0.7849 -0.0037 0.61 0.027 Uiso calc 1 . . H
C003 0.88158(7) 0.07795(9) 0.64676(13) 0.0221(3) Uani d 1 . . C
C004 0.67892(6) 0.28908(8) 0.91419(12) 0.0164(2) Uani d 1 . . C
C005 1.01777(7) 0.38986(9) 1.02439(14) 0.0244(3) Uani d 1 . . C
H003 1.0419 0.4402 1.0707 0.029 Uiso calc 1 . . H
C006 1.04655(7) 0.33559(9) 0.95181(13) 0.0220(3) Uani d 1 . . C
C007 0.93410(6) 0.28129(8) 0.93822(12) 0.0172(2) Uani d 1 . . C
C008 0.73740(6) 0.27872(8) 0.86454(12) 0.0171(2) Uani d 1 . . C
C009 0.94774(7) 0.35727(9) 1.01689(13) 0.0214(2) Uani d 1 . . C
C010 0.86958(6) 0.22430(8) 0.89314(12) 0.0173(2) Uani d 1 . . C
C011 0.79868(6) 0.09356(8) 0.75204(12) 0.0197(2) Uani d 1 . . C
C012 0.85853(6) 0.15780(8) 0.79903(12) 0.0174(2) Uani d 1 . . C
C013 0.91988(7) 0.04517(10) 0.55788(14) 0.0271(3) Uani d 1 . . C
```

H04A 0.9377 0.092 0.5181 0.041 Uiso calc 1 . . H
H04B 0.8824 0.0113 0.4808 0.041 Uiso calc 1 . . H
H04C 0.9649 0.0106 0.6161 0.041 Uiso calc 1 . . H
C014 0.72233(7) 0.31098(9) 0.71864(13) 0.0230(3) Uani d 1 . . C
H05A 0.6704 0.3368 0.6756 0.034 Uiso calc 1 . . H
H05B 0.7621 0.3527 0.7264 0.034 Uiso calc 1 . . H
H05C 0.7248 0.2644 0.6594 0.034 Uiso calc 1 . . H
C015 0.73222(7) 0.07912(9) 0.79253(15) 0.0245(3) Uani d 1 . . C
H06A 0.6927 0.1229 0.7507 0.037 Uiso calc 1 . . H
H06B 0.7516 0.0807 0.8958 0.037 Uiso calc 1 . . H
H06C 0.7088 0.0243 0.7576 0.037 Uiso calc 1 . . H
C016 0.80834(6) 0.23861(8) 0.94969(12) 0.0165(2) Uani d 1 . . C
C017 0.89931(8) 0.39909(10) 1.08052(17) 0.0291(3) Uani d 1 . . C
H07A 0.9223 0.4535 1.1191 0.044 Uiso calc 1 . . H
H07B 0.8978 0.3641 1.1566 0.044 Uiso calc 1 . . H
H07C 0.846 0.4071 1.0077 0.044 Uiso calc 1 . . H
C018 1.11735(8) 0.34581(11) 0.92111(16) 0.0300(3) Uani d 1 . . C
H08A 1.1419 0.2912 0.9258 0.045 Uiso calc 1 . . H
H08B 1.1548 0.3834 0.9913 0.045 Uiso calc 1 . . H
H08C 1.1015 0.3695 0.8263 0.045 Uiso calc 1 . . H

loop_
    _atom_site_aniso_label
    _atom_site_aniso_U_11
    _atom_site_aniso_U_22
    _atom_site_aniso_U_33
    _atom_site_aniso_U_12
    _atom_site_aniso_U_13
    _atom_site_aniso_U_23
Zn01 0.01510(19) 0.0220(3) 0.0226(2) 0 0.01048(15) 0
N001 0.0148(4) 0.0271(6) 0.0222(5) -0.0014(4) 0.0104(4) -0.0017(4)
N002 0.0166(4) 0.0224(6) 0.0220(5) 0.0027(4) 0.0100(4) -0.0004(4)
C001 0.0139(5) 0.0269(7) 0.0221(5) 0.0028(4) 0.0069(4) 0.0021(4)
C002 0.0186(5) 0.0212(6) 0.0250(6) -0.0004(5) 0.0068(4) -0.0031(4)
C003 0.0210(5) 0.0242(7) 0.0214(5) 0.0028(5) 0.0092(4) -0.0007(4)
C004 0.0127(4) 0.0185(6) 0.0185(5) 0.0003(4) 0.0070(4) -0.0006(4)
C005 0.0196(5) 0.0241(7) 0.0284(6) -0.0039(5) 0.0089(5) -0.0028(5)
C006 0.0171(5) 0.0261(7) 0.0237(5) -0.0043(5) 0.0094(4) -0.0004(5)
C007 0.0133(4) 0.0197(6) 0.0201(5) 0.0008(4) 0.0086(4) -0.0011(4)
C008 0.0127(4) 0.0198(6) 0.0194(5) 0.0010(4) 0.0074(4) -0.0006(4)
C009 0.0185(5) 0.0221(6) 0.0255(6) -0.0025(4) 0.0110(4) -0.0020(4)
C010 0.0126(4) 0.0207(6) 0.0195(5) 0.0022(4) 0.0077(4) 0.0025(4)
C011 0.0140(5) 0.0224(6) 0.0218(5) 0.0007(4) 0.0067(4) 0.0001(4)
C012 0.0126(4) 0.0205(6) 0.0201(5) 0.0009(4) 0.0079(4) 0.0001(4)
C013 0.0256(6) 0.0326(8) 0.0258(6) 0.0033(5) 0.0133(5) -0.0050(5)
C014 0.0188(5) 0.0311(7) 0.0210(5) 0.0043(5) 0.0102(4) 0.0037(5)
C015 0.0186(5) 0.0268(7) 0.0301(6) -0.0041(5) 0.0122(5) -0.0021(5)
C016 0.0120(4) 0.0187(6) 0.0203(5) 0.0003(4) 0.0082(4) -0.0004(4)
C017 0.0256(6) 0.0280(8) 0.0396(7) -0.0037(5) 0.0195(6) -0.0110(6)
C018 0.0205(6) 0.0436(9) 0.0288(6) -0.0092(6) 0.0133(5) -0.0014(6)

#==========
==========

# MOLECULAR GEOMETRY

_geom_special_details
;
 All esds (except the esd in the dihedral angle between two l.s. planes)
 are estimated using the full covariance matrix.  The cell esds are taken
 into account individually in the estimation of esds in distances, angles
 and torsion angles; correlations between esds in cell parameters are only
 used when they are defined by crystal symmetry.  An approximate (isotropic)
 treatment of cell esds is used for estimating esds involving l.s. planes.
;
loop_
    _geom_bond_atom_site_label_1
    _geom_bond_atom_site_label_2
    _geom_bond_site_symmetry_2
    _geom_bond_distance
    _geom_bond_publ_flag
Zn01 N002 . 1.8949(11) ?
Zn01 N002 2_756 1.8949(11) ?
Zn01 N001 2_756 1.9398(11) ?
Zn01 N001 . 1.9398(11) ?
N001 C006 . 1.3432(17) ?
N001 C007 . 1.3990(14) ?
N002 C003 . 1.3301(17) ?
N002 C012 . 1.4123(15) ?
C001 C004 . 1.5098(16) ?
C001 H01A . 0.98 ?
C001 H01B . 0.98 ?
C001 H01C . 0.98 ?
C002 C011 . 1.3766(18) ?
C002 C003 . 1.4350(18) ?
C002 H002 . 0.95 ?
C003 C013 . 1.4860(17) ?
C004 C008 . 1.4079(16) ?
C004 C016 7_657 1.4055(16) ?
C005 C009 . 1.3886(17) ?
C005 C006 . 1.3998(19) ?
C005 H003 . 0.95 ?
C006 C018 . 1.5036(18) ?
C007 C010 . 1.4309(17) ?
C007 C009 . 1.4269(18) ?
C008 C016 . 1.4099(16) ?
C008 C014 . 1.5135(17) ?
C009 C017 . 1.4905(19) ?
C010 C012 . 1.4007(17) ?
C010 C016 . 1.5148(15) ?
C011 C012 . 1.4496(17) ?
C011 C015 . 1.4954(16) ?
C013 H04A . 0.98 ?
C013 H04B . 0.98 ?
C013 H04C . 0.98 ?
C014 H05A . 0.98 ?
C014 H05B . 0.98 ?
C014 H05C . 0.98 ?
C015 H06A . 0.98 ?
C015 H06B . 0.98 ?
C015 H06C . 0.98 ?
C016 C004 7_657 1.4055(16) ?
C017 H07A . 0.98 ?
C017 H07B . 0.98 ?
C017 H07C . 0.98 ?
C018 H08A . 0.98 ?
C018 H08B . 0.98 ?
C018 H08C . 0.98 ?

loop_
    _geom_angle_atom_site_label_1
    _geom_angle_atom_site_label_2
    _geom_angle_atom_site_label_3

```
    _geom_angle
    _geom_angle_site_symmetry_1
    _geom_angle_site_symmetry_3
    _geom_angle_publ_flag
N002 Zn01 N002 121.17(7) . 2_756 ?
N002 Zn01 N001 121.48(4) . 2_756 ?
N002 Zn01 N001 91.69(4) 2_756 2_756 ?
N002 Zn01 N001 91.69(4) . . ?
N002 Zn01 N001 121.48(4) 2_756 . ?
N001 Zn01 N001 111.67(7) 2_756 . ?
C006 N001 C007 109.25(11) . . ?
C006 N001 Zn01 119.89(8) . . ?
C007 N001 Zn01 127.12(8) . . ?
C003 N002 C012 107.68(10) . . ?
C003 N002 Zn01 122.67(8) . . ?
C012 N002 Zn01 129.60(9) . . ?
C004 C001 H01A 109.5 . . ?
C004 C001 H01B 109.5 . . ?
H01A C001 H01B 109.5 . . ?
C004 C001 H01C 109.5 . . ?
H01A C001 H01C 109.5 . . ?
H01B C001 H01C 109.5 . . ?
C011 C002 C003 107.29(12) . . ?
C011 C002 H002 126.4 . . ?
C003 C002 H002 126.4 . . ?
N002 C003 C002 110.63(11) . . ?
N002 C003 C013 122.66(12) . . ?
C002 C003 C013 126.70(12) . . ?
C008 C004 C016 120.22(10) . 7_657 ?
C008 C004 C001 119.18(10) . . ?
C016 C004 C001 120.60(10) 7_657 . ?
C009 C005 C006 108.03(12) . . ?
C009 C005 H003 126 . . ?
C006 C005 H003 126 . . ?
N001 C006 C005 109.05(11) . . ?
N001 C006 C018 122.18(12) . . ?
C005 C006 C018 128.66(13) . . ?
N001 C007 C010 122.29(11) . . ?
N001 C007 C009 106.79(10) . . ?
C010 C007 C009 130.87(10) . . ?
C016 C008 C004 120.18(10) . . ?
C016 C008 C014 121.05(10) . . ?
C004 C008 C014 118.77(10) . . ?
C005 C009 C007 106.87(10) . . ?
C005 C009 C017 123.31(13) . . ?
C007 C009 C017 129.82(11) . . ?
C012 C010 C007 124.73(10) . . ?
C012 C010 C016 118.16(10) . . ?
C007 C010 C016 117.10(10) . . ?
C002 C011 C012 106.50(11) . . ?
C002 C011 C015 123.89(12) . . ?
C012 C011 C015 129.62(12) . . ?
C010 C012 N002 122.26(11) . . ?
C010 C012 C011 129.84(10) . . ?
N002 C012 C011 107.89(11) . . ?
C003 C013 H04A 109.5 . . ?
C003 C013 H04B 109.5 . . ?
H04A C013 H04B 109.5 . . ?
C003 C013 H04C 109.5 . . ?
H04A C013 H04C 109.5 . . ?
H04B C013 H04C 109.5 . . ?
C008 C014 H05A 109.5 . . ?
C008 C014 H05B 109.5 . . ?
H05A C014 H05B 109.5 . . ?
C008 C014 H05C 109.5 . . ?
H05A C014 H05C 109.5 . . ?
H05B C014 H05C 109.5 . . ?
C011 C015 H06A 109.5 . . ?
C011 C015 H06B 109.5 . . ?
H06A C015 H06B 109.5 . . ?
C011 C015 H06C 109.5 . . ?
H06A C015 H06C 109.5 . . ?
H06B C015 H06C 109.5 . . ?
C008 C016 C004 119.58(10) . 7_657 ?
C008 C016 C010 119.91(10) . . ?
C004 C016 C010 120.50(10) 7_657 . ?
C009 C017 H07A 109.5 . . ?
C009 C017 H07B 109.5 . . ?
H07A C017 H07B 109.5 . . ?
C009 C017 H07C 109.5 . . ?
H07A C017 H07C 109.5 . . ?
H07B C017 H07C 109.5 . . ?
C006 C018 H08A 109.5 . . ?
C006 C018 H08B 109.5 . . ?
H08A C018 H08B 109.5 . . ?
C006 C018 H08C 109.5 . . ?
H08A C018 H08C 109.5 . . ?
H08B C018 H08C 109.5 . . ?

loop_
    _geom_torsion_atom_site_label_1
    _geom_torsion_atom_site_label_2
    _geom_torsion_atom_site_label_3
    _geom_torsion_atom_site_label_4
    _geom_torsion
    _geom_torsion_site_symmetry_1
    _geom_torsion_site_symmetry_2
    _geom_torsion_site_symmetry_3
    _geom_torsion_site_symmetry_4
    _geom_torsion_publ_flag
N002 Zn01 N002 C003 -43.43(9) 2_756 . . . ?
N001 Zn01 N002 C003 70.82(12) 2_756 . . . ?
N001 Zn01 N002 C003 -172.36(10) . . . . ?
N002 Zn01 N002 C012 133.96(12) 2_756 . . . ?
N001 Zn01 N002 C012 -111.79(11) 2_756 . . . ?
N001 Zn01 N002 C012 5.04(11) . . . . ?
C012 N002 C003 C002 -0.90(14) . . . . ?
Zn01 N002 C003 C002 177.00(8) . . . . ?
C012 N002 C003 C013 -179.84(12) . . . . ?
Zn01 N002 C003 C013 -1.95(18) . . . . ?
C011 C002 C003 N002 0.93(15) . . . . ?
C011 C002 C003 C013 179.83(13) . . . . ?
C007 N001 C006 C005 1.15(15) . . . . ?
Zn01 N001 C006 C005 160.87(9) . . . . ?
C007 N001 C006 C018 -175.39(12) . . . . ?
Zn01 N001 C006 C018 -15.67(17) . . . . ?
C009 C005 C006 N001 -0.84(16) . . . . ?
C009 C005 C006 C018 175.41(13) . . . . ?
C006 N001 C007 C010 176.55(11) . . . . ?
Zn01 N001 C007 C010 18.69(17) . . . . ?
C006 N001 C007 C009 -1.01(14) . . . . ?
Zn01 N001 C007 C009 -158.87(9) . . . . ?
C016 C004 C008 C016 1.6(2) 7_657 . . . ?
C001 C004 C008 C016 -177.75(11) . . . . ?
```

C016 C004 C008 C014 -178.69(11) 7_657 . . . ?
C001 C004 C008 C014 1.94(18) . . . . ?
C006 C005 C009 C007 0.20(15) . . . . ?
C006 C005 C009 C017 -178.95(13) . . . . ?
N001 C007 C009 C005 0.48(14) . . . . ?
C010 C007 C009 C005 -176.80(12) . . . . ?
N001 C007 C009 C017 179.55(14) . . . . ?
C010 C007 C009 C017 2.3(2) . . . . ?
N001 C007 C010 C012 -6.42(19) . . . . ?
C009 C007 C010 C012 170.49(12) . . . . ?
N001 C007 C010 C016 174.87(11) . . . . ?
C009 C007 C010 C016 -8.21(19) . . . . ?
C003 C002 C011 C012 -0.55(14) . . . . ?
C003 C002 C011 C015 179.77(11) . . . . ?
C007 C010 C012 N002 -4.83(18) . . . . ?
C016 C010 C012 N002 173.86(10) . . . . ?
C007 C010 C012 C011 176.04(12) . . . . ?
C016 C010 C012 C011 -5.26(19) . . . . ?
C003 N002 C012 C010 -178.76(11) . . . . ?
Zn01 N002 C012 C010 3.54(17) . . . . ?
C003 N002 C012 C011 0.53(13) . . . . ?
Zn01 N002 C012 C011 -177.16(8) . . . . ?
C002 C011 C012 C010 179.26(12) . . . . ?
C015 C011 C012 C010 -1.1(2) . . . . ?
C002 C011 C012 N002 0.04(14) . . . . ?
C015 C011 C012 N002 179.69(12) . . . . ?
C004 C008 C016 C004 -1.6(2) . . . 7_657 ?
C014 C008 C016 C004 178.71(11) . . . 7_657 ?
C004 C008 C016 C010 177.34(11) . . . . ?
C014 C008 C016 C010 -2.35(18) . . . . ?
C012 C010 C016 C008 -78.40(15) . . . . ?
C007 C010 C016 C008 100.39(13) . . . . ?
C012 C010 C016 C004 100.52(13) . . . 7_657 ?
C007 C010 C016 C004 -80.68(15) . . . 7_657 ?

# END of CIF

## Crystallographic data of CuCP

```
#------------------ SECTION 1. GLOBAL INFORMATION --------------------------#

data_global

#==========================================================
==================
#
# SUBMISSION DETAILS
# Name and address of author for correspondence

_publ_contact_author_name          'Professor Hiroshi Nishihara'
_publ_contact_author_address
;Department of Chemistry, Graduate School of Science, The University of Tokyo,
7-3-1, Hongo, Bunkyo-ku, Tokyo 113-0033, Japan

;
_publ_contact_author_email         nishihara@chem.s.u-tokyo.ac.jp
_publ_contact_author_phone         '+81-3-5841-4346 '
_publ_contact_author_fax           '+81-3-5841-8063 '
loop_
  _publ_author_name
'Matsuoka, Ryota'
'Toyoda, Ryojun'
'Sakamoto, Ryota'
'Tsuchiya, Mizuho'
'Hoshiko, Ken'
'Tatsuhiro, Nagayama'
'Nonoguchi, Yoshiyuki'
'Nishibori, Eiji'
'Kawai, Tsuyoshi'
'Nishihara, Hiroshi'

_publ_requested_journal            Chem.Sci.

#==========================================================
==================
#

#------------------    SECTION 2. COMPOUND(S) DETAILS ------------------------#

#==========================================================
==================

# CHEMICAL DATA

_chemical_name_systematic
;
  ?
;
_chemical_formula_moiety           'C36 H40 Cu0.50 N4'
_chemical_formula_sum              'C36 H40 Cu0.50 N4'
_chemical_formula_weight           560.49

#==========================================================
==================

# CRYSTAL DATA

_symmetry_cell_setting             monoclinic
_symmetry_space_group_name_H-M     'C 2/c'
_symmetry_space_group_name_Hall    '-C 2yc'
loop_
    _symmetry_equiv_pos_as_xyz
'x, y, z'
'-x, y, -z+1/2'
'x+1/2, y+1/2, z'
'-x+1/2, y+1/2, -z+1/2'
'-x, -y, -z'
'x, -y, z-1/2'
'-x+1/2, -y+1/2, -z'
'x+1/2, -y+1/2, z-1/2'

_cell_length_a                     18.8080(8)
_cell_length_b                     16.1023(7)
_cell_length_c                     10.3382(4)
_cell_angle_alpha                  90
_cell_angle_beta                   115.201(8)
_cell_angle_gamma                  90
_cell_volume                       2832.9(3)
_cell_formula_units_Z              4
_cell_measurement_temperature      100(2)
_exptl_crystal_size_max            0.09
_exptl_crystal_size_mid            0.07
_exptl_crystal_size_min            0.01
_cell_measurement_reflns_used      32265
_cell_measurement_theta_min        1.715
_cell_measurement_theta_max        44.46
_exptl_crystal_description         platlet
_exptl_crystal_colour              green
_exptl_crystal_density_diffrn      1.314
_exptl_crystal_density_method      'not measured'
_exptl_crystal_F_000               1194
_exptl_absorpt_coefficient_mu      0.386
_exptl_absorpt_correction_type     none

#==========================================================
==================

# EXPERIMENTAL DATA

_exptl_special_details
;
  ?
;
_diffrn_ambient_temperature        100(2)
_diffrn_radiation_type             synchrotron
_diffrn_radiation_wavelength       0.7
_diffrn_source                     'bending magnet'
_diffrn_radiation_monochromator    silicon
_diffrn_measurement_device_type
cylindrical_IP_camera_at_SPring-8_BL02B1
_diffrn_measurement_method         'phi or omega oscillation scans'
_diffrn_detector_area_resol_mean   10
_diffrn_reflns_number              39666
_diffrn_reflns_av_R_equivalents    0.0787
_diffrn_reflns_theta_min           1.715
_diffrn_reflns_theta_max           27.496
_diffrn_reflns_theta_full          24.835
_diffrn_measured_fraction_theta_max
                                   0.973
```

```
_diffrn_measured_fraction_theta_full
                                        0.989
_diffrn_reflns_Laue_measured_fraction_full
                                        0.989
_diffrn_reflns_Laue_measured_fraction_max
                                        0.973
_diffrn_reflns_point_group_measured_fraction_full
                                        0.989
_diffrn_reflns_point_group_measured_fraction_max
                                        0.973
_diffrn_reflns_limit_h_min              -31
_diffrn_reflns_limit_h_max              31
_diffrn_reflns_limit_k_min              -26
_diffrn_reflns_limit_k_max              25
_diffrn_reflns_limit_l_min              -17
_diffrn_reflns_limit_l_max              17
_diffrn_reflns_reduction_process
;
  Scaled and merged with Sortav
  R.H. Blessing, (1987) Cryst. Rev. 1, 3-58
  R.H. Blessing, (1989) J. Appl. Cryst. 22, 396-397
;

#=============================================================
==================

# STRUCTURE SOLUTION

_atom_sites_solution_hydrogens          geom
```

```
#=============================================================
==================

# REFINEMENT DATA

_refine_special_details
;
  The occupancy of 'CU01' was fixed as 0.25
  (a half of the ideal value) during the refinement.
;
_reflns_number_total                    3319
_reflns_number_gt                       1444
_reflns_threshold_expression            'I > 2¥s(I)'
_refine_ls_structure_factor_coef        Fsqd
_refine_ls_matrix_type                  full
_refine_ls_R_factor_all                 0.0818
_refine_ls_R_factor_gt                  0.057
_refine_ls_wR_factor_ref                0.1169
_refine_ls_goodness_of_fit_ref          0.891
_refine_ls_restrained_S_all             0.891
_refine_ls_number_reflns                3319
_refine_ls_number_parameters            189
_refine_ls_number_restraints            0
_refine_ls_number_constraints           0
_refine_ls_hydrogen_treatment           constr
_refine_ls_weighting_scheme             calc
_refine_ls_weighting_details
                    'w=1/[¥s^2^(Fo^2^)+(0.0286P)^2^]          where
P=(Fo^2^+2Fc^2^)/3'
_refine_ls_shift/su_max                 0
_refine_ls_shift/su_mean                0
```

```
_refine_diff_density_max                0.399
_refine_diff_density_min                -0.525
_refine_diff_density_rms                0.057
_refine_ls_extinction_method            none
loop_
    _atom_type_symbol
    _atom_type_description
    _atom_type_scat_dispersion_real
    _atom_type_scat_dispersion_imag
    _atom_type_scat_source
C C 0.003 0.0016 'International Tables Vol C Tables 4.2.6.8 and 6.1.1.4'
H H 0 0 'International Tables Vol C Tables 4.2.6.8 and 6.1.1.4'
N N 0.0059 0.0032 'International Tables Vol C Tables 4.2.6.8 and 6.1.1.4'
Cu Cu 0.3261 1.2361 'International Tables Vol C Tables 4.2.6.8 and 6.1.1.4'

_computing_data_collection              'CrystalClear (Rigaku/MSC Inc., 2006)'
_computing_cell_refinement              'CrystalClear (Rigaku/MSC Inc., 2006)'
_computing_data_reduction
                    'CrystalClear (Rigaku/MSC Inc., 2006), SORTAV (Blessing, 1995)'
_computing_structure_solution           'SIR 92'
_computing_structure_refinement         'SHELXL-2014 (Sheldrick, 2014)'
_computing_molecular_graphics           'Mercury 3.3, CCDC, 2013'
_computing_publication_material         'enCIFer 1.4, CCDC, 2011'

#=============================================================
==================

# ATOMIC COORDINATES AND DISPLACEMENT PARAMETERS

loop_
    _atom_site_label
    _atom_site_fract_x
    _atom_site_fract_y
    _atom_site_fract_z
    _atom_site_U_iso_or_equiv
    _atom_site_adp_type
    _atom_site_calc_flag
    _atom_site_occupancy
    _atom_site_disorder_assembly
    _atom_site_disorder_group
    _atom_site_type_symbol
Cu01 1 0.20440(6) 0.75 0.0224(3) Uani d 0.5 . . Cu
N001 0.91097(12) 0.14287(14) 0.7361(2) 0.0209(5) Uani d 1 . . N
N002 0.99452(12) 0.27331(16) 0.8957(2) 0.0247(5) Uani d 1 . . N
C004 0.81591(15) 0.04351(17) 0.6607(3) 0.0212(5) Uani d 1 . . C
H001 0.787 -0.004 0.6117 0.025 Uiso calc 1 . . H
C005 0.86945(14) 0.22418(16) 0.8931(3) 0.0183(5) Uani d 1 . . C
C006 0.67840(14) 0.28900(15) 0.9128(3) 0.0160(5) Uani d 1 . . C
C007 0.60195(15) 0.32908(16) 0.8168(3) 0.0213(5) Uani d 1 . . C
H02A 0.6123 0.3831 0.7846 0.032 Uiso calc 1 . . H
H02B 0.5697 0.3369 0.8694 0.032 Uiso calc 1 . . H
H02C 0.5739 0.2934 0.7337 0.032 Uiso calc 1 . . H
C008 0.94640(15) 0.35790(17) 1.0153(3) 0.0215(5) Uani d 1 . . C
C009 1.01684(16) 0.38981(17) 1.0213(3) 0.0251(6) Uani d 1 . . C
H003 1.0419 0.4393 1.0691 0.03 Uiso calc 1 . . H
C010 0.73255(15) 0.07864(18) 0.7907(3) 0.0243(6) Uani d 1 . . C
H04A 0.7057 0.027 0.7461 0.036 Uiso calc 1 . . H
H04B 0.6956 0.1251 0.7561 0.036 Uiso calc 1 . . H
H04C 0.7523 0.0742 0.8948 0.036 Uiso calc 1 . . H
C011 0.88470(15) 0.07654(17) 0.6524(3) 0.0220(6) Uani d 1 . . C
C012 0.79957(14) 0.09316(17) 0.7528(3) 0.0205(5) Uani d 1 . . C
C013 0.73717(14) 0.27826(15) 0.8623(3) 0.0168(5) Uani d 1 . . C
```

C014 0.80765(13) 0.23804(15) 0.9497(3) 0.0160(5) Uani d 1 . . C
C015 0.86040(14) 0.15668(15) 0.8022(3) 0.0167(5) Uani d 1 . . C
C016 0.93270(13) 0.28180(17) 0.9354(3) 0.0191(5) Uani d 1 . . C
C017 0.89899(17) 0.39745(19) 1.0823(3) 0.0298(6) Uani d 1 . . C
H05A 0.9226 0.4509 1.124 0.045 Uiso calc 1 . . H
H05B 0.8979 0.3611 1.1574 0.045 Uiso calc 1 . . H
H05C 0.8453 0.4064 1.0096 0.045 Uiso calc 1 . . H
C018 0.72122(17) 0.30955(17) 0.7166(3) 0.0235(6) Uani d 1 . . C
H06A 0.6691 0.3355 0.6737 0.035 Uiso calc 1 . . H
H06B 0.7612 0.3506 0.7238 0.035 Uiso calc 1 . . H
H06C 0.7229 0.2631 0.6567 0.035 Uiso calc 1 . . H
C003 1.04398(15) 0.33791(18) 0.9469(3) 0.0234(6) Uani d 1 . . C
C002 0.92244(16) 0.04341(18) 0.5624(3) 0.0271(6) Uani d 1 . . C
H07A 0.8934 -0.0055 0.5098 0.041 Uiso calc 1 . . H
H07B 0.9219 0.0862 0.4945 0.041 Uiso calc 1 . . H
H07C 0.9769 0.0277 0.6236 0.041 Uiso calc 1 . . H
C001 1.11561(16) 0.3480(2) 0.9168(3) 0.0338(7) Uani d 1 . . C
H08A 1.1439 0.3986 0.9631 0.051 Uiso calc 1 . . H
H08B 1.1502 0.2998 0.9543 0.051 Uiso calc 1 . . H
H08C 1.099 0.352 0.8134 0.051 Uiso calc 1 . . H

loop_
_atom_site_aniso_label
_atom_site_aniso_U_11
_atom_site_aniso_U_22
_atom_site_aniso_U_33
_atom_site_aniso_U_12
_atom_site_aniso_U_13
_atom_site_aniso_U_23
Cu01 0.0213(5) 0.0228(5) 0.0274(5) 0 0.0144(4) 0
N001 0.0178(11) 0.0244(12) 0.0221(11) 0.0013(9) 0.0100(10) -0.0031(9)
N002 0.0169(11) 0.0363(14) 0.0249(11) -0.0047(10) 0.0127(10) -0.0094(10)
C004 0.0182(13) 0.0183(12) 0.0249(14) -0.0029(10) 0.0070(11) -0.0037(10)
C005 0.0144(12) 0.0262(13) 0.0147(11) 0.0021(10) 0.0065(10) 0.0021(10)
C006 0.0099(12) 0.0186(13) 0.0164(12) 0.0008(9) 0.0028(10) -0.0005(9)
C007 0.0155(13) 0.0266(14) 0.0214(13) 0.0022(10) 0.0074(11) 0.0016(11)
C008 0.0178(13) 0.0250(14) 0.0201(13) -0.0016(11) 0.0066(11) 0.0002(11)
C009 0.0239(15) 0.0286(15) 0.0228(14) -0.0063(11) 0.0100(12) -0.0018(11)
C010 0.0196(14) 0.0292(15) 0.0249(14) -0.0062(11) 0.0103(12) -0.0007(12)
C011 0.0153(13) 0.0281(15) 0.0195(13) 0.0024(10) 0.0044(11) 0.0002(10)
C012 0.0140(12) 0.0251(14) 0.0209(13) 0.0016(10) 0.0060(11) 0.0014(10)
C013 0.0138(12) 0.0160(12) 0.0210(12) -0.0006(9) 0.0078(11) 0.0014(10)
C014 0.0079(11) 0.0204(13) 0.0193(12) -0.0016(9) 0.0054(10) -0.0028(9)
C015 0.0125(12) 0.0201(12) 0.0191(12) 0.0019(9) 0.0083(10) 0.0020(10)
C016 0.0140(13) 0.0279(14) 0.0180(13) -0.0012(10) 0.0093(11) -0.0016(10)
C017 0.0216(15) 0.0310(16) 0.0369(16) -0.0027(11) 0.0127(13) -0.0114(12)
C018 0.0193(14) 0.0330(15) 0.0210(13) 0.0036(11) 0.0112(12) 0.0021(11)
C003 0.0206(14) 0.0332(16) 0.0184(14) -0.0100(11) 0.0102(12) -0.0037(11)
C002 0.0246(15) 0.0314(15) 0.0287(15) -0.0022(12) 0.0145(13) -0.0102(12)
C001 0.0236(15) 0.058(2) 0.0231(15) -0.0180(14) 0.0135(13) -0.0105(14)

#==========
==========

# MOLECULAR GEOMETRY

_geom_special_details
;
All esds (except the esd in the dihedral angle between two l.s. planes)
are estimated using the full covariance matrix. The cell esds are taken
into account individually in the estimation of esds in distances, angles
and torsion angles; correlations between esds in cell parameters are only
used when they are defined by crystal symmetry. An approximate (isotropic)
treatment of cell esds is used for estimating esds involving l.s. planes.
;
loop_
_geom_bond_atom_site_label_1
_geom_bond_atom_site_label_2
_geom_bond_site_symmetry_2
_geom_bond_distance
_geom_bond_publ_flag
Cu01 N001 . 1.898(2) ?
Cu01 N001 2_756 1.898(2) ?
Cu01 N002 . 1.908(2) ?
Cu01 N002 2_756 1.908(2) ?
N001 C011 . 1.330(3) ?
N001 C015 . 1.405(3) ?
N002 C003 . 1.345(4) ?
N002 C016 . 1.395(3) ?
C004 C012 . 1.374(3) ?
C004 C011 . 1.435(3) ?
C004 H001 . 0.95 ?
C005 C015 . 1.399(4) ?
C005 C016 . 1.423(4) ?
C005 C014 . 1.524(3) ?
C006 C014 7_657 1.400(3) ?
C006 C013 . 1.420(3) ?
C006 C007 . 1.501(4) ?
C007 H02A . 0.98 ?
C007 H02B . 0.98 ?
C007 H02C . 0.98 ?
C008 C009 . 1.397(4) ?
C008 C016 . 1.438(4) ?
C008 C017 . 1.485(4) ?
C009 C003 . 1.373(4) ?
C009 H003 . 0.95 ?
C010 C012 . 1.489(3) ?
C010 H04A . 0.98 ?
C010 H04B . 0.98 ?
C010 H04C . 0.98 ?
C011 C002 . 1.489(3) ?
C012 C015 . 1.455(4) ?
C013 C014 . 1.405(3) ?
C013 C018 . 1.493(4) ?
C014 C006 7_657 1.400(3) ?
C017 H05A . 0.98 ?
C017 H05B . 0.98 ?
C017 H05C . 0.98 ?
C018 H06A . 0.98 ?
C018 H06B . 0.98 ?
C018 H06C . 0.98 ?
C003 C001 . 1.515(3) ?
C002 H07A . 0.98 ?
C002 H07B . 0.98 ?
C002 H07C . 0.98 ?
C001 H08A . 0.98 ?
C001 H08B . 0.98 ?
C001 H08C . 0.98 ?

loop_
_geom_angle_atom_site_label_1
_geom_angle_atom_site_label_2
_geom_angle_atom_site_label_3

```
    _geom_angle
    _geom_angle_site_symmetry_1
    _geom_angle_site_symmetry_3
    _geom_angle_publ_flag
N001 Cu01 N001 117.05(14) . 2_756 ?
N001 Cu01 N002 91.21(9) . . ?
N001 Cu01 N002 125.88(9) 2_756 . ?
N001 Cu01 N002 125.88(9) . 2_756 ?
N001 Cu01 N002 91.20(9) 2_756 2_756 ?
N002 Cu01 N002 108.90(16) . 2_756 ?
C011 N001 C015 107.6(2) . . ?
C011 N001 Cu01 122.68(16) . . ?
C015 N001 Cu01 129.69(18) . . ?
C003 N002 C016 109.4(2) . . ?
C003 N002 Cu01 119.98(16) . . ?
C016 N002 Cu01 128.39(18) . . ?
C012 C004 C011 107.4(2) . . ?
C012 C004 H001 126.3 . . ?
C011 C004 H001 126.3 . . ?
C015 C005 C016 124.1(2) . . ?
C015 C005 C014 118.5(2) . . ?
C016 C005 C014 117.4(2) . . ?
C014 C006 C013 119.8(2) 7_657 . ?
C014 C006 C007 121.15(19) 7_657 . ?
C013 C006 C007 119.1(2) . . ?
C006 C007 H02A 109.5 . . ?
C006 C007 H02B 109.5 . . ?
H02A C007 H02B 109.5 . . ?
C006 C007 H02C 109.5 . . ?
H02A C007 H02C 109.5 . . ?
H02B C007 H02C 109.5 . . ?
C009 C008 C016 105.9(2) . . ?
C009 C008 C017 124.6(2) . . ?
C016 C008 C017 129.5(2) . . ?
C003 C009 C008 108.8(2) . . ?
C003 C009 H003 125.6 . . ?
C008 C009 H003 125.6 . . ?
C012 C010 H04A 109.5 . . ?
C012 C010 H04B 109.5 . . ?
H04A C010 H04B 109.5 . . ?
C012 C010 H04C 109.5 . . ?
H04A C010 H04C 109.5 . . ?
H04B C010 H04C 109.5 . . ?
N001 C011 C004 110.7(2) . . ?
N001 C011 C002 123.4(2) . . ?
C004 C011 C002 125.9(2) . . ?
C004 C012 C015 106.1(2) . . ?
C004 C012 C010 123.7(2) . . ?
C015 C012 C010 130.1(2) . . ?
C014 C013 C006 119.3(2) . . ?
C014 C013 C018 122.3(2) . . ?
C006 C013 C018 118.5(2) . . ?
C006 C014 C013 120.92(19) 7_657 . ?
C006 C014 C005 120.0(2) 7_657 . ?
C013 C014 C005 119.0(2) . . ?
C005 C015 N001 122.4(2) . . ?
C005 C015 C012 129.4(2) . . ?
N001 C015 C012 108.2(2) . . ?
N002 C016 C005 122.6(2) . . ?
N002 C016 C008 106.5(2) . . ?
C005 C016 C008 130.9(2) . . ?
C008 C017 H05A 109.5 . . ?
C008 C017 H05B 109.5 . . ?
H05A C017 H05B 109.5 . . ?
C008 C017 H05C 109.5 . . ?
H05A C017 H05C 109.5 . . ?
H05B C017 H05C 109.5 . . ?
C013 C018 H06A 109.5 . . ?
C013 C018 H06B 109.5 . . ?
H06A C018 H06B 109.5 . . ?
C013 C018 H06C 109.5 . . ?
H06A C018 H06C 109.5 . . ?
H06B C018 H06C 109.5 . . ?
N002 C003 C009 109.4(2) . . ?
N002 C003 C001 121.9(2) . . ?
C009 C003 C001 128.7(3) . . ?
C011 C002 H07A 109.5 . . ?
C011 C002 H07B 109.5 . . ?
H07A C002 H07B 109.5 . . ?
C011 C002 H07C 109.5 . . ?
H07A C002 H07C 109.5 . . ?
H07B C002 H07C 109.5 . . ?
C003 C001 H08A 109.5 . . ?
C003 C001 H08B 109.5 . . ?
H08A C001 H08B 109.5 . . ?
C003 C001 H08C 109.5 . . ?
H08A C001 H08C 109.5 . . ?
H08B C001 H08C 109.5 . . ?

loop_
    _geom_torsion_atom_site_label_1
    _geom_torsion_atom_site_label_2
    _geom_torsion_atom_site_label_3
    _geom_torsion_atom_site_label_4
    _geom_torsion
    _geom_torsion_site_symmetry_1
    _geom_torsion_site_symmetry_2
    _geom_torsion_site_symmetry_3
    _geom_torsion_site_symmetry_4
    _geom_torsion_publ_flag
N001 Cu01 N001 C011 -43.47(19) 2_756 . . . ?
N002 Cu01 N001 C011 -175.5(2) . . . . ?
N002 Cu01 N001 C011 70.0(2) 2_756 . . . ?
N001 Cu01 N001 C015 138.5(3) 2_756 . . . ?
N002 Cu01 N001 C015 6.5(2) . . . . ?
N002 Cu01 N001 C015 -108.0(2) 2_756 . . . ?
C016 C008 C009 C003 1.4(3) . . . . ?
C017 C008 C009 C003 -179.4(3) . . . . ?
C015 N001 C011 C004 -0.4(3) . . . . ?
Cu01 N001 C011 C004 -178.82(18) . . . . ?
C015 N001 C011 C002 178.9(2) . . . . ?
Cu01 N001 C011 C002 0.5(4) . . . . ?
C012 C004 C011 N001 0.8(3) . . . . ?
C012 C004 C011 C002 -178.5(2) . . . . ?
C011 C004 C012 C015 -0.8(3) . . . . ?
C011 C004 C012 C010 -179.4(2) . . . . ?
C014 C006 C013 C014 2.1(4) 7_657 . . . ?
C007 C006 C013 C014 -177.7(2) . . . . ?
C014 C006 C013 C018 -178.6(2) 7_657 . . . ?
C007 C006 C013 C018 1.7(4) . . . . ?
C006 C013 C014 C006 -2.1(4) . . . 7_657 ?
C018 C013 C014 C006 178.6(2) . . . 7_657 ?
C006 C013 C014 C005 178.0(2) . . . . ?
C018 C013 C014 C005 -1.3(4) . . . . ?
```

C015 C005 C014 C006 98.9(3) . . . 7_657 ?
C016 C005 C014 C006 -81.7(3) . . . 7_657 ?
C015 C005 C014 C013 -81.2(3) . . . . ?
C016 C005 C014 C013 98.2(3) . . . . ?
C016 C005 C015 N001 -4.4(4) . . . . ?
C014 C005 C015 N001 174.9(2) . . . . ?
C016 C005 C015 C012 179.1(3) . . . . ?
C014 C005 C015 C012 -1.6(4) . . . . ?
C011 N001 C015 C005 -177.2(2) . . . . ?
Cu01 N001 C015 C005 1.0(4) . . . . ?
C011 N001 C015 C012 -0.1(3) . . . . ?
Cu01 N001 C015 C012 178.18(18) . . . . ?
C004 C012 C015 C005 177.4(3) . . . . ?
C010 C012 C015 C005 -4.0(5) . . . . ?
C004 C012 C015 N001 0.5(3) . . . . ?
C010 C012 C015 N001 179.1(3) . . . . ?
C003 N002 C016 C005 178.0(2) . . . . ?
Cu01 N002 C016 C005 15.3(4) . . . . ?
C003 N002 C016 C008 0.6(3) . . . . ?
Cu01 N002 C016 C008 -162.1(2) . . . . ?
C015 C005 C016 N002 -3.7(4) . . . . ?
C014 C005 C016 N002 177.0(2) . . . . ?
C015 C005 C016 C008 173.1(3) . . . . ?
C014 C005 C016 C008 -6.3(4) . . . . ?
C009 C008 C016 N002 -1.2(3) . . . . ?
C017 C008 C016 N002 179.6(3) . . . . ?
C009 C008 C016 C005 -178.3(3) . . . . ?
C017 C008 C016 C005 2.5(5) . . . . ?
C016 N002 C003 C009 0.3(3) . . . . ?
Cu01 N002 C003 C009 164.70(19) . . . . ?
C016 N002 C003 C001 -177.7(3) . . . . ?
Cu01 N002 C003 C001 -13.3(4) . . . . ?
C008 C009 C003 N002 -1.1(3) . . . . ?
C008 C009 C003 C001 176.8(3) . . . . ?

## Crystallographic data of NiCP

```
#------------------ SECTION 1. GLOBAL INFORMATION --------------------------#

data_global

#==========================================================
==================
#
# SUBMISSION DETAILS
# Name and address of author for correspondence

_publ_contact_author_name          'Professor Hiroshi Nishihara'
_publ_contact_author_address
;Department of Chemistry, Graduate School of Science, The University of Tokyo,
7-3-1, Hongo, Bunkyo-ku, Tokyo 113-0033, Japan

;
_publ_contact_author_email         nishihara@chem.s.u-tokyo.ac.jp
_publ_contact_author_phone         '+81-3-5841-4346 '
_publ_contact_author_fax           '+81-3-5841-8063 '
loop_
  _publ_author_name
'Matsuoka, Ryota'
'Toyoda, Ryojun'
'Sakamoto, Ryota'
'Tsuchiya, Mizuho'
'Hoshiko, Ken'
'Tatsuhiro, Nagayama'
'Nonoguchi, Yoshiyuki'
'Nishibori, Eiji'
'Kawai, Tsuyoshi'
'Nishihara, Hiroshi'

_publ_requested_journal            Chem.Sci.

#==========================================================
==================
#

#------------------    SECTION 2. COMPOUND(S) DETAILS ------------------------#

#==========================================================
==================

# CHEMICAL DATA

_chemical_name_systematic
;
  ?
;
_chemical_formula_moiety           'C36 H40 N4 Ni0.50'
_chemical_formula_sum              'C36 H40 N4 Ni0.50'
_chemical_formula_weight           558.07

#==========================================================
==================

# CRYSTAL DATA

_symmetry_cell_setting             monoclinic
_symmetry_space_group_name_H-M     'C 2/c'
_symmetry_space_group_name_Hall    '-C 2yc'
loop_
    _symmetry_equiv_pos_as_xyz
'x, y, z'
'-x, y, -z+1/2'
'x+1/2, y+1/2, z'
'-x+1/2, y+1/2, -z+1/2'
'-x, -y, -z'
'x, -y, z-1/2'
'-x+1/2, -y+1/2, -z'
'x+1/2, -y+1/2, z-1/2'

_cell_length_a                     18.8249(10)
_cell_length_b                     15.9650(10)
_cell_length_c                     10.4056(6)
_cell_angle_alpha                  90
_cell_angle_beta                   114.696(8)
_cell_angle_gamma                  90
_cell_volume                       2841.3(3)
_cell_formula_units_Z              4
_cell_measurement_temperature      100(2)
_exptl_crystal_size_max            0.07
_exptl_crystal_size_mid            0.06
_exptl_crystal_size_min            0.01
_cell_measurement_reflns_used      64773
_cell_measurement_theta_min        1.72
_cell_measurement_theta_max        44.43
_exptl_crystal_description         platlet
_exptl_crystal_colour              green
_exptl_crystal_density_diffrn      1.305
_exptl_crystal_density_method      'not measured'
_exptl_crystal_F_000               1192
_exptl_absorpt_coefficient_mu      0.343
_exptl_absorpt_correction_type     none

#==========================================================
==================

# EXPERIMENTAL DATA

_exptl_special_details
;
  ?
;
_diffrn_ambient_temperature        100(2)
_diffrn_radiation_type             synchrotron
_diffrn_radiation_wavelength       0.7
_diffrn_source                     'bending magnet'
_diffrn_radiation_monochromator    silicon
_diffrn_measurement_device_type
cylindrical_IP_camera_at_SPring-8_BL02B1
_diffrn_measurement_method         'phi or omega oscillation scans'
_diffrn_detector_area_resol_mean   10
_diffrn_reflns_number              64773
_diffrn_reflns_av_R_equivalents    0.0598
_diffrn_reflns_theta_min           1.719
_diffrn_reflns_theta_max           27.5
_diffrn_reflns_theta_full          24.835
_diffrn_measured_fraction_theta_max
                                   0.964
```

```
_diffrn_measured_fraction_theta_full
                                        0.984
_diffrn_reflns_Laue_measured_fraction_full
                                        0.984
_diffrn_reflns_Laue_measured_fraction_max
                                        0.964
_diffrn_reflns_point_group_measured_fraction_full
                                        0.984
_diffrn_reflns_point_group_measured_fraction_max
                                        0.964
_diffrn_reflns_limit_h_min              -34
_diffrn_reflns_limit_h_max              26
_diffrn_reflns_limit_k_min              -31
_diffrn_reflns_limit_k_max              30
_diffrn_reflns_limit_l_min              -15
_diffrn_reflns_limit_l_max              20
_diffrn_reflns_reduction_process
;
  Scaled and merged with Sortav
  R.H. Blessing, (1987) Cryst. Rev. 1, 3-58
  R.H. Blessing, (1989) J. Appl. Cryst. 22, 396-397
;

#=============================================================
==================

# STRUCTURE SOLUTION

_atom_sites_solution_hydrogens          geom
```

```
#=============================================================
==================

# REFINEMENT DATA

_refine_special_details
;
  The occupancy of 'NI01' was fixed as 0.25
  (a half of the ideal value) during the refinement.
;
_reflns_number_total                    3297
_reflns_number_gt                       2741
_reflns_threshold_expression            'I > 2¥s(I)'
_refine_ls_structure_factor_coef        Fsqd
_refine_ls_matrix_type                  full
_refine_ls_R_factor_all                 0.0629
_refine_ls_R_factor_gt                  0.0578
_refine_ls_wR_factor_ref                0.1291
_refine_ls_goodness_of_fit_ref          1.129
_refine_ls_restrained_S_all             1.129
_refine_ls_number_reflns                3297
_refine_ls_number_parameters            189
_refine_ls_number_restraints            0
_refine_ls_number_constraints           0
_refine_ls_hydrogen_treatment           constr
_refine_ls_weighting_scheme             calc
_refine_ls_weighting_details
                    'w=1/[¥s^2^(Fo^2^)+(0.0351P)^2^]          where
P=(Fo^2^+2Fc^2^)/3'
_refine_ls_shift/su_max                 0
_refine_ls_shift/su_mean                0
```

```
_refine_diff_density_max                0.535
_refine_diff_density_min                -0.589
_refine_diff_density_rms                0.061
_refine_ls_extinction_method            none
loop_
    _atom_type_symbol
    _atom_type_description
    _atom_type_scat_dispersion_real
    _atom_type_scat_dispersion_imag
    _atom_type_scat_source
C C 0.003 0.0016 'International Tables Vol C Tables 4.2.6.8 and 6.1.1.4'
H H 0 0 'International Tables Vol C Tables 4.2.6.8 and 6.1.1.4'
N N 0.0059 0.0032 'International Tables Vol C Tables 4.2.6.8 and 6.1.1.4'
Ni Ni 0.3431 1.0865 'International Tables Vol C Tables 4.2.6.8 and 6.1.1.4'

_computing_data_collection              'CrystalClear (Rigaku/MSC Inc., 2006)'
_computing_cell_refinement              'CrystalClear (Rigaku/MSC Inc., 2006)'
_computing_data_reduction
                    'CrystalClear (Rigaku/MSC Inc., 2006), SORTAV (Blessing, 1995)'
_computing_structure_solution           'SIR 92'
_computing_structure_refinement         'SHELXL-2014 (Sheldrick, 2014)'
_computing_molecular_graphics           'Mercury 3.3, CCDC, 2013'
_computing_publication_material         'enCIFer 1.4, CCDC, 2011'

#=============================================================
==================

# ATOMIC COORDINATES AND DISPLACEMENT PARAMETERS

loop_
    _atom_site_label
    _atom_site_fract_x
    _atom_site_fract_y
    _atom_site_fract_z
    _atom_site_U_iso_or_equiv
    _atom_site_adp_type
    _atom_site_calc_flag
    _atom_site_occupancy
    _atom_site_disorder_assembly
    _atom_site_disorder_group
    _atom_site_type_symbol
Ni01 0.5 0.20225(4) 0.75 0.0161(2) Uani d 0.5 . . Ni
N001 0.49713(10) 0.27047(11) 0.90204(17) 0.0178(4) Uani d 1 . . N
N002 0.40809(9) 0.14495(11) 0.72995(18) 0.0178(4) Uani d 1 . . N
C004 0.36960(11) 0.22406(12) 0.8935(2) 0.0162(4) Uani d 1 . . C
C005 0.32110(11) 0.21101(11) 1.08583(19) 0.0141(4) Uani d 1 . . C
C006 0.31374(12) 0.04451(13) 0.6580(2) 0.0201(4) Uani d 1 . . C
H001 0.2846 -0.0031 0.6094 0.024 Uiso calc 1 . . H
C007 0.26233(11) 0.22121(11) 1.1353(2) 0.0151(4) Uani d 1 . . C
C008 0.39742(12) 0.17079(12) 1.1808(2) 0.0182(4) Uani d 1 . . C
H02A 0.4257 0.2077 1.2614 0.027 Uiso calc 1 . . H
H02B 0.4291 0.1615 1.1276 0.027 Uiso calc 1 . . H
H02C 0.3871 0.117 1.2153 0.027 Uiso calc 1 . . H
C009 0.35873(11) 0.15786(12) 0.7994(2) 0.0150(4) Uani d 1 . . C
C010 0.29870(11) 0.09354(12) 0.7513(2) 0.0175(4) Uani d 1 . . C
C011 0.30836(11) 0.23846(12) 0.94948(19) 0.0142(4) Uani d 1 . . C
C012 0.38183(12) 0.07826(13) 0.6470(2) 0.0203(4) Uani d 1 . . C
C013 0.51773(13) 0.38953(13) 1.0246(2) 0.0219(4) Uani d 1 . . C
H003 0.5419 0.4398 1.0713 0.026 Uiso calc 1 . . H
C014 0.54694(12) 0.33540(13) 0.9520(2) 0.0194(4) Uani d 1 . . C
C015 0.44767(12) 0.35738(13) 1.0167(2) 0.0197(4) Uani d 1 . . C
C016 0.23220(12) 0.07882(14) 0.7916(2) 0.0227(5) Uani d 1 . . C
```

H04A 0.1926 0.1225 0.7496 0.034 Uiso calc 1 . . H
H04B 0.2515 0.0805 0.8948 0.034 Uiso calc 1 . . H
H04C 0.209 0.0238 0.7568 0.034 Uiso calc 1 . . H
C017 0.43413(11) 0.28118(12) 0.9382(2) 0.0156(4) Uani d 1 . . C
C018 0.41988(13) 0.04522(15) 0.5576(2) 0.0245(5) Uani d 1 . . C
H05A 0.3911 -0.004 0.5053 0.037 Uiso calc 1 . . H
H05B 0.4197 0.0885 0.4907 0.037 Uiso calc 1 . . H
H05C 0.4739 0.0293 0.618 0.037 Uiso calc 1 . . H
C003 0.27759(12) 0.18884(13) 1.2810(2) 0.0198(4) Uani d 1 . . C
H06A 0.3295 0.1629 1.3236 0.03 Uiso calc 1 . . H
H06B 0.2754 0.2355 1.3405 0.03 Uiso calc 1 . . H
H06C 0.2378 0.1472 1.2735 0.03 Uiso calc 1 . . H
C002 0.39957(14) 0.39919(14) 1.0808(3) 0.0266(5) Uani d 1 . . C
H07A 0.422 0.4542 1.1175 0.04 Uiso calc 1 . . H
H07B 0.3991 0.3647 1.1583 0.04 Uiso calc 1 . . H
H07C 0.346 0.4062 1.0088 0.04 Uiso calc 1 . . H
C001 0.61771(12) 0.34497(16) 0.9214(2) 0.0268(5) Uani d 1 . . C
H08A 0.6461 0.3959 0.967 0.04 Uiso calc 1 . . H
H08B 0.6519 0.2963 0.9582 0.04 Uiso calc 1 . . H
H08C 0.6013 0.349 0.819 0.04 Uiso calc 1 . . H

loop_
    _atom_site_aniso_label
    _atom_site_aniso_U_11
    _atom_site_aniso_U_22
    _atom_site_aniso_U_33
    _atom_site_aniso_U_12
    _atom_site_aniso_U_13
    _atom_site_aniso_U_23
Ni01 0.0116(4) 0.0197(4) 0.0197(4) 0 0.0090(3) 0
N001 0.0121(9) 0.0248(9) 0.0184(8) -0.0010(6) 0.0084(7) -0.0017(6)
N002 0.0144(9) 0.0216(8) 0.0186(8) 0.0033(7) 0.0080(7) -0.0005(6)
C004 0.0122(10) 0.0225(9) 0.0151(9) 0.0032(7) 0.0067(8) 0.0030(7)
C005 0.0073(10) 0.0172(9) 0.0174(9) 0.0004(7) 0.0046(7) -0.0003(7)
C006 0.0152(10) 0.0203(9) 0.0221(10) -0.0002(8) 0.0050(8) -0.0014(8)
C007 0.0103(10) 0.0170(8) 0.0175(9) -0.0005(7) 0.0053(7) -0.0012(7)
C008 0.0128(10) 0.0242(10) 0.0171(9) 0.0040(7) 0.0056(8) 0.0037(7)
C009 0.0096(10) 0.0198(9) 0.0166(9) 0.0015(7) 0.0064(8) 0.0017(7)
C010 0.0109(11) 0.0207(9) 0.0184(9) 0.0003(7) 0.0037(8) 0.0015(7)
C011 0.0073(10) 0.0175(9) 0.0183(9) -0.0013(7) 0.0058(8) -0.0022(7)
C012 0.0182(11) 0.0238(10) 0.0183(9) 0.0034(8) 0.0070(8) 0.0006(7)
C013 0.0158(11) 0.0241(10) 0.0239(10) -0.0049(8) 0.0066(8) -0.0021(8)
C014 0.0124(11) 0.0256(10) 0.0204(10) -0.0029(7) 0.0069(8) 0.0015(7)
C015 0.0173(11) 0.0214(9) 0.0206(10) -0.0020(8) 0.0081(8) -0.0005(7)
C016 0.0145(12) 0.0286(11) 0.0277(11) -0.0046(8) 0.0113(9) -0.0006(9)
C017 0.0108(10) 0.0216(9) 0.0166(9) 0.0018(7) 0.0081(7) -0.0001(7)
C018 0.0226(12) 0.0293(11) 0.0248(11) 0.0008(9) 0.0132(9) -0.0051(9)
C003 0.0143(11) 0.0276(10) 0.0195(9) 0.0049(8) 0.0088(8) 0.0046(8)
C002 0.0203(12) 0.0276(11) 0.0360(12) -0.0055(9) 0.0159(10) -0.0117(9)
C001 0.0160(12) 0.0411(13) 0.0249(11) -0.0072(9) 0.0101(9) 0.0007(9)

#==========
==========

# MOLECULAR GEOMETRY

_geom_special_details
;
 All esds (except the esd in the dihedral angle between two l.s. planes)
 are estimated using the full covariance matrix.  The cell esds are taken
 into account individually in the estimation of esds in distances, angles
 and torsion angles; correlations between esds in cell parameters are only
 used when they are defined by crystal symmetry.  An approximate (isotropic)
 treatment of cell esds is used for estimating esds involving l.s. planes.
;
loop_
    _geom_bond_atom_site_label_1
    _geom_bond_atom_site_label_2
    _geom_bond_site_symmetry_2
    _geom_bond_distance
    _geom_bond_publ_flag
Ni01 N002 2_656 1.8899(17) ?
Ni01 N002 . 1.8900(17) ?
Ni01 N001 2_656 1.9399(17) ?
Ni01 N001 . 1.9400(17) ?
N001 C014 . 1.348(3) ?
N001 C017 . 1.397(2) ?
N002 C012 . 1.329(3) ?
N002 C009 . 1.411(2) ?
C004 C009 . 1.396(3) ?
C004 C017 . 1.432(3) ?
C004 C011 . 1.511(3) ?
C005 C011 . 1.407(3) ?
C005 C007 . 1.411(3) ?
C005 C008 . 1.506(3) ?
C006 C010 . 1.365(3) ?
C006 C012 . 1.439(3) ?
C006 H001 . 0.95 ?
C007 C011 7_557 1.408(3) ?
C007 C003 . 1.512(3) ?
C008 H02A . 0.98 ?
C008 H02B . 0.98 ?
C008 H02C . 0.98 ?
C009 C010 . 1.452(3) ?
C010 C016 . 1.496(3) ?
C011 C007 7_557 1.408(3) ?
C012 C018 . 1.487(3) ?
C013 C015 . 1.385(3) ?
C013 C014 . 1.403(3) ?
C013 H003 . 0.95 ?
C014 C001 . 1.501(3) ?
C015 C017 . 1.427(3) ?
C015 C002 . 1.488(3) ?
C016 H04A . 0.98 ?
C016 H04B . 0.98 ?
C016 H04C . 0.98 ?
C018 H05A . 0.98 ?
C018 H05B . 0.98 ?
C018 H05C . 0.98 ?
C003 H06A . 0.98 ?
C003 H06B . 0.98 ?
C003 H06C . 0.98 ?
C002 H07A . 0.98 ?
C002 H07B . 0.98 ?
C002 H07C . 0.98 ?
C001 H08A . 0.98 ?
C001 H08B . 0.98 ?
C001 H08C . 0.98 ?

loop_
    _geom_angle_atom_site_label_1
    _geom_angle_atom_site_label_2
    _geom_angle_atom_site_label_3

```
    _geom_angle
    _geom_angle_site_symmetry_1
    _geom_angle_site_symmetry_3
    _geom_angle_publ_flag
N002 Ni01 N002 122.10(10) 2_656 . ?
N002 Ni01 N001 91.47(7) 2_656 2_656 ?
N002 Ni01 N001 121.18(7) . 2_656 ?
N002 Ni01 N001 121.18(7) 2_656 . ?
N002 Ni01 N001 91.47(7) . . ?
N001 Ni01 N001 111.70(11) 2_656 . ?
C014 N001 C017 109.52(17) . . ?
C014 N001 Ni01 119.63(13) . . ?
C017 N001 Ni01 127.21(13) . . ?
C012 N002 C009 107.69(17) . . ?
C012 N002 Ni01 122.30(14) . . ?
C009 N002 Ni01 129.89(14) . . ?
C009 C004 C017 124.47(16) . . ?
C009 C004 C011 118.26(16) . . ?
C017 C004 C011 117.24(16) . . ?
C011 C005 C007 120.18(17) . . ?
C011 C005 C008 120.58(16) . . ?
C007 C005 C008 119.24(16) . . ?
C010 C006 C012 107.36(18) . . ?
C010 C006 H001 126.3 . . ?
C012 C006 H001 126.3 . . ?
C011 C007 C005 120.29(17) 7_557 . ?
C011 C007 C003 121.21(16) 7_557 . ?
C005 C007 C003 118.50(17) . . ?
C005 C008 H02A 109.5 . . ?
C005 C008 H02B 109.5 . . ?
H02A C008 H02B 109.5 . . ?
C005 C008 H02C 109.5 . . ?
H02A C008 H02C 109.5 . . ?
H02B C008 H02C 109.5 . . ?
C004 C009 N002 122.32(17) . . ?
C004 C009 C010 129.95(17) . . ?
N002 C009 C010 107.71(16) . . ?
C006 C010 C009 106.74(17) . . ?
C006 C010 C016 123.76(19) . . ?
C009 C010 C016 129.50(17) . . ?
C007 C011 C005 119.50(16) 7_557 . ?
C007 C011 C004 120.12(16) 7_557 . ?
C005 C011 C004 120.38(16) . . ?
N002 C012 C006 110.50(18) . . ?
N002 C012 C018 122.99(19) . . ?
C006 C012 C018 126.51(19) . . ?
C015 C013 C014 108.50(19) . . ?
C015 C013 H003 125.7 . . ?
C014 C013 H003 125.7 . . ?
N001 C014 C013 108.39(18) . . ?
N001 C014 C001 122.17(19) . . ?
C013 C014 C001 129.3(2) . . ?
C013 C015 C017 106.74(17) . . ?
C013 C015 C002 123.33(19) . . ?
C017 C015 C002 129.93(18) . . ?
C010 C016 H04A 109.5 . . ?
C010 C016 H04B 109.5 . . ?
H04A C016 H04B 109.5 . . ?
C010 C016 H04C 109.5 . . ?
H04A C016 H04C 109.5 . . ?
H04B C016 H04C 109.5 . . ?
N001 C017 C004 122.32(17) . . ?
N001 C017 C015 106.84(16) . . ?
C004 C017 C015 130.79(16) . . ?
C012 C018 H05A 109.5 . . ?
C012 C018 H05B 109.5 . . ?
H05A C018 H05B 109.5 . . ?
C012 C018 H05C 109.5 . . ?
H05A C018 H05C 109.5 . . ?
H05B C018 H05C 109.5 . . ?
C007 C003 H06A 109.5 . . ?
C007 C003 H06B 109.5 . . ?
H06A C003 H06B 109.5 . . ?
C007 C003 H06C 109.5 . . ?
H06A C003 H06C 109.5 . . ?
H06B C003 H06C 109.5 . . ?
C015 C002 H07A 109.5 . . ?
C015 C002 H07B 109.5 . . ?
H07A C002 H07B 109.5 . . ?
C015 C002 H07C 109.5 . . ?
H07A C002 H07C 109.5 . . ?
H07B C002 H07C 109.5 . . ?
C014 C001 H08A 109.5 . . ?
C014 C001 H08B 109.5 . . ?
H08A C001 H08B 109.5 . . ?
C014 C001 H08C 109.5 . . ?
H08A C001 H08C 109.5 . . ?
H08B C001 H08C 109.5 . . ?

loop_
    _geom_torsion_atom_site_label_1
    _geom_torsion_atom_site_label_2
    _geom_torsion_atom_site_label_3
    _geom_torsion_atom_site_label_4
    _geom_torsion
    _geom_torsion_site_symmetry_1
    _geom_torsion_site_symmetry_2
    _geom_torsion_site_symmetry_3
    _geom_torsion_site_symmetry_4
    _geom_torsion_publ_flag
N002 Ni01 N002 C012 -42.84(14) 2_656 . . . ?
N001 Ni01 N002 C012 71.68(18) 2_656 . . . ?
N001 Ni01 N002 C012 -171.71(16) . . . . ?
N002 Ni01 N002 C009 132.85(18) 2_656 . . . ?
N001 Ni01 N002 C009 -112.63(17) 2_656 . . . ?
N001 Ni01 N002 C009 3.98(18) . . . . ?
C011 C005 C007 C011 -2.2(3) . . . 7_557 ?
C008 C005 C007 C011 177.55(17) . . . 7_557 ?
C011 C005 C007 C003 178.47(17) . . . . ?
C008 C005 C007 C003 -1.8(3) . . . . ?
C017 C004 C009 N002 -5.2(3) . . . . ?
C011 C004 C009 N002 173.07(16) . . . . ?
C017 C004 C009 C010 176.57(18) . . . . ?
C011 C004 C009 C010 -5.2(3) . . . . ?
C012 N002 C009 C004 -179.09(18) . . . . ?
Ni01 N002 C009 C004 4.7(3) . . . . ?
C012 N002 C009 C010 -0.5(2) . . . . ?
Ni01 N002 C009 C010 -176.69(13) . . . . ?
C012 C006 C010 C009 -0.6(2) . . . . ?
C012 C006 C010 C016 -179.94(19) . . . . ?
C004 C009 C010 C006 179.1(2) . . . . ?
N002 C009 C010 C006 0.7(2) . . . . ?
C004 C009 C010 C016 -1.6(3) . . . . ?
N002 C009 C010 C016 180.00(19) . . . . ?
```

C007 C005 C011 C007 2.2(3) . . . 7_557 ?
C008 C005 C011 C007 -177.56(17) . . . 7_557 ?
C007 C005 C011 C004 -177.14(17) . . . . ?
C008 C005 C011 C004 3.1(3) . . . . ?
C009 C004 C011 C007 -78.4(2) . . . 7_557 ?
C017 C004 C011 C007 100.0(2) . . . 7_557 ?
C009 C004 C011 C005 101.0(2) . . . . ?
C017 C004 C011 C005 -80.6(2) . . . . ?
C009 N002 C012 C006 0.2(2) . . . . ?
Ni01 N002 C012 C006 176.70(13) . . . . ?
C009 N002 C012 C018 -179.5(2) . . . . ?
Ni01 N002 C012 C018 -3.0(3) . . . . ?
C010 C006 C012 N002 0.3(2) . . . . ?
C010 C006 C012 C018 179.9(2) . . . . ?
C017 N001 C014 C013 1.0(2) . . . . ?
Ni01 N001 C014 C013 161.02(14) . . . . ?
C017 N001 C014 C001 -175.62(18) . . . . ?
Ni01 N001 C014 C001 -15.6(3) . . . . ?
C015 C013 C014 N001 -1.0(2) . . . . ?
C015 C013 C014 C001 175.4(2) . . . . ?
C014 C013 C015 C017 0.5(2) . . . . ?
C014 C013 C015 C002 -179.2(2) . . . . ?
C014 N001 C017 C004 176.86(17) . . . . ?
Ni01 N001 C017 C004 18.8(3) . . . . ?
C014 N001 C017 C015 -0.7(2) . . . . ?
Ni01 N001 C017 C015 -158.76(14) . . . . ?
C009 C004 C017 N001 -6.7(3) . . . . ?
C011 C004 C017 N001 175.05(17) . . . . ?
C009 C004 C017 C015 170.2(2) . . . . ?
C011 C004 C017 C015 -8.0(3) . . . . ?
C013 C015 C017 N001 0.1(2) . . . . ?
C002 C015 C017 N001 179.8(2) . . . . ?
C013 C015 C017 C004 -177.2(2) . . . . ?
C002 C015 C017 C004 2.6(4) . . . . ?

## Acknowledgement

This work was established by a lot of supports of many people. I would like to express my gratitude to all of them.

This research was totally supervised by Professor Dr. Hiroshi Nishihara. Professor Nishihara gave me not only the opportunity to study this interesting research, but also valuable discussion, hearty suggestion and encouragement. I express my deep gratitude to Professor Dr. Hiroshi Nishihara.

I am greatly thankful to Assistant Professor Dr. Ryota Sakamoto. He gave me a lot of guidance and advices which provided the direction of this study. I have been learning a lot of skills improving my research life from Assistant Professor Sakamoto.

I would like to express my thank to Associate Professor Dr. Yoshinori Yamanoi, Assistant Professor Dr. Tetsuro Kusamoto, Project Assistant Professor Dr. Mariko Miyachi, Project Assistant Professor Dr. Wu Kuo Hui, and Project Assistant Professor Dr. Hiroaki Maeda, for helpful comments and suggestions.

Many researchers technically supported my study. I appreciate Mr. Kohei Okitsu in Research Hub in Advanced Nano Characterization (Graduate School of Engineering, The University of Tokyo) for XPS measurements, Professor Dr. Tsuyoshi Kawai and Assistant Professor Dr. Yoshiyuki Nonoguchi (Graduate School of Materials Science, Nara Institute of Science and Technology) for thermoelectric power factor measurements, Prof. Dr. Eiji Nishibori (Graduate School of Pure andApplied Sciences, University of Tsukuba) and Dr. Kunihisa Sugimoto (Japan Synchrotron Radiation Research Institute) for synchrotron radiation single crystal X-ray diffraction measurements, Prof. Dr. Sono Sasaki (Department of Biobased Materials Science, Kyoto Institute of Technology) and Dr. Hiroyasu Masunaga (Japan Synchrotron Radiation

Research Institute) for synchrotron radiation 2D WAXS measurements, Associate Professor Kosuke Nagashio (Graduate School of Engineering, The University of Tokyo) for handling the graphdiyne nanosheet and optical microscopy, and Dr. Zheng Liu (National Institute of Advanced Industrial Science and Technology) for TEM measurements.

I would like to deeply acknowledge to all members in Nishihara Lab. Especially, I appreciate Dr. Kenji Takada, Dr. Tigmansu Pal, Dr. Amalia Rapakousiou, Mr. Xinsen Sun, Ms. Eunice Jia Han Phua, Mr. Tatsuhiro Nagayama, Mr. Keisuke Wada, Mr. Tan Choon Meng, Mr. Toshiki Yagi, Mr. Cao Jian, Mr. Ryojun Toyoda, Mr. Toshiki Iwashima, Mr. Ukyo Nakajima, Ms. Risa Aoki, and Mr. Ryo Shiotsuki, who are members of the CONASH research team. They kindly supported my study and shared the joys and sorrows of research life with me. I also thank to my classmates, Ms. Yasuyo Ogino, Mr. Mizuho Tsuchiya, and Mr. Ken Hoshiko. We have always encouraged and helped each other, and overcome many ordeals.

I am indebted to JSPS Fellowship for Young Scientists.

The most of Figures in Chapter 2 and 3 are reproduced from my publication on *Chemical Science* published in 2015 and *Journal of the American Chemical Society* published in 2017, respectively. I also thank to Royal Society of Chemistry and American Chemical Society for allow me to reuse them in this thesis.

Finally, I would like to express my sincere gratitude to my partner Aimi for giving a lot of support, encouragement, and unconditional love throughout my research period.

December 2016

Ryota Matsuoka

# List of publications

## Publication related to the thesis

1. "Bis(dipyrrinato)metal(II) coordination polymers: Crystallization, exfoliation into single wires, and electric conversion ability", R. Matsuoka, R. Toyoda, R. Sakamoto, M. Tsuchiya, K. Hoshiko, T. Nagayama, Y. Nonoguchi, K. Sugimoto, E. Nishibori, T. Kawai, H. Nishihara, *Chem. Sci.* **2015**, *6*, 2853–2858.
2. "Crystalline Graphdiyne Nanosheets Produced at a Gas/Liquid or Liquid/Liquid Interface", R. Matsuoka, R. Sakamoto, K. Hoshiko, S. Sasaki, H. Masunaga, K. Nagashio, H. Nishihara, *J. Am. Chem. Soc.* in press. DOI: 10.1021/jacs.6b12776.

## Publications not related to the thesis

1. "Heteroleptic bis(dipyrrinato)copper(II) and nickel(II) complexes", R. Toyoda, M. Tsuchiya, R. Sakamoto, R. Matsuoka, K.-H. Wu, Y. Hattori, H. Nishihara, *Dalton Trans.* **2015**, *44*, 15103–15106.
2. "New aspects in bis and tris(dipyrrinato)metal complexes: bright luminescence, self-assembled nanoarchitectures, and materials applications", R. Sakamoto, T. Iwashima, M. Tsuchiya, R. Toyoda, R. Matsuoka, J. F. Kögel, S. Kusaka, K. Hoshiko, T. Yagi, T. Nagayama, H. Nishihara, *J. Mater. Chem. A.* **2015**, *3*, 15357–15371.
3. "π-Conjugated bis(terpyridine)metal complex molecular wires", R. Sakamoto, K.-H. Wu, R. Matsuoka, H. Maeda, H. Nishihara, *Chem. Soc. Rev.* **2015**, *44*, 7698–7714.
4. "Interfacial Synthesis of Electrically Conducting Palladium Bis(dithiolene) Complex Nanosheet", T. Pal, T. Kambe, T. Kusamoto, M. L. Foo, R. Matsuoka, R. Sakamoto, H. Nishihara, *ChemPlusChem* **2015**, *80*, 1255–1258.
5. "Heteroleptic [Bis(oxazoline)](dipyrrinato)zinc(II) Complexes: Bright and Circularly Polarized Luminescence from an Originally Achiral Dipyrrinato Ligand", J. F. Koegel, S. Kusaka, R. Sakamoto, T. Iwashima, R. Toyoda, M. Tsuchiya, R. Matsuoka, T. Takamasa, J. Yuasa, Y. Kitagawa, T. Kawai, H. Nishihara, *Angew. Chem. Int. Ed.* **2016**, *55*, 1377–1381.